

**Late Quaternary climate history of Northern Siberia –
evidence from ground ice**

**Die spätquartäre Klimageschichte Nordsibiriens –
Ergebnisse aus Untersuchungen an Grundeis**

Hanno Meyer

**Ber. Polarforsch. Meeresforsch. 461 (2003)
ISSN 1618 - 3193**

Hanno Meyer
Alfred-Wegener-Institut für
Polar- und Meeresforschung
Forschungsstelle Potsdam
Telegrafenberg A43
14473 Potsdam

Diese Arbeit ist die leicht veränderte Fassung einer Dissertation, die im April 2001 dem Fachbereich Geowissenschaften der Universität Potsdam vorgelegt wurde.

Table of contents

Table of contents	i
Abstract.....	iv
Kurzfassung.....	v
1. Introduction.....	1
1.1 Scientific background.....	1
1.2. Aims for paleoclimate studies in ground ice.....	3
2. Study area.....	5
2.1. Geology	5
2.2. Ice Complex.....	6
3. Isotope studies of hydrogen and oxygen in ground ice – Experiences with the equilibration technique	
3.1. Abstract.....	9
3.2. Introduction	10
3.3. Analytical procedure	11
3.4. Calibration.....	14
3.5. Equilibration technique and small sample sizes.....	18
3.6. Sampling strategy for ground ice	22
3.7. First results	25
3.8. Conclusions	25
4. Paleoclimate studies on Bykovsky Peninsula, North Siberia - Hydrogen and oxygen isotopes in ground ice	
4.1. Abstract.....	26
4.2. Introduction	27

4.3. The working area	28
4.4. The outcrop.....	30
4.5. Sampling strategy	34
4.6. Analytical procedure	35
4.7. Geochronology	35
4.7.1. Age estimate of the Ice Complex	35
4.7.2. Age estimate of the Holocene genetic units	40
4.8. Results and discussion	41
4.8.1. Recent precipitation.....	41
4.8.2. Stable isotopes in ice wedges	43
4.8.3. Paleoclimatic evolution as revealed from stable isotope data	48
4.8.4. Sources	54
4.9. Conclusions	57

5. Paleoclimate reconstruction on Big Lyakhovsky Island, North Siberia – hydrogen and oxygen isotopes in ice wedges

5.1. Abstract.....	59
5.2. Introduction	60
5.3. Working area and climatic background.....	61
5.4. Methods	62
5.5. Results of the field studies	64
5.6. Geochronology	68
5.7. Recent precipitation	70
5.8. Stable isotopes in ice wedges and their paleoclimatic interpretation	73
5.9. Conclusions	81

6. Synthesis 83

6.1. Paleoclimatic history of Northern Siberia.....	83
6.2 Moisture sources for ice wedges	90
6.3 Absolute temperatures	92

7. Conclusions	96
8. References	99
List of Figures	107
List of Tables	108
Acknowledgements	110

Abstract

Large areas of Russia, especially in Northern Siberia, are characterised by a severe continental climate and continuous permafrost conditions. On Bykovsky Peninsula and Big Lyakhovsky Island, located in the Laptev Sea region, ice-rich permafrost deposits were studied in order to decipher the climatic variations of the Late Quaternary. Ground ice and in particular ice wedges were analysed by means of stable hydrogen and oxygen isotopes in the framework of the multidisciplinary research project "Paleoclimate signals in ice-rich permafrost". The main goals of the research program are the reconstruction of the paleoclimatic and paleoenvironmental conditions in ice-rich permafrost areas of Northern Siberia.

The Ice Complex, a peculiar cryolithogenic formation, is typical for the non-glaciated lowland areas of Northern Siberia. It was formed between 60 ka and 12 ka BP, and is characterised by syngenetic ice wedge growth in ice-rich deposits. As shown in the stable isotopes, ice wedges are mainly fed by meltwater of the winter precipitation and, thus reflect winter temperatures. Water from the adjacent sediment may alter the isotopic composition of an ice wedge at its margins. The presence of ice wedges as indicative feature for permafrost conditions since 60 ka BP, implies that a large glacier extending over the Laptev Sea shelf did not exist during the Late Glacial Maximum. Sediment and ice wedges with an age of 200 ka underlay the Ice Complex on Big Lyakhovsky Island. This is the oldest ground ice ever analysed by hydrogen and oxygen isotopes.

The comparison between the stable isotope records of ice wedges from the individual sites reveal a period of extremely cold winter temperatures between 60 and 50 ka BP. Between 50 and 20 ka BP, the winters were relatively cold and stable. A sharp rise in the stable isotope ratios of ice wedges is found for the Pleistocene-Holocene boundary, interpreted as a climatic warming trend. For the Early Holocene warm period (8-4.5 ka BP), thermokarst processes formed lacustrine environments, which restricted ice wedge growth. After 4.5 ka BP, Holocene ice wedges grew until present in thermo-erosional valleys and in thermo-karst depressions after the lakes fell dry. The isotopic composition of

recent ice wedges was used for the reconstruction of absolute winter and January temperatures of the older units. The combination of H and O isotope analyses of precipitation and ground ice is useful to identify moisture sources for the Laptev Sea region. For the winter precipitation of the western Laptev Sea, a change in the moisture source to the present North Atlantic source was proved between 18.5 and 11.2 ka BP.

Kurzfassung

Weite Gebiete Russlands, insbesondere im nördlichen Sibirien sind durch ein strenges kontinentales Klima und kontinuierliche Permafrost-Bedingungen gekennzeichnet. Im Gebiet der Laptew-See, auf der Bykowski-Halbinsel und der Großen Ljachow-Insel, wurden eisreiche Permafrost-Ablagerungen untersucht, um die spätquartäre Klima-Entwicklung zu rekonstruieren. Grundeis, insbesondere Eiskeile wurden mittels stabiler Sauerstoff- und Wasserstoff-Isotope im Rahmen des deutsch-russischen Forschungsprogramms "System Laptew-See 2000" im multi-disziplinären Teilprojekt "Paläo-Klimasignale in eisreichem Permafrost" untersucht. Das Ziel des Projektes ist die Rekonstruktion der Paläo-Klima- und Umweltbedingungen in eisreichen Permafrost-Abfolgen Nordsibiriens.

Der Eis-Komplex ist eine einzigartige kryolithogenetische Bildung, die typisch für die nicht vergletscherten Akkumulationsgebiete Nordsibiriens ist. Der Eis-Komplex ist durch syngenetisches Eiskeil-Wachstum in eisreichem Sediment gekennzeichnet und wurde zwischen 60 ka und 12 ka BP gebildet. Eiskeile werden durch Schmelzwässer aus den Winter-Niederschlägen gespeist und spiegeln daher Winter-Temperaturen wider. Allerdings kann die Migration von Feuchtigkeit aus dem benachbarten Sediment die Isotopen-Zusammensetzung von Eiskeilen im Randbereich verändern. Eiskeile sind an Permafrost-Bedingungen gebunden. Dies belegt, dass der Schelf der Laptew-See während des letzten glazialen Maximums nicht von Gletschereis bedeckt gewesen sein kann. Auf der Großen Ljachow-Insel wird der Eis-Komplex von Sedimenten und

Eiskeilen unterlagert, die bis zu 200.000 Jahre alt sind. Dies ist das älteste Grundeis, das je mit stabilen Sauerstoff- und Wasserstoff-Isotopen untersucht wurde.

Die Kombination der stabilen Isotopen-Daten der Untersuchungsgebiete zeigt eine Phase extrem kalter Winter zwischen 60 und 50 ka BP. Die Zeit von 50 bis 20 ka BP ist durch stabile, weiterhin relativ kalte Wintertemperaturen gekennzeichnet. Ein deutlicher Anstieg der stabilen Isotopen-Verhältnisse in Eiskeilen wurde am Übergang Pleistozän-Holozän festgestellt und als Klima-Erwärmung interpretiert. Die wärmste Phase war während des Frühholozäns (8 - 4.5 ka BP), als durch Thermokarst-Prozesse weite Gebiete von Seen eingenommen wurden, die die Eiskeil-Bildung einschränkten. Holozänes Eiskeil-Wachstum begann in Thermokarst-Senken nach dem Trockenfallen der Seen und in Thermo-Erosionstälern, und setzte sich bis heute fort. Die Isotopen-Verhältnisse rezenter Eiskeile wurden als Basis für die Rekonstruktion absoluter Winter- und Januar-Temperaturen der Vergangenheit verwendet. Die Kombination von Sauerstoff- und Wasserstoff-Isotopenanalysen an Grundeis und Rezent-Niederschlägen ermöglicht eine Zuordnung von Feuchtigkeitsquellen für die Laptew-See-Region. Für die westliche Laptew-See-Region fand zwischen 18.5 and 11.2 ka BP ein Wechsel der Quellgebiete für die Winter-Niederschläge zur heutigen nordatlantischen Feuchtigkeitsquelle statt.

1. INTRODUCTION

1.1 Scientific background

Ice is a natural archive of paleoclimatic information. The ice cores from Greenland are the most important records for the understanding for the Northern hemisphere climate history. The ice cores GRIP (Greenland Ice Core Project), GISP2 (Greenland Ice Sheet Project II), Dye-3 and Camp Century reached bedrock, and provide high resolution archives covering the last 250 ka. All Greenland ice cores show climatically different conditions for the Late Pleistocene and the Holocene (e.g. Dansgaard *et al.*, 1984; Grootes *et al.*, 1993). The stable oxygen isotope records of Greenland ice cores show large and fast oscillations for the pre-Holocene period, where up to 24 interstadial episodes with relatively high $\delta^{18}\text{O}$ values were distinguished (Dansgaard *et al.*, 1993). The Holocene is characterised by a more stable climate, with much lower variations in $\delta^{18}\text{O}$. These are principle characteristics of Greenland ice cores, which can be correlated between the cores, and are also found in deep sea sediments (e. g. Bond *et al.*, 1992).

Except the large Greenland ice sheet, glaciers are rather rare and limited in distribution in the Northern hemisphere (Fig. 1.1). In large parts of the Siberian Arctic, glacier ice cores are not available and restricted to islands such as the Severnaya Zemlya archipelago (Vaikmäe & Punning, 1984; Klementyev *et al.*, 1991) or to mountain areas. It rises the question whether the $\delta^{18}\text{O}$ curves of glaciers reflect the general climatic situation of the Northern hemisphere or, to a large amount, local or regional processes.

Presently, approximately a quarter of the world's continental surface is characterised by permafrost conditions (French, 1996). In Fig. 1.1, the regional extent of the periglacial zones in the Northern hemisphere is displayed (Karte, 1979). Most of the Siberian and Canadian Arctic are within the zones of continuous, discontinuous or sporadic permafrost. Permafrost is defined by ground temperatures below or at 0°C for two or more successive years (International Permafrost Association, 1998). Russia has the largest extent of permafrost with ca. $11 \times 10^6 \text{ km}^2$, corresponding to about 50% of its territory. The

oldest permafrost sequences in the Siberian Arctic have been dated to Late Pliocene age (Kaplina, 1981). In Tiksi, Northern Siberia, near the working area, continuous permafrost reaches a thickness of 630 m (Yefimov & Dukhin, 1966; cited in Washburn, 1979).

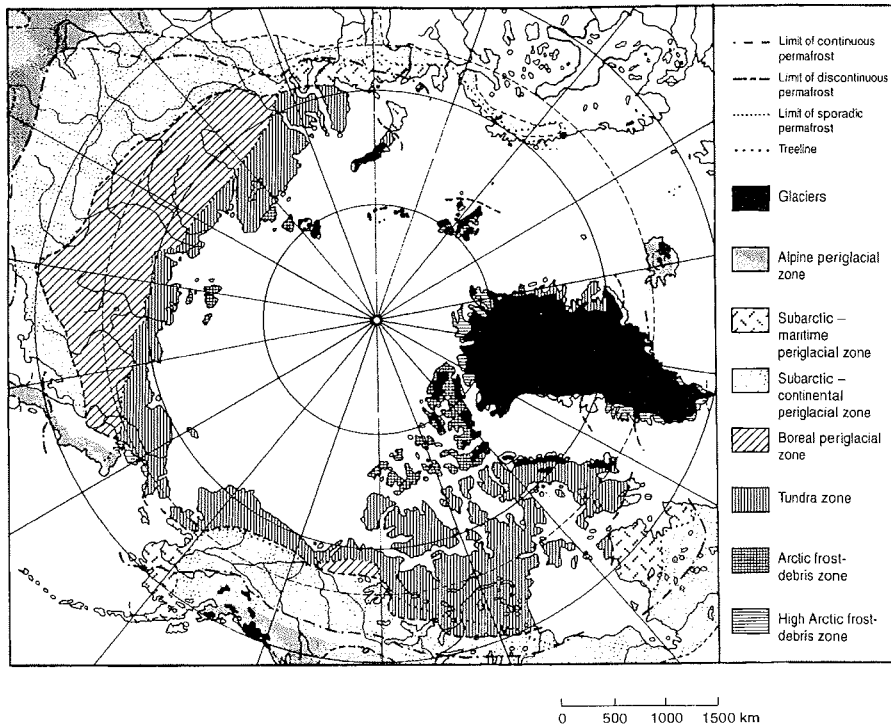


Fig. 1.1: Permafrost regions in the Northern hemisphere (Karte, 1979)

A major component of permafrost is the ground ice, which is a term used for all types of ice in freezing or frozen ground (International Permafrost Association, 1998). Wide areas of Russia, especially in Northern Siberia contain high amounts of ground ice, such as ice wedges, pingo ice, pore ice and segregated ice. Most ground ice types are fed by precipitation (Vaikmäe, 1989), which is dependent upon the condensation temperature out of an air mass (Dansgaard, 1964). Therefore, the stable isotopic composition of ground ice reflects climatic conditions. The formation mechanisms are different for the various types of ground ice (MacKay, 1972). These processes must be considered for the interpretation of isotopic analysis of ground ice. Ice wedges

are believed to be the most promising ground ice climatic archives because they are fed by snow melt water and consequently closely correlated with mean winter temperatures (Vaikmäe, 1989).

In general, permafrost is linked with low precipitation and negative air temperatures for 75% of the year, rarely exceeding 20°C in summer (Washburn, 1979). The most important factor controlling the extent and the distribution of permafrost are changes in climate. A world-wide increase in air temperatures may result in dramatic changes in the Arctic region. These are i. e. the release of large amounts of greenhouse gases (such as methane) stored in the permafrost or changes in the sea ice cover, which controls the gas and energy exchange between Arctic ocean and atmosphere (Aagaard *et al.*, 1985). On one hand, ice-rich permafrost is extremely sensitive to thawing processes. The reactions of Arctic permafrost to global climate and environmental change are yet insufficiently understood and subject to concern. On the other hand, the sediments and ground ice of ice-rich permafrost deposits are excellent archives of climatic and environmental information.

1.1 Aims for paleoclimate studies in ground ice

The multidisciplinary research project „Paleoclimate signals in ice-rich permafrost“ was established in the frame of German-Russian cooperation „System Laptev Sea 2000“. During the expeditions „Lena Delta 1998-2000“, ice-rich permafrost sequences were studied in detail in the coastal areas of the Laptev Sea, North Siberia. For the first time a major comprehensive research program unified scientific approaches such as geocryology, sedimentology, geochemistry, mineralogy, paleobotany, pedology and micropaleontology.

The thesis covers a paleoclimate reconstruction based on stable isotope geochemistry and hydrochemistry applied to recent, Holocene and Pleistocene ground ice, especially ice wedges. For that purpose, we used the combination of hydrogen and oxygen isotopes, which up to now has been rarely applied to ground ice, and the most intensive sampling effort ever performed for ground ice exceeding 2000 stable isotope analyses. The main objective of the thesis is a reconstruction of the local and regional climatic and environmental history of

Northern Siberia during the Late Quaternary. Mostly ice-rich permafrost sequences of two key localities in the eastern Laptev Sea were studied with the aim to differentiate regional and site-specific peculiarities from climatic trends. Based on this fundamental research and on well-established geochronology, the construction of a stable isotope curve for ground ice analogously to the $\delta^{18}\text{O}$ curves in glacier ice cores is aimed. The thesis includes results derived from three expeditions to Bykovsky Peninsula from July to August, 1998, to Big Lyakhovsky Island between July and September, 1999 and to different locations in the Lena delta in 2000. First field data and results are described in three field reports (Rachold, 1999; 2000; Rachold & Grigoriev, 2001).

The thesis is written in “cumulative” form containing three independent papers, which are published in different journals. Chapter 3 describes the stable isotope method used with equilibration technique and its applicability to ground ice. It includes a new approach for the measurement of small sample volumes and the calibration of the mass spectrometer, during which the new standard NGT, suitable for ground ice, is introduced. Chapter 4 deals with stable isotope and field data of the first sampling site, the Bykovsky Peninsula. Main results are the differentiation of three stratigraphic units alas, log and Ice Complex with stable water isotopes, the identification of water migration processes between ice wedges and segregated ice as well as the establishment of a stable isotope curve covering the last 60 ka. For the second sampling site, Big Lyakhovsky Island (Chapter 5), stable isotopes are used for the distinction of six different generations of ice wedges, including ground ice as old as 200 ka. These are the oldest ice wedges ever analysed by means of stable oxygen and hydrogen isotopes. In Chapter 6, the results of Bykovsky Peninsula and Big Lyakhovsky Island are synthesised and combined with own unpublished data and data from the literature in order to derive a regional climate picture including a reconstruction of absolute winter and January temperatures from ice wedge stable isotope data. The last chapter concludes the results and suggests possible directions for future research related to paleoclimate studies on ground ice.

2. STUDY AREA

The Laptev Sea, being a part of the Arctic Ocean, is a shallow epicontinental shelf sea, with water depths in general below 60 m. The Laptev Sea is limited by the Taymyr Peninsula in the West, the New Siberian Archipelago in the East and the Siberian continent in the South. The main tributary is the Lena River forming a large delta of 32.000 km² (Gordeev & Sidorov, 1993). The water supply of the Lena and other Siberian rivers forms a layer of fresh water with low salinity and density, which freezes in winter. As a consequence, the Laptev Sea is covered by a 3 m thick layer of pack ice during winter and for large parts of the year, leaving only the so called "polynya", a belt of several kilometres in extension, free of ice. During the Late Glacial Maximum (LGM), the world-wide sea level was approximately 120 m lower than today (Fairbanks, 1989). The sea level of the Laptev Sea started rising around 16 ka (Rozenbaum & Shpolyanskaya, 1998) reaching its modern position approximately 5-6 ka BP (Romanovskii *et al.*, 1999, Bauch *et al.*, 1999). Therefore, large parts of the Laptev Sea shelf were continental areas during large parts of the Weichselian to Middle Holocene history.

Presently, the peculiar strongly continental climate of the Laptev Sea region is dominated by the influence of the Siberian anticyclone. The winters are severe, 6 to 9 months long, and characterised by mean January temperatures of about -30°C, interrupted by short summers with mean July temperatures of about 10°C (Atlas Arktiki, 1985). The mean annual precipitation is low especially in winter, and ranges in general between 200-300 mm. The region is located to the north of the Arctic Circle. Therefore, the solar net radiation is near zero in the winter months.

2.1 Geology

The Laptev Sea region is influenced by four tectonic elements: The Siberian Craton and the Early Mesozoic Taymyr fold belt characterise the western Laptev Sea region. The Mesozoic Verkhoyansk-Kolyma and the New Siberian-Chukchi fold belts are located in the eastern part and divided by the mid-

Cretaceous Lyakhov-South Anyui ophiolitic suture (Drachev *et al.*, 1999). The study area belongs to the Laptev Rift System, which is linked to the sea floor spreading of the Gakkel Ridge, and characterised by vertical block tectonic and high seismic activity. The Gakkel ridge, which occurs since 56 Ma until present time, proceeds in the eastern Laptev Sea region to the Eurasian continent. The Laptev Rift system is characterised by rift basins in the western, the U'st Lena rift in the central part and horst structures in the eastern part of the Laptev Sea. The deformed Paleozoic to Mesozoic basement is discordantly overlain by mostly undisturbed Late Cretaceous to Cenozoic clastic sequences, which fill the rift-related sedimentary basins (Drachev *et al.*, 1999). The thickness of these sediments varies between 10-12 km in the western Laptev Sea region to about 2 km in the eastern Laptev Sea horst structures. Lungersgauzen (1967, cited in: Romanovskii, 1978) stated the occurrence of neotectonic uplift of the Kharaulakh mountains, a western extension of the Verkhoyansk-Kolyma fold belt, between 150 and 50 ka before present. Approximately at this time during the marine isotope stages 5 to 3 started the formation of the Ice Complex, which is probably linked to the marine regression after the Eemian sea-level maximum (Romanovskii *et al.*, 2000).

2.2 Ice Complex

Large areas of Northern Siberia are characterised by this specific permafrost formation called "Ice Complex", which was the main object of our studies.

Ice Complex is widely distributed in different relief elements in Northern Siberia (Fig. 2.1), especially in the coastal lowlands of the Laptev and East Siberian Seas, and along the large Siberian rivers Lena, Yana, Kolyma and Indigirka (Romanovskii, 1993). In Western and Eastern Siberia, Ice Complex formation is restricted to river and lake depressions.

The formation of the Ice Complex is generally related to areas of sediment accumulation. The sediments of the Ice Complex reach a maximum thickness of about 60 m, and, in the study area, derive from the nearby mountain areas (Schwamborn *et al.*, 2002; Siegert *et al.*, 2002). Some authors consider the Ice Complex as a cold-climatic equivalent of the loess formation (Tomirdiaro *et al.*,

1984). In general, the Ice Complex is related to high continental areas with low precipitation. Being composed of large syngenetic ice wedge polygons in ice-rich sediments indicative for permafrost conditions, the Ice Complex is a proof for the absence of glaciers.

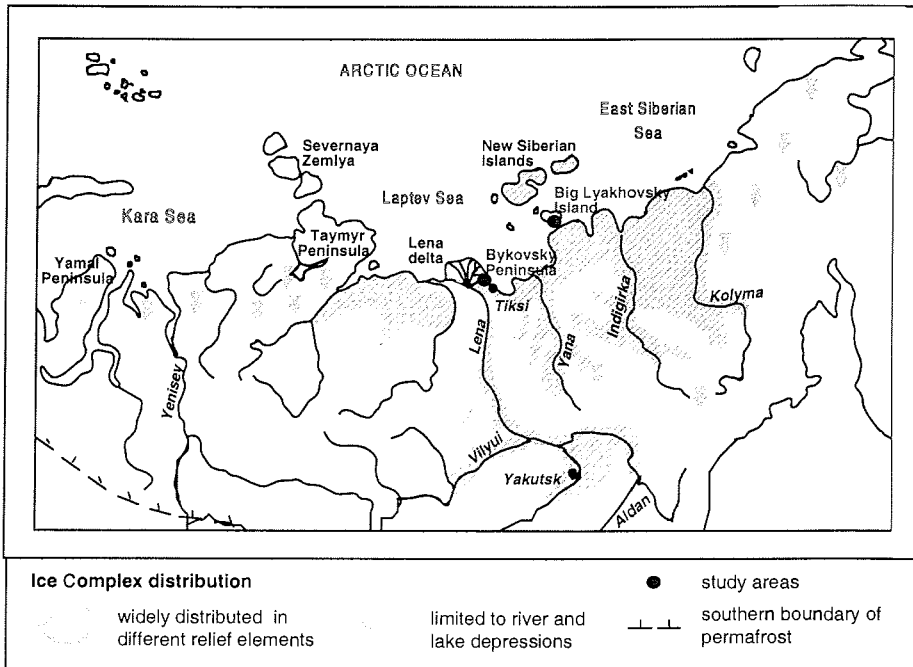


Fig. 2.1: Distribution of the Ice Complex in Northern Siberia (after Romanovskii, 1993) and the position of the study areas

The maximum age of the Ice Complex decreases from the East to the West. The oldest Ice Complex is found in Eastern Siberia (Kaplina, 1981) dated to Early Weichselian times. The analysed sequences of Ice Complex on Bykovsky Peninsula and Big Lyakhovskiy Island are of Middle to Late Weichselian age. At Yamal Peninsula, Western Siberia, Vasil'chuk *et al.* (2000) dated the Ice Complex to 35 ka BP and younger. These differences of the beginning of Ice Complex formation are related to progressive aridification from the East to the West. In Western Siberia, the Ice Complex started growing after the disappearance of glaciers.

3. ISOTOPE STUDIES OF HYDROGEN AND OXYGEN IN GROUND ICE – EXPERIENCES WITH THE EQUILIBRATION TECHNIQUE

Hanno Meyer, Lutz Schönicke, Ulrich Wand, Hans-Wolfgang Hubberten and Hans Friedrichsen

Reprinted with permission from **Isotopes in Environmental and Health Studies** 36, p. 133-149, 2000, Copyright © 2000.

3.1 Abstract

Equilibration technique suitable for a large amount of samples is described for hydrogen and oxygen isotope analyses of ground ice, especially ice wedges, including the sampling strategy and the analytical procedure as well as the calibration of the Finnigan MAT Delta-S mass spectrometer in June, 1999. Since for future analyses of ice wedges, a higher sampling resolution with limited sample volume is required, the limit of the equilibration technique for small water sample sizes of between 0.05 and 5 ml was checked. For water samples smaller than 1 ml, corresponding to a molar ratio $[H_2O]/[H_2]$ of smaller than 0.994, a balance correction has to be applied. The experimental errors due to partial evaporation during evacuation, the balance calculation of the isotope equilibration process, the linearity as well as memory effects of the mass spectrometer for samples with large differences in $\delta^{18}O$ and δD are tackled in this paper.

In the polar regions of Northern Siberia without Late Pleistocene and Holocene glaciation, ground ice is used as an archive for paleoclimate studies. First results of stable isotope measurements on ice wedges clearly show a shift towards heavier isotopes and thus warmer winter temperatures as well as a change in the source of the precipitation between Late Pleistocene and Holocene. These results indicate the high potential of ground ice for paleoclimate studies.

3.2 Introduction

In former times, hydrogen isotopes of water samples were measured by Zn, U or Cr reduction method. Automated equilibration technique is used since 1953 (Epstein & Mayeda, 1953) for oxygen isotope analysis, but can only be applied for hydrogen isotopes since a few years (Horita *et al.*, 1989). There are some major advantages of this technique:

- a. the whole procedure is fully automatic and both elements can be measured in one run,
- b. oxygen isotope analysis by equilibration is less time consuming than converting the oxygen of the water into either O₂ by the fluorination or into carbon monoxide by high temperature conversion, which are both difficult to be automated besides possible memory effects,
- c. hydrogen isotope determination by reducing the water to hydrogen with either zinc, chromium or uranium involves the possibility of considerable memory effects (Scrimgeour *et al.*, 1993).

Hydrogen and oxygen isotopes are well known as useful tools for paleoclimate studies in ice bodies, especially for paleotemperature reconstruction and for the identification of the source of the precipitation (Dansgaard, 1964). During the last 30 years, many efforts have been made in isotope analysis of the ice caps of Greenland and Antarctica in order to provide information on climate changes through time (Johnsen *et al.*, 1972; Oeschger, 1985). In polar regions without actual glaciation, such as most of the Eurasian Arctic, glacier ice cores are not available and, therefore, other climatic archives have to be considered for paleoclimate reconstruction.

The equilibration technique of hydrogen and oxygen isotopes was applied by the authors to a high number of Siberian ground ice samples. In our studies, carried out at the Bykovsky Peninsula in the Lena Delta area, NE Siberia, we mainly used ice-rich sediments with huge polygonal ice wedge systems (Meyer *et al.*, 1999) These ice wedges consist of thin subvertical annual ice veins, which have been formed since the Weichselian period. An annual sampling

resolution with limited sample volume is desired for future analyses. Therefore, we checked the equilibration technique to small water sample sizes.

3.3 Analytical procedure

Our measurements were carried out with a Finnigan MAT Delta-S mass spectrometer endowed with two equilibration units (MS Analysentechnik, Berlin). Each unit has a capacity of 24 sample bottles. Both oxygen and hydrogen isotopes of ground ice have been analysed using common equilibration technique.

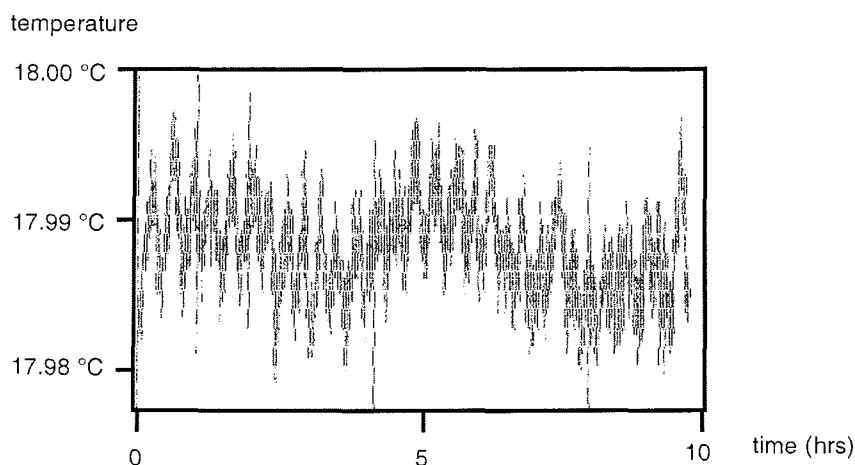


Fig. 3.1: 10 hour temperature plot of a water bath (type GFL 1086, modified)
 mean value: 17.988°C maximum: 18.002°C
 standard deviation: 0.003°C minimum: 17.976°C

Since the fractionation factor for deuterium (H_2O/H_2) has a temperature coefficient of $-5.4\text{‰}/^\circ\text{C}$ (Friedman & O'Neil, 1977), the temperature of the water shaking bath (actually the surface of the catalyst sticks where equilibration happens) has to be constant within $\pm 0.05^\circ\text{C}$ or better.

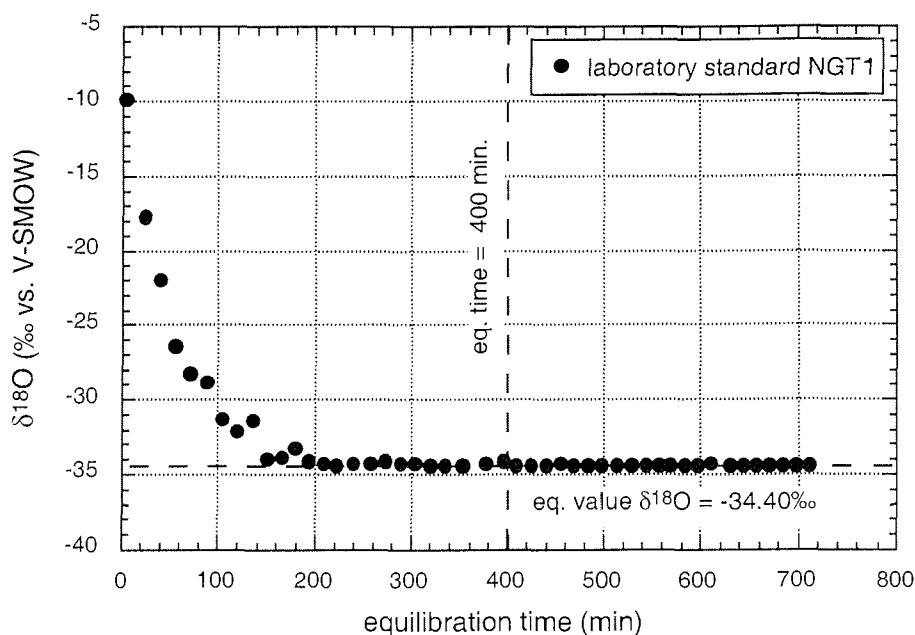


Fig. 3.2: Determination of the equilibration time for $\delta^{18}\text{O}$

A two stage rotary pump (type E2M1.5, Edwards Vacuum Products) evacuates the bottles. As a first step, hydrogen isotope measurements are carried out. Hydrogen isotopes are equilibrated between the water and the H_2 gas for 120 min. Activated platinum condensed on a hydrophobic stick (MS Analysentechnik, Berlin) is used as catalyst for the hydrogen isotope exchange. After finishing the complete hydrogen measuring sequence, the same sample aliquots are equilibrated with CO_2 for $\delta^{18}\text{O}$ measurement. For the determination of the time necessary for complete equilibration of oxygen isotopes in the water- CO_2 system, test measurements were carried out for different equilibration times with our standard NGT1 until the known $\delta^{18}\text{O}$ of -34.40‰ was achieved (see Fig. 3.2). As can be seen from these experiments, equilibrium is complete after 200 min. For safety reasons, an equilibration time of 400 min is used in our laboratory during routine analyses with 5 ml samples.

The first bottle of each unit is equipped with our laboratory standard NGT1 (snow, North Greenland Traverse). The H_2 and CO_2 gas equilibrated with NGT1

is subsequently transferred into the standard bellow of the inlet system and used as reference standard for the whole unit. We prefer this technique since normal tank gas differs considerably in its isotopic composition from natural water samples. Both possible errors in connection with measuring large isotopic differences – uncertainties of δ -determinations and varying H_3^+ -contributions – are limited. After equilibration of the water sample with H_2 or CO_2 , an aliquot of equilibrated gas is separated from water vapour by freezing the water in a cooling trap at $-78^\circ C$ and then transferred into the sample bellow. With the dual inlet method, sample and reference gases are alternately introduced from the bellows through a viscous leak into the mass spectrometer. Ten measurements are carried out at 5 nA H_2 signal for δD and at 10 nA mass 44 intensity for $\delta^{18}O$. In order to avoid any changes of the isotopic composition of the standard gases caused by demixing during the run of the samples, the pressure in the standard bellow was chosen higher (150 to 200 mbar) compared to the pressure in the sample bellow (30 to 50 mbar). A standard gas in the standard bellow measured against the same standard gas in the sample bellow yields a difference of -1‰ for δD . These differences caused by the experimental set-up are linear and have to be corrected. For $\delta^{18}O$, no demixing of the standard gas could be observed.

δD and $\delta^{18}O$ values are calculated by the commercial software ISODAT (Version 5.2) and displayed as permil differences relative to V-SMOW. ^{17}O and H_3^+ corrections are carried out automatically. The measured H_3^+ factor was determined routinely and was normally less than 5 ppm/nA H_2 signal (the mean value from June to September 1999 is 4.44 ± 0.11 ppm/nA). For both isotope systems, 48 samples are measured in less than two days including preparation time. Three standard samples per unit are used for quality control, for isotopically light samples NGT1 is selected. In general, all samples are analysed twice in order to check the quality and reproducibility of the measuring process. The internal 1σ error is generally better than 0.8‰ for δD and better than 0.1‰ for $\delta^{18}O$ for all measurements.

3.4 Calibration

Our Delta-S mass spectrometer was calibrated for $\delta^{18}\text{O}$ and δD in June, 1999, using IAEA standards V-SMOW, SLAP and GISP and laboratory standards OCE2, ANST3, NGT1, PAK5 and HL1. In order to demonstrate the analytical precision of the measurements, the results of the calibration and the accepted values for IAEA standards are shown in Tab. 3.1.

Tab. 3.1: δD and $\delta^{18}\text{O}$ of IAEA and laboratory standards (vs. V-SMOW)

Standard	δD (‰)		$\delta^{18}\text{O}$ (‰)		$\delta^{18}\text{O}_{\text{corrected}}$ (‰)	
	mean value \pm S.D.		mean value		mean value \pm S.D. ^a	
V-SMOW	+0.1	\pm 0.1	+0.01	+0.01	\pm	0.00
OCE 2	-5.3	\pm 0.4	-0.71	-0.73	\pm	0.07
GISP	-189.7	\pm 0.1	-24.28	-24.81	\pm	0.01
ANST 3	-220.4	\pm 0.2	-27.56	-28.16	\pm	0.00
NGT 1	-265.4	\pm 0.5	-33.66	-34.40	\pm	0.03
PAK 5	-288.6	\pm 0.0	-35.67	-36.46	\pm	0.00
HL 1	-363.2	\pm 0.5	-45.17	-46.17	\pm	0.03
SLAP	-428.8	\pm 0.1	-54.32	-55.52	\pm	0.01
International accepted values as given in Gonfiantini <i>et al.</i> (1995).						
V-SMOW	0.0				0.00	
GISP	-189.7				-24.78	
SLAP	-428.0				-55.50	

a.) a correction factor of 1.022 was applied.

In Figs. 3.3.1 and 3.3.2, the excellent precision for both $\delta^{18}\text{O}$ and δD is displayed. V-SMOW was set zero, then scaled to SLAP ($\delta\text{D} = -428\text{‰}$ and $\delta^{18}\text{O} = -55.5\text{‰}$) and controlled by GISP ($\delta\text{D} = -189.7\text{‰}$ and $\delta^{18}\text{O} = -24.8\text{‰}$).

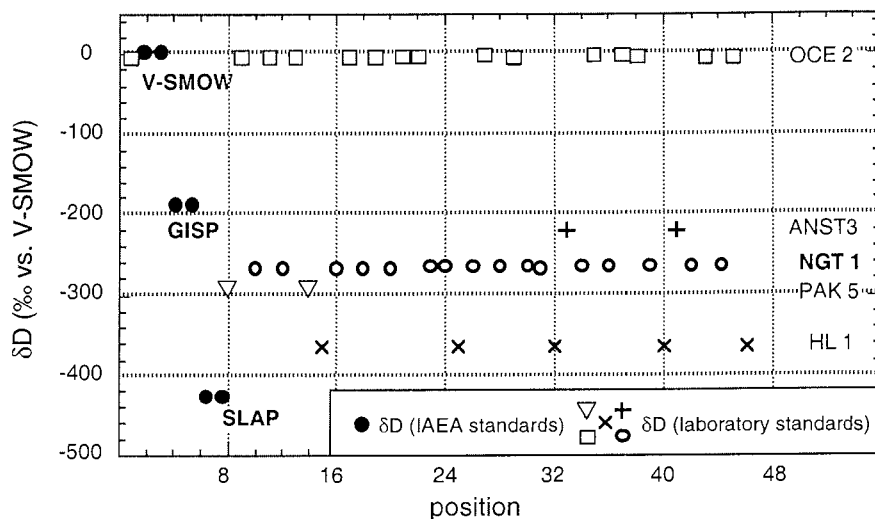


Fig. 3.3.1: δD -calibration of Delta-S mass spectrometer

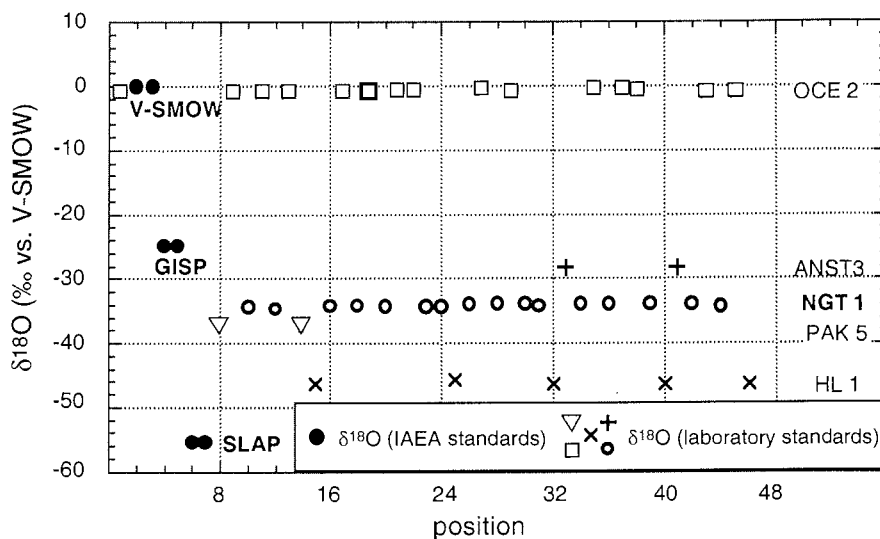


Fig. 3.3.2: $\delta^{18}O$ -calibration of Delta-S mass spectrometer

The δD and $\delta^{18}O$ values of GISP are within the analytical precision identical to those published by Gonfiantini *et al.* (1995). Additionally, the standard deviation of the isotopically lighter laboratory standard NGT1 ($\delta D = -265.4 \pm 0.5\text{‰}$ and $\delta^{18}O = -34.40 \pm 0.03\text{‰}$, $N = 16$) is slightly better than for the isotopically heavier OCE2 ($\delta D = -5.3 \pm 0.4\text{‰}$ and $\delta^{18}O = -0.73 \pm 0.07\text{‰}$, $N = 15$).

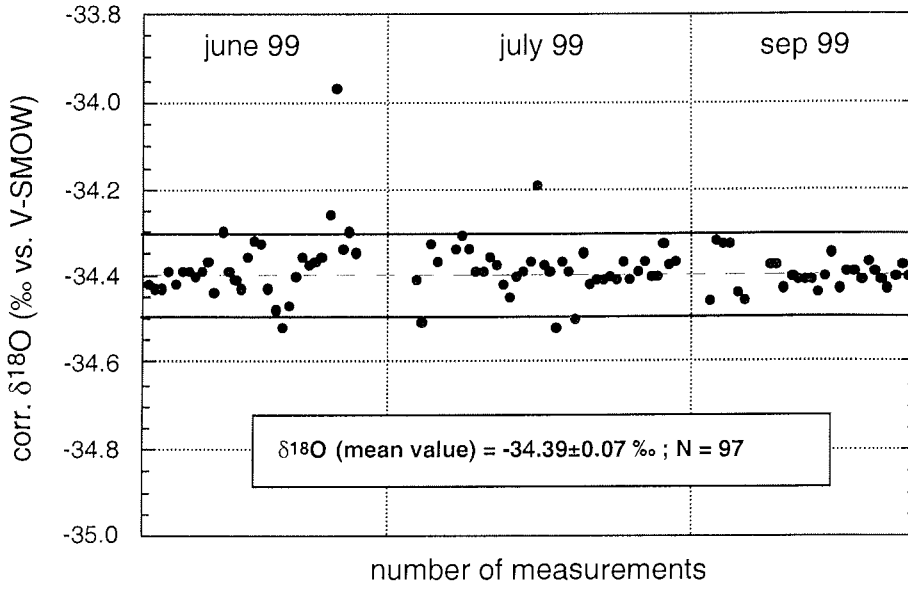


Fig. 3.4.1: Temporal variation of δD for the laboratory standard NGT1. The shaded field displays the maximal accepted internal 1σ error ($\delta D_{int.} = 0.8\text{‰}$)

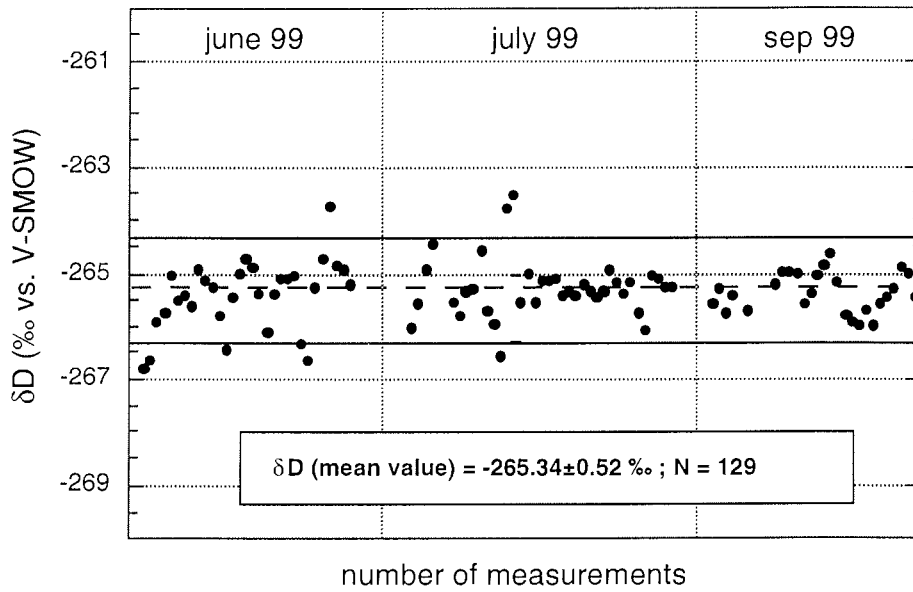


Fig. 3.4.2: Temporal variation of $\delta^{18}O$ for the laboratory standard NGT1. The shaded field displays the maximal accepted internal 1σ error ($\delta^{18}O_{int.} = 0.1\text{‰}$)

Thus, we conclude that the calibration is accurate, especially for isotopically light samples such as ground ice. $\delta^{18}\text{O}$ measurements of NGT1 carried out at the UFZ Leipzig-Halle (Kowski, pers. comm.) support our calibration ($\delta^{18}\text{O} = -34.44 \pm 0.06\text{‰}$, $N = 14$).

From June to October, 1999, NGT1 had a mean value of $-34.39 \pm 0.06\text{‰}$ for $\delta^{18}\text{O}$ and of $-265.3 \pm 0.5\text{‰}$ for δD relative to V-SMOW corresponding well with the calibrated value (see Figs. 3.4.1 and 3.4.2). After a careful determination of the H_3 -contribution on mass 3, a δD of $-427.9 \pm 0.4 \text{‰}$ was measured for V-SMOW-SLAP, giving evidence that a "stretching-correction" had not to be applied. Within our limits of error, we have no indication for any memory effects of neither the equilibration line nor the mass spectrometer when we used samples with up to 700 ‰ enrichments in the δD -values.

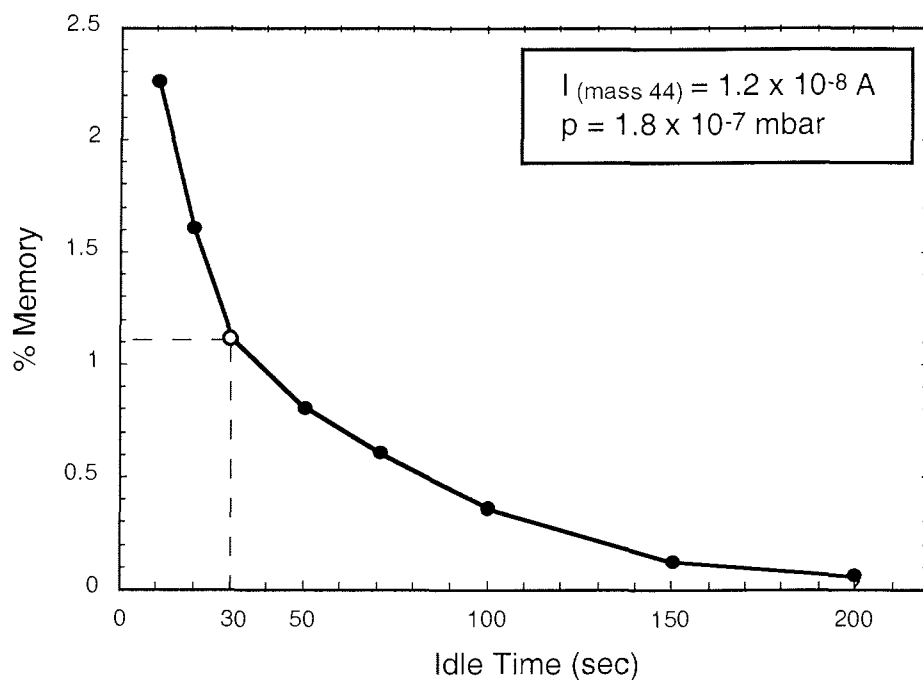


Fig. 3.5: Memory effects (in %) for different idle times between changeover of standard and sample inlet

For $\delta^{18}\text{O}$, a correction factor of 1.022 was applied to all samples due to the memory effect in the mass spectrometer. A possible memory can be checked easily by changing the idle time before measuring a gas after changeover.

Fig. 3.5 displays the memory (in %) vs. idle time of between 10 and 200 sec for CO_2 at an inlet rate of $3 \cdot 10^{-14}$ molecules per sec. The raw data have to be corrected for the double of this "mixing-effect", because memory occurs between sample and standard, and also *vice versa* between standard and sample. In our case for an idle time of 30 sec, a memory of 2.2% was observed. The memory is very constant and for V-SMOW-SLAP, a $\delta^{18}\text{O}$ of -55.5% has been analysed several times after correction. The new generation of instrumentation has a considerably lower memory (FINNIGAN-MAT, pers. comm.).

3.5 Equilibration technique and small sample sizes

During equilibration between water and hydrogen, the isotopic composition of both phases, liquid water and hydrogen gas, are altered. Therefore, the isotope shift of the water during this reaction has to be calculated in order to get an information on the original D/H-ratio of the liquid. If ample liquid is available, the molar ratio of the two phases $[\text{H}_2\text{O}]/[\text{H}_2]$ is higher than 0.998 (for 5 ml H_2O and 7 ml H_2) and the isotopic composition of hydrogen in the liquid phase does not change significantly during equilibration. A balance calculation is therefore not necessary. In some environmental and medical applications, only a small amount of water is available. Therefore, the equilibration technique was checked for small sample sizes.

Aliquots of 5, 1, 0.5, 0.25, 0.1 and 0.05 ml of an Antarctic water sample were analysed for their hydrogen isotope compositions (see Fig. 3.6 and Tab. 3.2). The weight or the volume of the water sample has to be determined accurately. We have used 7 ml of H_2 gas for equilibration. The initial and the final isotopic composition of the gases were determined and a mass balance calculation for the exchange reaction was performed as follows (see also Scrimgeour *et al.*, 1993). The D/H-ratio of the water to be analysed is:

$$\delta D (H_2O_{corr.}) = \delta D (H_2O_{meas.}) + \{ [H_2]/[H_2O] * \delta D (H_2) \} * f (H_2-H_2O),$$

where $\delta D (H_2O_{meas.})$ is the raw delta between hydrogen gas equilibrated with the water sample and hydrogen equilibrated with the reference water (V-SMOW), $[H_2]/[H_2O]$ is the molar ratio of these phases, $f (H_2-H_2O)$ the isotopic fractionation of the D/H-ratio between these substances (at 18°C, $f = 0.2720$; Friedman & O'Neil, 1977) and $\delta D (H_2)$ is the isotopic shift of the hydrogen gas during equilibration.

Tab. 3.2: δD values for small sample sizes of between 0.05 and 5 ml for an Antarctic water

sample	sample (ml)	H ₂ (ml)	$\delta D (H_2O_{meas.})$ (‰)	calculated correction	$\delta D (H_2O_{corr.})$ (‰)
Antarctic water	0.05	7	-295.0	-9.1	-304.1
	0.1	7	-300.3	-4.6	-304.9
	0.25	7	-302.4	-1.9	-304.2
	0.5	7	-303.5	-0.9	-304.4
	1.0	7	-304.2	-0.5	-304.7
	5.0	7	-304.4	-0.1	-304.5

In the case of the equilibration line used in this study, the correction is:

$$\delta D (H_2O_{corr.}) = \delta D (H_2O_{meas.}) + 0.00022 * \delta D (H_2) * a/b,$$

where a = ml (hydrogen gas, STP) and b = ml water (liquid).

The original composition of the hydrogen can be analysed by the same line filling one of the bottles only with hydrogen and no catalyst. In Fig. 3.6, results for the equilibration of water samples with the same isotopic composition of between 50 µl and 5 ml are displayed. These waters have been equilibrated with a hydrogen gas enriched in its D/H-ratio by 304.2 ‰ in comparison to the

equilibrated hydrogen. Filled dots represent the measured values, open dots the corrected values.

Thielecke *et al.* (1998) recently published an algorithm for D/H isotope ratios of small sample volumes. The main difference between Thielecke *et al.* (1998) and our approach is the fact that they did not consider the isotope fractionation factor for their balance correction.

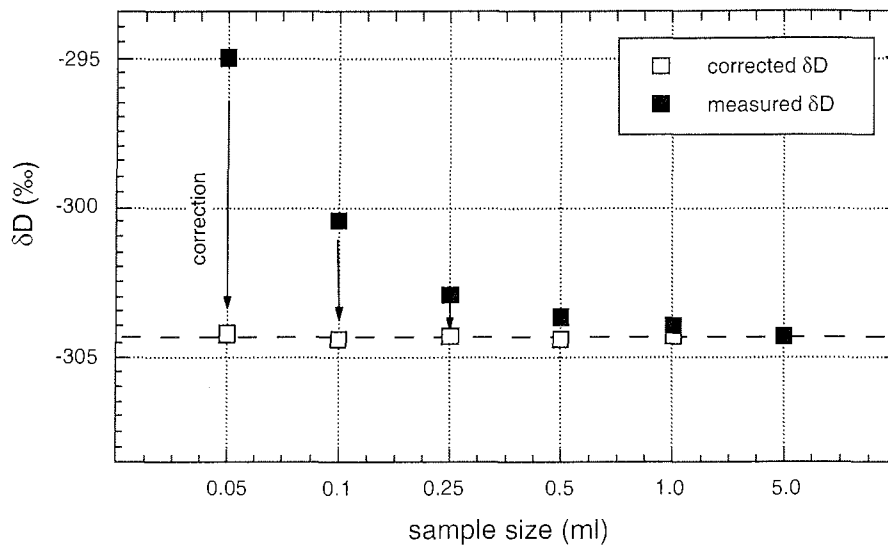


Fig. 3.6: Equilibration technique applied to small sample sizes

Since at 18°C the water is enriched in deuterium (fractionation factor near 4), normally deuterium is transferred into the water phase. It is recommended to use a hydrogen gas for the equilibration with a deuterium content of one fourth of the D/H-ratio of the water to be analysed (close to equilibrium). Hydrogen of this isotopic composition can be purchased from Messer-Griesheim, Duisburg or it can be produced by a small appendix in the equilibration line. Depending on the total isotope shift of the gases, a correction of the δ -values has to be applied for sample sizes smaller than 1 ml, corresponding to a molar ratio $[H_2]/[H_2O]$ of smaller than 0.994. The correction is smaller for hydrogen than for oxygen due to the low deuterium content of the equilibrated gas.

Publications

The equilibration of the oxygen isotopes ^{18}O and ^{16}O between H_2O and CO_2 in a shaking water bath at 18°C is completed after more than 24 h for small amounts of water down to 0.05 ml.

Tab. 3.3: Small sample sizes and large differences in δD and $\delta^{18}\text{O}$ values

sample	sample (mg)	H_2 (ml)	δD ($\text{H}_2\text{O}_{\text{meas.}}$) (‰)	δD ($\text{H}_2\text{O}_{\text{corr.}}$) (‰)	CO_2 (ml)	Δ ($^{18}\text{O}_{\text{meas.}}$) (‰)	Δ ($^{18}\text{O}-\text{H}_2\text{O}_{\text{true}}$) (‰)
water 1	1.05	7.2	43.4	43.2	7.3	13.07	13.32
	0.55	7.2	43.7	43.4	7.3	12.86	13.33
	0.37	7.2	44.3	43.8	7.3	12.66	13.36
water 2	0.94	7.2	-49.2	-49.5	7.3	-7.12	-7.10
	0.67	7.2	-49.1	-49.6	7.3	-7.18	-7.16
	0.27	7.2	-48.6	-49.8	7.3	-7.00	-6.94
water 3	0.96	7.2	-71.1	-71.5	7.3	-7.16	-7.14
	0.53	7.2	-70.6	-71.3	7.3	-7.05	-7.02
	0.25	7.2	-69.6	-71.0	7.3	-7.06	-6.99
water 4	0.97	7.2	172.4	172.4	7.3	39.66	40.27
	0.51	7.2	173.4	173.4	7.3	39.33	40.48
	0.37	7.2	173.6	173.6	7.3	38.95	40.52
	0.42	7.2	173.9	173.8	7.3	38.97	40.35
water 5	1.13	7.2	693.2	692.5	7.3	153.51	155.26
	0.51	7.2	692.6	691.0	7.3	151.41	155.24
	0.26	7.2	693.2	690.1	7.3	148.32	155.69
	0.19	7.2	694.0	689.7	7.3	145.08	154.96

Since at equilibrium the fractionation factor between CO_2 and H_2O is near unity (at 18°C , $f(\text{CO}_2-\text{H}_2\text{O}) = 1.0425$; Friedman & O'Neil, 1977) and the molar ratio of oxygen between CO_2 and H_2O is 2, the balance correction for the $^{18}\text{O}/^{16}\text{O}$ ratio is higher by a factor of 8 compared to hydrogen.

$$\Delta (^{18}\text{O}-\text{H}_2\text{O}_{\text{true}}) = \Delta (^{18}\text{O}_{\text{meas.}}) + 2 \cdot \left\{ \frac{[\text{CO}_2]}{[\text{H}_2\text{O}]} \right\} \cdot \Delta (^{18}\text{O}-\text{CO}_2) \cdot f(\text{CO}_2-\text{H}_2\text{O}),$$

where $\Delta(^{18}\text{O}_{\text{meas.}})$ is $\delta^{18}\text{O}(\text{CO}_2_{\text{sample}}) - \delta^{18}\text{O}(\text{CO}_2_{\text{standard}})$, $[\text{CO}_2]/[\text{H}_2\text{O}]$ the molar ratio of these phases and $\Delta(^{18}\text{O}-\text{CO}_2)$ is the isotopic shift of the CO_2 towards equilibration.

The equations for small volumes have been checked with water and urine samples of between 1.13 g and 0.19 g (supplied by Dr. E. Forsum, Karolinska Hospital, Stockholm). The δD and $\delta^{18}\text{O}$ values of the H_2 and CO_2 gas used for equilibration are +152‰ and -8.43‰ on the V-SMOW scale. Five liquids were analysed for large differences in $\delta^{18}\text{O}$ and δD values of up to 150 ‰ and 700‰, respectively, confirming the suitable application of the algorithms (see Tab. 3.3). After the correction, the δ -values for the D/H-ratio did not differ by more than 1.5‰ and for the $^{18}\text{O}/^{16}\text{O}$ ratio by more than 0.25 ‰ from the values analysed with 5 ml of liquid. The equilibration time for oxygen however had to be extended to more than 24 hours for these samples sizes. We have not observed any isotopic shifts of small water samples during the analytical procedure due to partial evaporation.

3.6 Sampling strategy for ground ice

The ground ice, defined as all types of ice contained in frozen or freezing ground (International Permafrost Association, 1998), is fed by meteoric water sources, and therefore can be studied as paleoclimate archive using hydrogen and oxygen isotope methods (Vaikmäe, 1989), similar to those in glaciers and ice caps. In the permafrost sequences studied at the Bykovsky Peninsula, two types of ground ice are found: ice wedges and segregated ice. The most promising archives for paleoclimate reconstruction are syngenetic ice wedges, which may reach widths of 5 m and heights of 40 m or more. Ice wedges are formed principally by frost cracking in the upper part of permafrost due to very cold winter temperatures and a thin snow cover with low heat insulation. During annual snow melt in spring, meltwater of previous years' winter precipitation penetrates into the frost cracks, in general in the middle of the ice wedge, and freezes immediately due to the low permafrost temperatures (at Bykovsky Peninsula presently ca. -10°C). Thus, the stable isotope composition of the ice

wedges reflects the mean annual winter temperature (Vaikmäe, 1991). Isotope fractionation during the fast freezing process can be neglected (MacKay, 1983). Repeated annual freezing and thawing leads to a succession of vertical ice veinlets. As a consequence of this process, in the ideal case, ice wedges get continuously older from the middle towards the margins. Syngenetic ice wedges also grow vertically, because they are formed in areas with sediment accumulation. Therefore, sampling was performed both in vertical and in horizontal directions (see Fig. 3.7).

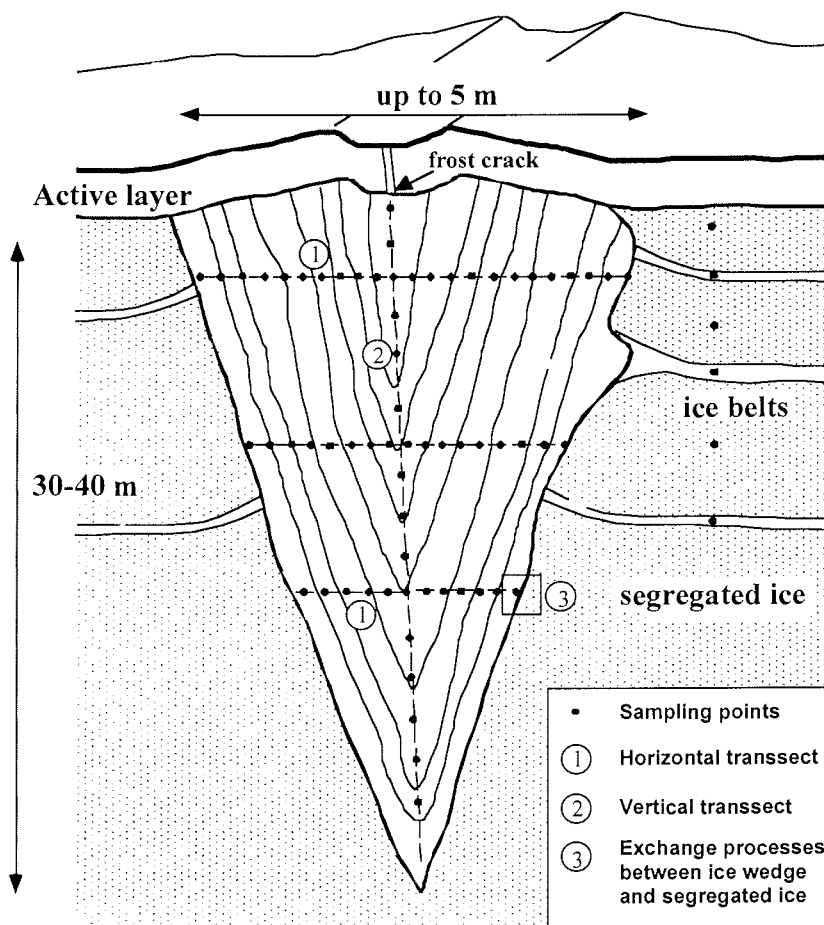


Fig. 3.7: Sampling strategy for ground ice (ice wedges and segregated ice)

We have observed single veinlets with widths of between 1 and 4 mm. Thus, the sampling resolution (10 cm intervals) in our studies corresponds probably to

time intervals of less than 100 years between two horizontal samples assuming frost cracking as an annual process. In order to verify the working hypothesis – one ice vein represents one year – we also have sampled along one vertical striking annual veinlet. Since for future analyses of ice wedges, an annual sampling resolution with limited sample volume is desired, we have extended the equilibration technique to water sample sizes of between 0.05 and 5 ml. In addition, the contact zone between ice and sediment was sampled carefully for the identification of exchange processes between ice wedge and frozen sediment.

Despite fractionation processes, which may occur during freezing and despite the participation of different water sources in its formation, segregated ice may also be used for paleoclimatic studies. This subject will be treated elsewhere. The ground ice was sampled using an ice screw or a chain saw, and was thawed on site. 30 ml of meltwater was collected in plastic bottles for stable isotope analysis.

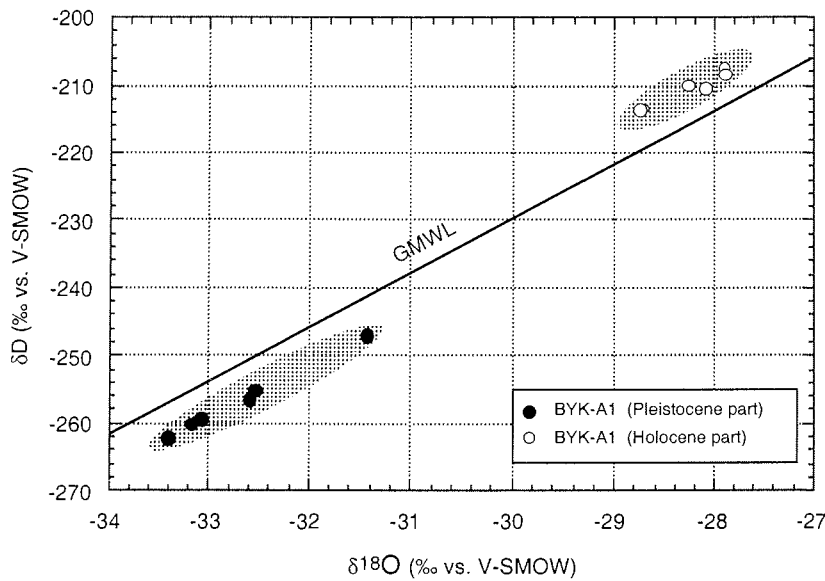


Fig. 3.8: First isotopic data of two Siberian ice wedges from the Bykovsky Peninsula. One ice wedge of Holocene age penetrates into a Late Pleistocene ice wedge

3.7 First results

In Fig. 3.8, first isotopic data are presented for two Siberian ice wedges of the Bykovsky Peninsula. One Holocene ice wedge penetrates into a Late Pleistocene ice wedge of the Ice Complex. In the $\delta^{18}\text{O}$ - δD diagram, we can clearly identify both generations of ice wedges by means of their absolute δ values showing lighter isotope ratios for the Pleistocene part and heavier isotope ratios for the Holocene part. This presumably reflects lower winter temperatures for the Late Pleistocene compared to the Holocene. Additionally, the position relative to the Global Meteoric Water Line changes towards the Holocene. This increase of the deuterium excess may probably be attributed to a change in the source of the precipitation. These first results show the potential of ground ice for the paleoclimate reconstruction in non-glaciated regions, which cover extent areas in Northern Siberia. Results of stable isotope measurements for ground ice samples obtained during field campaigns in 1998 and 1999 will be published in detail elsewhere.

3.8 Conclusions

The equilibration technique allows a sufficiently high number of isotopic analyses of approximately 24 samples per day for both δD and $\delta^{18}\text{O}$. The Delta-S mass spectrometer at the Alfred Wegener Institute in Potsdam was calibrated accurately in June, 1999. Its analytical precision is excellent, especially for isotopically light samples such as ground ice as shown by the new laboratory standard NGT1. The equilibration technique was checked for small sample sizes in order to extend the method and to enable a higher, possibly annual sampling resolution for ice wedges. A balance correction has to be applied to water samples smaller than 1 ml. Ground ice and especially ice wedges are promising paleoclimate archives. First results of hydrogen and oxygen isotope measurements on ice wedges indicate a shift towards warmer winter temperatures as well as a change in the source of the precipitation between Late Pleistocene and Holocene. These first results indicate the high potential of ground ice for paleoclimate studies.

4. PALEOCLIMATE STUDIES ON BYKOVSKY PENINSULA, NORTH SIBERIA - HYDROGEN AND OXYGEN ISOTOPES IN GROUND ICE

Hanno Meyer, Alexander Dereviagin, Christine Siegert, Hans-W. Hubberten

Reprinted from **Polarforschung** 70, p. 37-51, 2000 (erschienen 2002),
Copyright © 2002 with permission from Polarforschung.

4.1 Abstract

In wide areas of Northern Siberia, glaciers have been absent since the Late Pleistocene. Therefore, ground ice and especially ice wedges are used as archives for paleoclimatic studies. In the present study, carried out on the Bykovsky Peninsula, eastern Lena Delta, we were able to distinguish ice wedges of different genetic units by means of oxygen and hydrogen isotopes. The results obtained by this study on the Ice Complex, a peculiar periglacial phenomenon, allowed the reconstruction of the climate history with a subdivision of a period of very cold winters (60-55 ka), followed by a long stable period of cold winter temperatures (50-24 ka). Between 20 ka and 11 ka, climate warming is indicated in stable isotope compositions, most probably after the Late Glacial Maximum. At that time, a change of the marine source of the precipitation from a more humid source to the present North Atlantic source region was assumed. For the Ice Complex, a continuous age-height relationship was established, indicating syngenetic vertical ice wedge growth and sediment accumulation rates of 0.7 m/ky. During the Holocene optimum, ice wedge growth was probably limited due to the extensive formation of lacustrine environments. Holocene ice wedges in thermokarst depressions (alases) and thermo-erosional valleys (logs) were formed after climate deterioration from about 4.5 ka until the present. Winter temperatures were warmer at this time as compared to the cooler Pleistocene. Migration of bound water between ice wedges and segregated ice may have altered the isotopic composition of old ice

wedges. The presence of ice wedges as diagnostic features for permafrost conditions since 60 ka, implies that a large glacier extending over the Laptev Sea shelf did not exist. For the remote non-glaciated areas of Northern Siberia, ice wedges were established as a powerful climate archive.

4.2 Introduction

Hydrogen and oxygen isotopes are well known as useful tools for paleoclimatic studies in ice bodies, especially for paleotemperature reconstruction and for the identification of the precipitation source (Merlivat & Jouzel, 1979). During the last 30 years, many efforts have been made in isotopic analysis of the ice caps of Greenland and Antarctica in order to provide information about climate changes through time (e. g. Johnsen *et al.*, 1972; Oeschger, 1985; Petit *et al.*, 1999). In most parts of the Eurasian Arctic, glacier ice cores are not available and therefore, other climatic archives have to be considered for paleoclimatic reconstruction. This study is included in the German-Russian scientific co-operation project "System Laptev Sea 2000" as a part of the multidisciplinary research program "Paleoclimate signals in ice-rich permafrost". The main goals of the research program are the reconstruction of the paleoclimatic and paleoenvironmental conditions in ice-rich permafrost areas of Northern Siberia.

On the Bykovsky Peninsula, 50 km SE of the Lena Delta, NE Siberia, huge polygonal ice wedge systems within very ice-rich sediments, the so-called "Ice Complex" were analysed. The Ice Complex is widely distributed in Northern Siberia (Romanovskii, 1985), especially in the coastal lowlands and along rivers like Lena, Yana or Indigirka. In Northern Canada, an equivalent of the Ice Complex is described for a few limited areas of the MacKenzie and Yukon river basins (French, 1996). The Ice Complex is a special syncryogenic feature formed under severe climatic conditions, and it is a clue for non-glaciated areas. In these areas, precipitation is bound in ground ice instead of glacier ice.

Ground ice, defined as all types of ice contained in frozen or freezing ground (International Permafrost Association, 1998), is fed by meteoric water sources. Therefore, ground ice can be studied as a paleoclimatic archive using stable

isotope methods (MacKay, 1983; Vaikmäe, 1989; Vaikmäe, 1991; Vasil'chuk, 1991) similar to that in glaciers and ice caps. Oxygen isotope data of ground ice are commonly also used for the distinction of genetically different types of (ground) ice (Vaikmäe, 1991), for a stratigraphic subdivision of permafrost (Arkhangelov *et al.*, 1986) or for the identification of thaw unconformities (Burn *et al.*, 1986). Our studies focus on a combination of H and O isotopes, which extends the possibility to understand the processes leading to ground ice formation considerably. The application of hydrogen and oxygen isotopes to ground ice is used for a stratigraphic subdivision of the Ice Complex and for a reconstruction of the paleoclimatic variations for the last 60 ka.

4.3 The working area

The Bykovsky Peninsula is situated approximately 50 km SE of the Lena Delta, Northern Siberia, between 71°40' - 71°80' N and 129°00' - 129°30' E (Fig. 4.1). The study area is part of the coastal lowlands of the Laptev Sea region with continuous permafrost up to 500-600 m in thickness (Yershov, 1989). The highest areas of the Bykovsky Peninsula reach about 40 m a.s.l. and are occupied by the Ice Complex. According to radiocarbon ages, its formation started about 60 ka BP (Schirrneister *et al.*, 2002a).

The genesis of the Ice Complex is still a matter of debate. Some authors explain the origin of the Ice Complex as part of a former alluvial plain (Slagoda, 1993), as fluvial (Nagaoka, 1994), others as cryogenic-eolian (Tomirdiaro *et al.*, 1984), as linked to nival processes of snow patches (Kunitsky, 1989), formed in ice-dammed lakes in front of shelf glaciers (Grosswald, 1998) or as polygenetic (Sher *et al.*, 1987).

The present climatic situation of the Bykovsky Peninsula can be drawn from the closest meteorological station in Tiksi (71°35'N 128°55'E; NOAA data archive). The mean annual precipitation and temperature calculated for a 7-year period (1994 to 2000), are 400 mm and -12.2°C, respectively. Additionally, NOAA provides mean annual precipitation data from 1932 to 1988 indicating a much lower precipitation of approximately 191 mm/year. Thus, the considered 7-year period may have been particularly moist.

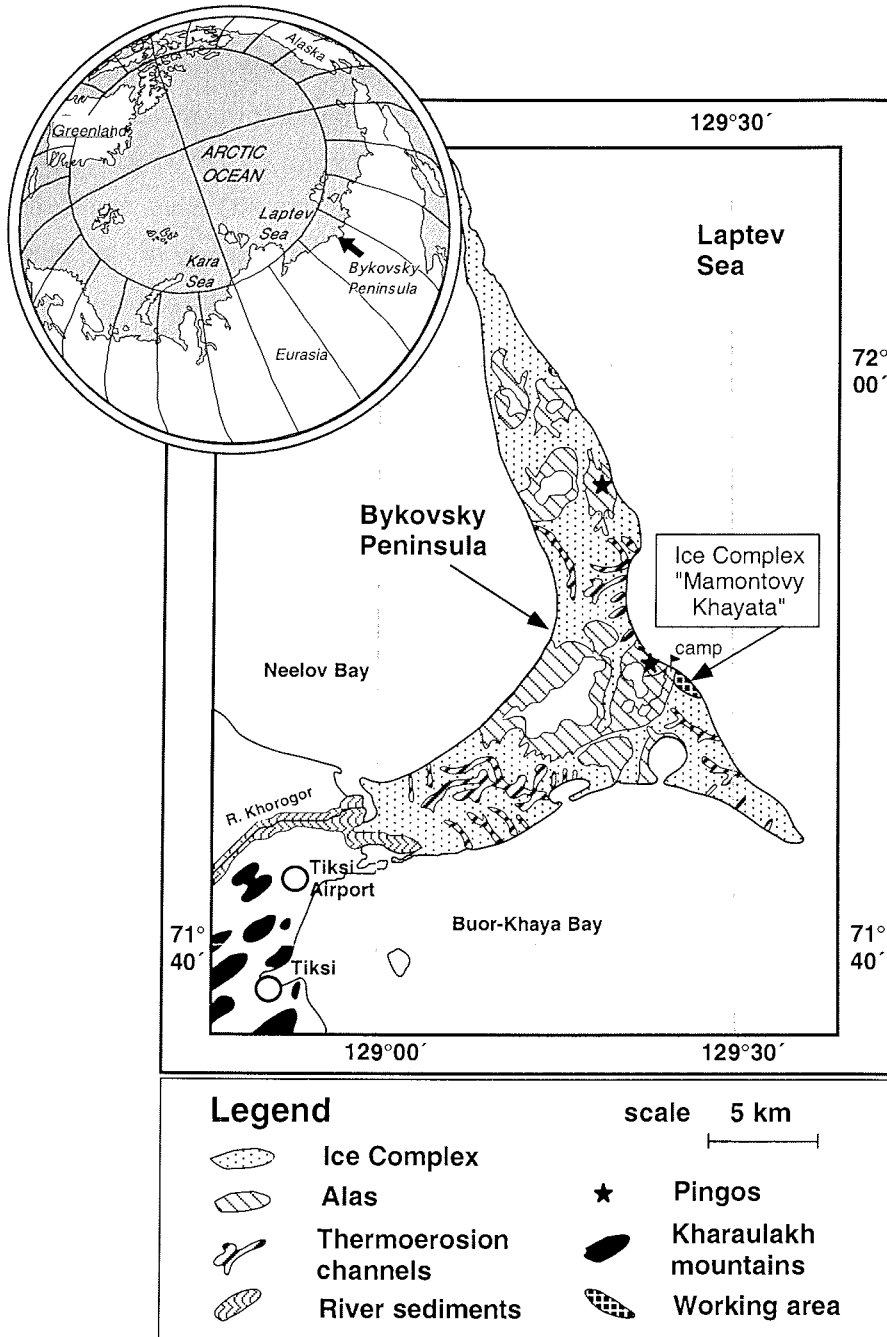


Fig. 4.1: Schematic map and geomorphological situation of the Bykovsky Peninsula.

The main period of precipitation is between June and September, with more than 60% of the annual volume. Severe winters and short cold summers are typical for the region. The coldest month is January (mean temperature -31.3°C), the warmest month is July (mean temperature 7.8°C). Mean daily temperatures as low as -42.0°C and as high as 18.0°C were measured, pointing to a highly continental climate despite of the proximity of the Laptev Sea. The study area belongs to the Northern Tundra (Atlas Arktiki, 1985).

Vast areas of the Bykovsky Peninsula are covered by the Ice Complex, which is subject to thermo-abrasion at the Laptev Sea coast and to different thermo-erosional and thermokarst processes (Fig. 4.1). Thermokarst depressions (or alases) are frequent geomorphologic features and some still contain residual thermokarst lakes, usually less than 2 m deep. The Ice Complex on the Bykovsky Peninsula is subject to thermo-erosion by small streams (or logs), forming characteristic steep gullies as well as wide and shallow valleys. A single, 28 m high pingo was observed in a large alas (Fig. 4.2).

4.4 The outcrop

The Laptev Sea coast of Bykovsky Peninsula is characterised by steep cliffs and wide shallow terraces containing numerous thermokarst mounds (or baydzerakhs). The main part of the field work was carried out at a 1.5 km long and 40 m high coastal outcrop, called „Mamontovy Khayata“ (Mammoth mountain) located at the east coast of the peninsula (Fig. 4.3).

The outcrop is subdivided into three very ice-rich cryolithogenic facies with different types of ground ice and sediment: a 40 m high vertical profile of the Ice Complex and two younger genetic units, alas and log. All facies show ice wedge growth and fine dispersed segregated ice, and are covered by a 0.2-0.5 m thick active layer. The oldest genetic unit is the Ice Complex. It is characterised by relatively uniform loess-like silty sediments and a belt-like cryogenic structure. The alternation of massive ice belts and sediment layers with a lens-like reticulated cryogenic structure both turned upward near ice wedges point to syngenetic freezing. The ice wedges may reach widths of 5 m and heights of more than 40 m and the ice wedge tips are not found in the outcrop.

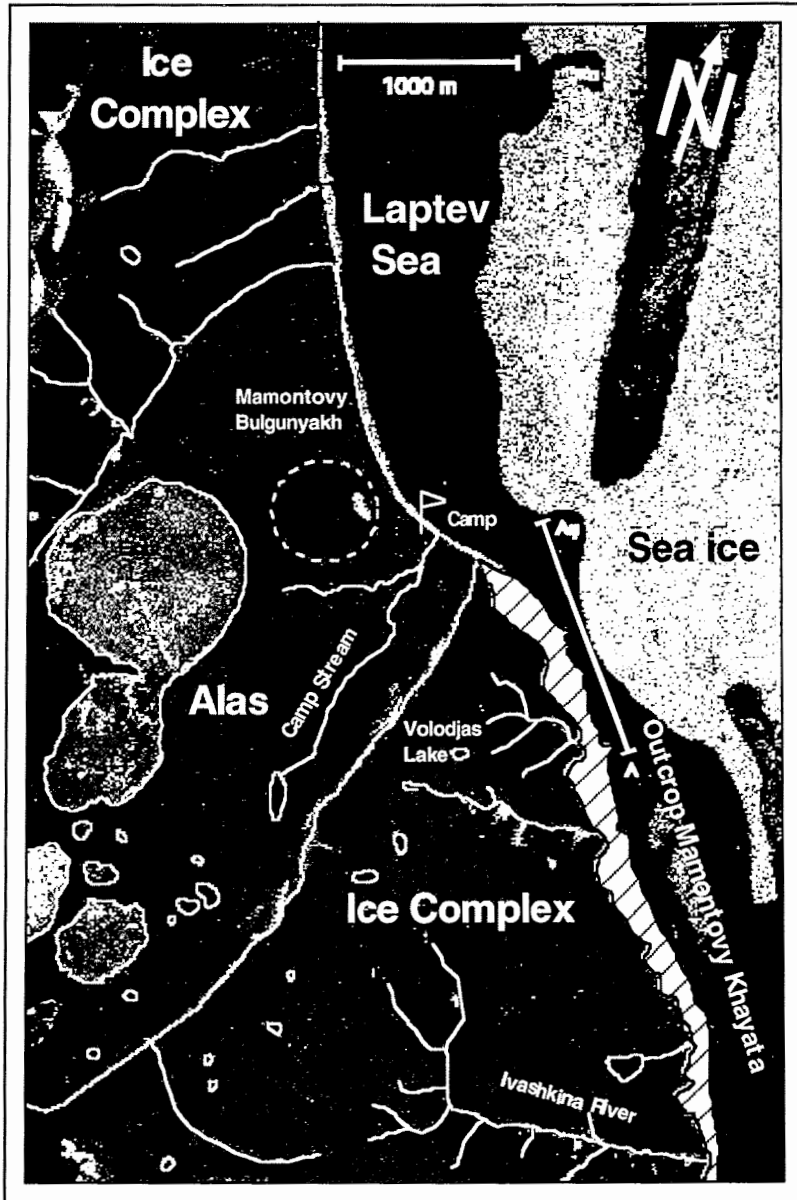


Fig. 4.2: Air photograph of the working area at the east coast of the Bykovsky Peninsula

Dirty, grey-coloured ice wedges are characteristic for the Ice Complex. In the uppermost part of the outcrop (Fig. 4.3), a few milky white ice wedges (parts of MKh-4.6) were observed, which reflects a higher content of gas bubbles. The total volumetric ice content in the Ice Complex may exceed 80%. Organic material is well-preserved and composed of autochthonous peat, insect and plant macrofossils and bones of mammals such as mammoth, horses, bison and rodents.

Schirromeister *et al.* (2002a) subdivided the evolution of the Ice Complex into three stages: a lower (0-10 m a.s.l.), a middle (10-25 m a.s.l.) and an upper horizon (25-39 m a.s.l.). The middle horizon (50-28 ka) is characterised by up to 15 peaty soil layers, whereas the lower (60-50 ka) and upper (25-12 ka) horizons have lower contents of organic material and a more uniform composition.

In the field, two younger facies (likely of Holocene age) discordantly overlying the Ice Complex could be distinguished sedimentologically and by different ice wedge generations. The alas is located in the NW of the outcrop and shaped by a polygonal landscape with numerous low-centre polygons (Fig. 4.2). Medium-grained sands are covered by peat layers up to 1 m in thickness. Ice wedge formation began after progressive freeze-back of the unfrozen zone (talik) below a thermokarst lake (French, 1996). Alas ice wedges are up to 3.6 m wide, more than 5 m high and extend beneath the sea level. Log deposits overlie the Ice Complex in the SE and are characterised by fine-grained sands partly covered by peat. Log ice wedges are smaller in width (maximum 1 m) and height (maximum 3.5 m). All ice wedges formed in environments younger than the Ice Complex are characterised by a milky white appearance. In some parts of the outcrop, we observed ice veins penetrating the active layer, which is subject to annual freezing and thawing. This suggests active ice wedge growth in the Holocene genetic units alas and log.

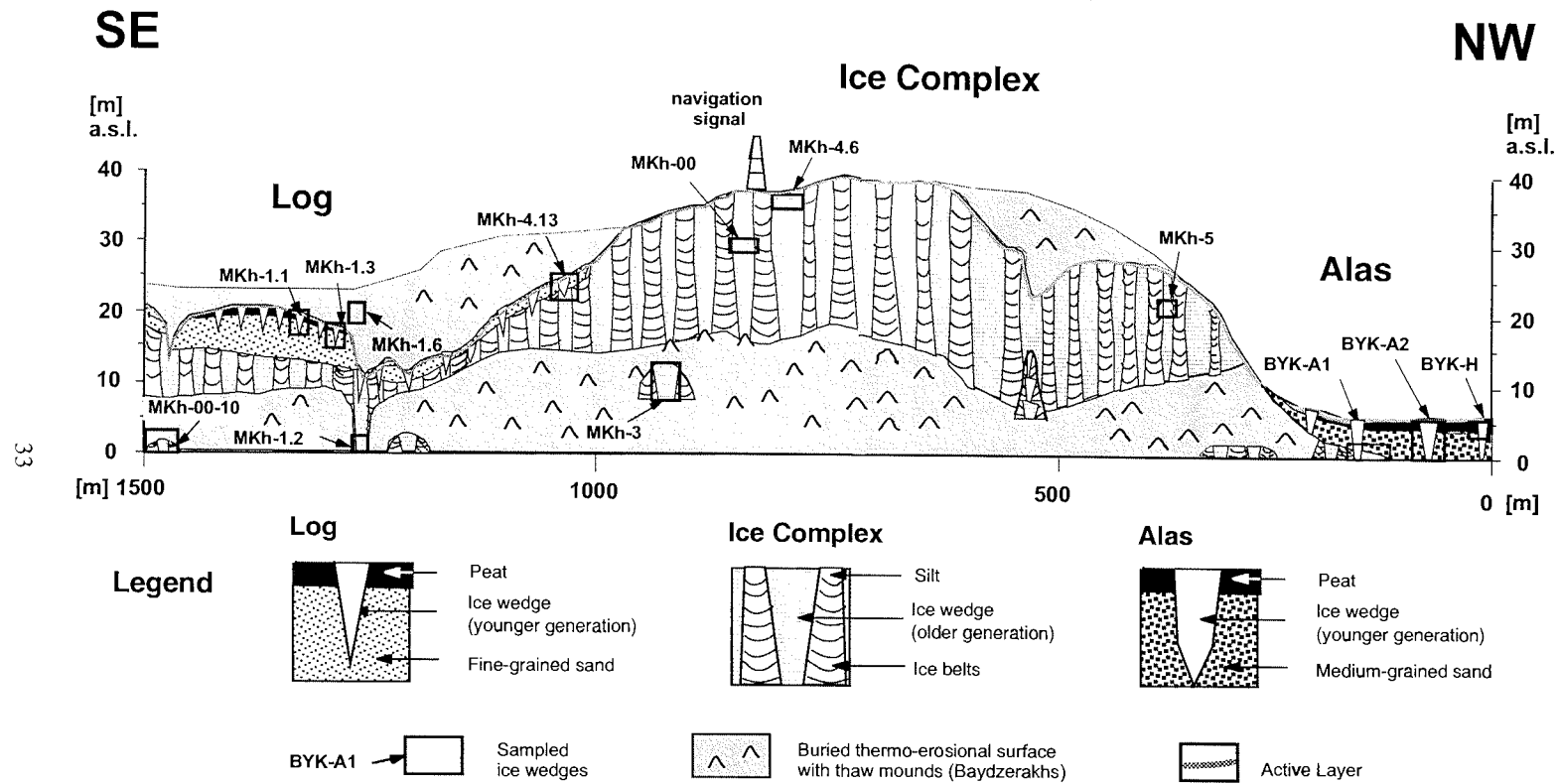


Fig. 4.3: Schematic profile of the outcrop "Mamontovy Khayata" (Mammoth mountain), east coast of Bykovsky Peninsula: Cryolithogenic units and the respective sampling locations for ice wedges.

4.5 Sampling strategy

In the studied permafrost sequences of the Bykovsky Peninsula, mainly two types of ground ice were found: ice wedges and segregated ice. Additionally, pingo ice occurs in the alas. The most promising archives for paleoclimatic reconstructions are ice wedges, which are formed principally by frost cracking in the upper part of permafrost due to rapid cooling at very low winter temperatures (Lachenbruch, 1962). During snow melt in spring, meltwater from the previous years' winter precipitation penetrates into the frost cracks, preferentially near the centre of the ice wedge and often at the same place (MacKay, 1974). The meltwater freezes immediately, due to the low permafrost temperatures (on the Bykovsky Peninsula presently ca. -10°C). Repeated annual freezing leads to a succession of vertical veinlets and finally to the formation of an ice wedge. As a consequence of this process, in the ideal case, ice wedges get continuously older from the middle towards the margins. The ice wedges, which occur in the studied Ice Complex, also grew upward with the sediment accumulation. Therefore, sampling was performed both in vertical and in horizontal directions (Fig. 3.7). In addition, the contact zone between the ice wedge and the sediment was sampled carefully to identify possible exchange processes between the ice wedge and the frozen sediment.

Segregated ice can also be used for paleoclimatic studies despite fractionation processes, which may occur during freezing and despite the participation of different water sources in its formation. Sediment accumulation or climatic cooling both result in an upward movement of the lower boundary of the active layer. The lower part of the former active layer is transferred into perennially frozen sediments with segregated ice. Mixing of water from atmospheric precipitation, surface waters and meltwater occurs in the active layer, resulting in a homogenisation of the isotopic composition, the variations of which are due to changes in climatic or facial conditions (Vaikmäe, 1989).

The ground ice was sampled using an ice screw or a chain saw, and was thawed on site. Samples for ^{14}C dating, hydrogen and oxygen isotopes, tritium and hydrochemical analyses were taken for the whole vertical profile of the Ice Complex and for the Holocene genetic units, alas and log. For stable isotope

and tritium analyses, meltwater was collected in 30 ml PE bottles, which were tightly closed to avoid evaporation (Meyer *et al.*, 1999).

4.6 Analytical procedure

The H and O isotope measurements were carried out with a Finnigan MAT Delta-S mass spectrometer with two equilibration units. Both, oxygen ($^{18}\text{O}/^{16}\text{O}$) and hydrogen (D/H) isotopes ratios were analysed for the same water sample using common equilibration techniques (Epstein & Mayeda, 1953). ^{17}O and H_3^+ corrections were carried out automatically. $^{18}\text{O}/^{16}\text{O}$ and D/H ratios are presented as $\delta^{18}\text{O}$ and δD . These δ values give the respective ‰-difference relative to the standard V-SMOW. The internal 1σ error is generally $<0.8\text{‰}$ for δD and $<0.1\text{‰}$ for $\delta^{18}\text{O}$, for all measurements (Meyer *et al.*, 2000). Tritium (^3H), as radioactive hydrogen isotope was used as an indicator for the "modern water contamination" in permafrost (Chizhov & Dereviagin, 1998) in order to check the validity of stable isotope analysis of ground ice. Tritium concentrations were determined at the Department of Radiochemistry, Moscow State University by a liquid-scintillation mass spectrometer Tricarb-1600 with an error of about 10%. Electrical conductivity was measured with a WTW instrument.

4.7 Geochronology

4.7.1 Age estimate of the Ice Complex

The ages of the sediments in the outcrop were estimated by conventional and Accelerator Mass Spectrometry (AMS) ^{14}C dating of plant remains (Schirrmeyer *et al.*, 2002a). Fig. 4.4 shows the continuous sedimentary evolution of the studied Ice Complex section between about 60 ka (at sea level) and 12.2 ka (at 37 m a.s.l.).

Tab. 4.1: New AMS ¹⁴C ages of organic material in ice wedges and in sediments enclosing ice wedges of the three genetic units Ice Complex, alas and log.

AMS dating of organic material close to ice wedges										
Lab. Number	sample	material	genetic unit	height (m, a.s.l.)	¹⁴ C age BP [a]	+	-	cal BP [a]	+2σ [a]	- 2σ [a]
KIA 11442	MKh-4.6-14C-3	peat	Active Layer above Ice Complex	37.0	300	30	30	313	471	288
KIA 6722	MKh-1.6-2	peat	peat covering log deposits	17.2	1080	35	35	969	1063	927
KIA 6723	MKh-1.6-3	peat	peat covering log deposits	17.4	1105	35	35	986	1167	931
KIA 8161	MKh-4.12-3a	peat inclusion, horizon 5	peat in log deposits	26.0	4455	35	35	5045	5295	4871
KIA 6720	MKh-4.6-1	peat, plant remains, wood	uppermost part of Ice Complex	36.6	8230	50	50	9212	9424	9027
KIA 11441	MKh-4.6-14C-2	peat	uppermost part of Ice Complex	36.5	10840	50	50	12902	13116	12641
KIA 6721	MKh-4.12-2a	peat	Ice Complex	24.1	24460	250	260	-	-	-
KIA 6727	MKh-3	peat inclusion	Ice Complex	10.0	45090	2770	2060	-	-	-
KIA 6730	MKh-1.2-14C-1	peat, wood residucs	Ice Complex	2.5	58400	4960	3040	-	-	-
AMS dating of organic material in ice wedges										
Lab. numbre	sample	material	genetic unit	height (m, a.s.l.)	age [a]	+	-	cal BP [a]	+	-
KIA 6743	BYK-A2-89a	plant remains (BYK A2)	alas ice wedge	4.5	1220	35	35	1171	1264	1008
KIA 6742	BYK-A2-I-58	plant remains (BYK A2)	alas ice wedge	2.5	2075	35	35	2027	2149	1927
KIA 6744	BYK-A2-Be8/9	plant remains (BYK A2)	alas ice wedge	2.7	2370	30	30	2352	2704	2334
KIA 6741	BYK-A2-I-2	plant remains (BYK A2)	alas ice wedge	2.5	3075	40	40	3285	3382	3082
KIA 6747	MKh-4.6-I-47	plant/wood remains (MKh-4.6)	uppermost part of Ice Complex	36.4	9390	60	60	10613	11041	10425
KIA 11457	MKh-4.6-I-25	plant remains (MKh-4.6)	uppermost part of Ice Complex	36.4	11180	100	100	13151	13758	12893
KIA 6746	MKh-5-1-11	plant/wood remains (MKh-5)	Ice Complex	19.8	26050	190	190	-	-	-
KIA 8168	MKh-3-mouse	lemming coprolith (MKh-3)	Ice Complex	10.0	41990	1050	930	-	-	-

In Tab. 4.1, new AMS ^{14}C ages of organic remains found in ice wedges and in sediments with direct contact to the sampled ice wedges are presented. All AMS ^{14}C age determinations were carried out in the Leibniz Laboratory in Kiel, Germany. Only leached residues were used. Since the abundance of organic material is quite low in the ice wedges, first direct AMS dating of micro-organic remains in the ice wedges was not published until recently (Vasil'chuk *et al.*, 2000). According to our experience bulk organic matter gets easily contaminated by younger material during sampling, whereas small leaves, twigs or lemming coprolithes proved to be less prone to contamination. To compare Pleistocene and Holocene samples, uncalibrated ^{14}C ages were used in Figs. 4.4 and 4.8. Additionally, samples younger than 24 ka were calibrated after INTCAL98 (Stuiver *et al.*, 1998) and given in Tab. 4.1.

In Fig. 4.4, a linear relationship between all conventional and AMS ^{14}C ages in the Ice Complex sediments and the heights of the samples in the outcrop is indicated. The AMS ^{14}C ages of organic remains in ice wedges (e. g. for ice wedge MKh-3) are in general slightly younger than those for the enclosing sediment. This is probably due to the fact that frost cracks always penetrate into slightly older sediment. A Scheffé test shows that the new ages in ice wedges and in the host sediments belong statistically to the same population. Mean values and variances do not differ significantly at a probability of $p = 0.05$. Therefore, a linear age-height relationship was established based on all samples available. Accordingly, continuous ice wedge growth occurring syngenetically to the sedimentation is assumed for the outcrop (Fig. 4.4).

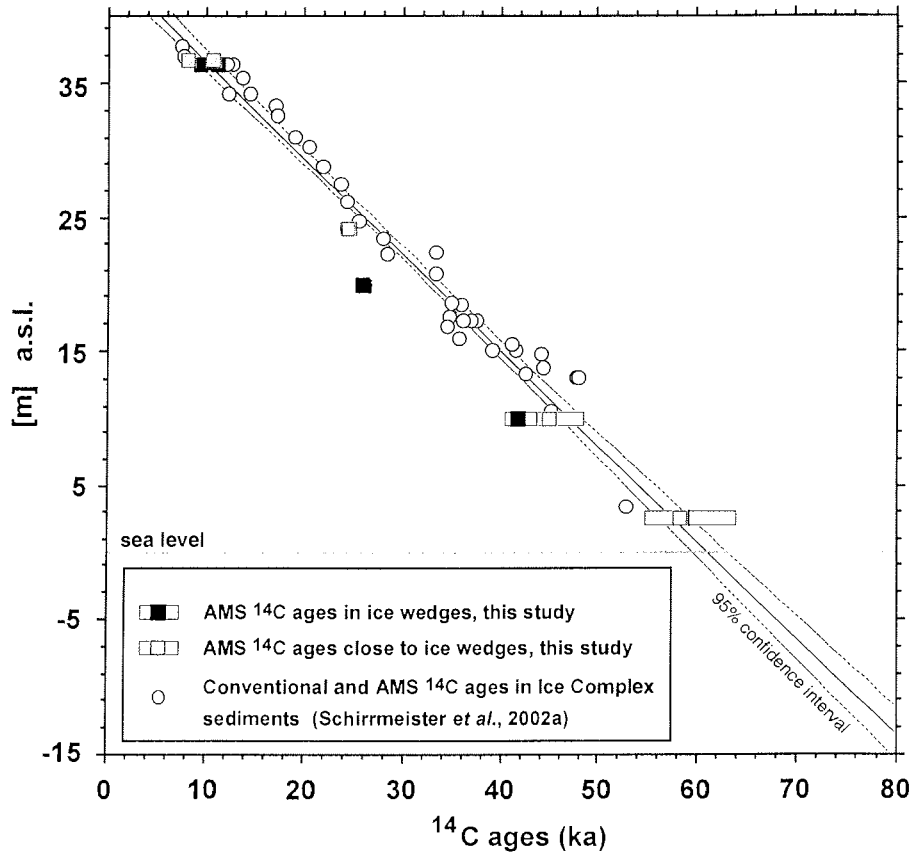


Fig. 4.4: New AMS ^{14}C ages of organic remains in ice wedges (black squares) and in the sediments in direct contact to the sampled ice wedges (grey squares) of the Ice Complex “Mamontovy Khayata”, with their respective error bars versus the height in the outcrop. White circles indicate conventional and AMS ^{14}C ages of organic material in the sediment sampled without relation to ice wedges, as published by Schirrmeister *et al.* (2002a). A Scheffé test has shown that ice wedge and sediment ages belong to the same population. Therefore, a linear correlation between ages and heights is given (straight line) based on all samples available including the 95% confidence interval (dashed lines).

The meaning of a continuous Ice Complex formation should not be overestimated because changes in sedimentation rates (Schirrmeister *et al.*, 2002a) and in vertical ice wedge growth can not be excluded. An approximate rate of Ice Complex evolution was assumed to be 0.7 m/ky. The age-height relationship for vertical Ice Complex and ice wedge growth is:

$$T = 59.9 - 1.33Z \quad (1)$$

where T denotes the age in ka and Z the height [m, a.s.l.]. The coefficient of determination ($R^2 = 0.97$) represents a large part of the variation. Vasil'chuk *et al.* (2000) calculated for Yamal a vertical ice wedge accumulation rate of 1.2-1.3 m/ky. This larger accumulation rate is probably caused by a higher sedimentation rate. Our equation was used: (1) to estimate the age of ice wedges at our study site, which had not been dated up to now (BYK-A1, MKh-00, MKh-00-10), in order to include them into the paleoclimatic reconstruction, and (2) to calculate the maximum age of the Bykovsky Ice Complex. Using equation (1), MKh-00 is 20 ky old, BYK-A1 59 ky and MKh-00-10 about 60 ky. Drilling of permafrost in the adjacent shelf near Bykovsky Peninsula has shown that the Ice Complex exists at 15 m below sea level (Grigoryev *et al.*, 1996; Romanovskii *et al.*, 2000). Assuming continuous Ice Complex growth for the whole period of its formation, Ice Complex ground ice and sediment on Bykovsky Peninsula could be as old as 80 ky.

MacKay (1992) reported that the frequency of ice wedge cracking was highly variable from 8% to 75%, for two nearby located sites on Garry Island, Canada between 1967 and 1987. Therefore, it is impossible to infer the age of an ice wedge by counting the annual ice veins. Nevertheless, it is possible to estimate ages. We observed single veinlets with mean widths of 2 to 2.5 mm, ranging between 1 and 4 mm. Thus, the sampling resolution (10 cm intervals) in our study corresponds to around 50, but certainly more than 25 and less than 100 cracking events between two horizontal samples. If we assume a frost cracking frequency of 75% (rather high; for Ice Complex growth, cracking must have occurred relatively often), a minimum of 1 ky, and an estimate of 2 ky are needed for the growth of a 3 m wide ice wedge.

For ice wedge MKh-4.6, an AMS ^{14}C age of 9.4 ka proves that ice wedge growth proceeded to the Early Holocene. This signifies that on this site, ice wedge growth continued after the end of Ice Complex sediment accumulation. An age of 11.2 ka in the same ice wedge shows that the growth of a horizontal transect of this ice wedge would take at least 1.8 ka.

4.7.2 Age estimate of the Holocene genetic units

The AMS ^{14}C dating was also carried out for the Holocene units, alas and log (Tab. 4.1). All AMS ages of alas ice wedges were dated "directly", whereas in log only organic matter in host sediments could be dated. For alas and log, no age-height relationship could be established. Therefore, all Holocene ice wedges, which could not be dated directly by AMS or ^3H methods, were put into a "logical" order.

According to four AMS ages of organic remains, ice wedge BYK-A2 in the alas was formed in the interval from 3.1 ka to 1.2 ka, whereas the surrounding sediment is slightly older (Schirrmester *et al.*, 2002a). BYK-A1 and BYK-H have not been dated. However, BYK-A1 should be older than BYK-A2 because it was sampled at sea level, where the sediments are older and closer to the margin of the alas. BYK-H is located closer to the centre and was sampled at 5.1 m. Hence, it should be younger because it fell dry later. In the alas, active ice wedge growth was observed (Fig. 4.2).

Log sediments in the southern part of Mamontovy Khayata outcrop (MKh-4.13) were formed around 4.5 ka. The AMS data point to an age of the log-covering peat layer (MKh-1.6) of about 1 ka. Ice wedge growth should have started synchronous to or later than peat formation. Elevated tritium concentrations of ice veins (or "heads") in the lowest part of the still frozen active layer (MKh-1.6, MKh-1.3) prove ice wedge growth during the last 50 years (Dereviagin *et al.*, 2002). MKh-1.1 belongs to the same ice wedge generation under the peat layer and is probably slightly older, because no tritium was detected. The occurrence of Holocene ice wedges is proved from around 3.1 ka until today (Tab. 4.1). From the Holocene warm period (8 - 5 ka), no ice wedges could be dated. This could be by chance or due to a missing ice wedge growth at the sampled sites in that time interval. The existence of large thermokarst lakes during the Holocene warm period may have prevented frost cracking at the studied sites.

4.8 Results and discussion

On a global scale, the δD and $\delta^{18}O$ of fresh surface waters are correlated linearly in the “Global Meteoric Water Line” (GMWL). This relationship between δD and $\delta^{18}O$ is due to temperature-dependent fractionation at the phase transitions of water (evaporation, condensation, melting or freezing) in the hydrological cycle, and is defined as:

$$\delta D = 8\delta^{18}O + 10\text{‰ SMOW (Craig, 1961)} \quad (2)$$

The lowest $\delta^{18}O$ and δD values are attributed to the coldest temperatures. The ocean is the main source for atmospheric water vapour. The movement of an air mass from a moisture source towards higher latitude, altitude or distance to the sea progressively removes the heavy isotopes from the cloud. Dansgaard (1964) introduced the deuterium excess (d) giving the position relative to the GMWL in a δD - $\delta^{18}O$ diagram, defined as:

$$d = \delta D - 8\delta^{18}O \text{ (Dansgaard, 1964)} \quad (3)$$

d reflects the sensitivity of H and O isotopes to kinetic fractionation processes in the hydrological cycle. Being a function of the relative humidity, sea surface temperature and wind speed (Merlivat & Jouzel, 1979) in the moisture source region, d may be used for the identification of the source of precipitation.

4.8.1 Recent precipitation

In Fig. 4.5, the seasonal variation of recent precipitation is displayed in the $\delta^{18}O$ - δD diagram for rain water and snow patch samples of Bykovsky Peninsula. The scatter of precipitation data in the diagram reflects seasonal variations due to different condensation temperatures of water vapour out of the air mass.

Mean, maximum and minimum isotopic compositions for rain and snow can be drawn from Tab. 4.2. Samples of snow patches ($N = 9$) were taken during the field season in summer 1998 on Bykovsky Peninsula. Snow samples move

along the GMWL, with a slope of 8.0 and an intercept of 9.6 points to the oceans being the main source for winter precipitation. A slope of 8.0 has also been described by Boike (1997) for snow in the Levinson-Lessing Lake area, Taymyr Peninsula.

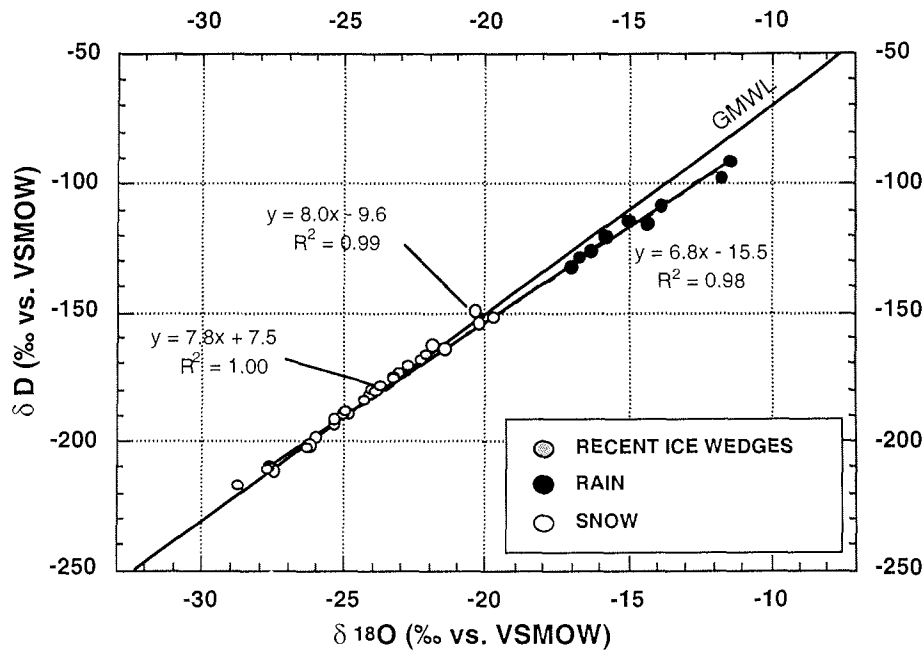


Fig. 4.5: $\delta^{18}\text{O}$ - δD diagram for samples from snow patches, rain and recent ice wedges collected in summer 1998 on Bykovsky Peninsula. GMWL is the Global Meteoric Water Line.

The combination of both studies reveals that sublimation, evaporation and melting of the snow did not lead to a significant change of d excess in the snow. Therefore, we can use these remnants of snow (already subject to melting) as our local source for ice wedge formation. Additionally, rain water ($N = 10$) was collected between 25 July and 17 August 1998. The samples are shifted from the GMWL towards a lower mean d excess of 2.7‰ and a smaller slope of 6.8. This enrichment in heavy isotopes is due to evaporation processes probably originating from surface waters or from the open Laptev Sea. Thus, winter and summer precipitation on Bykovsky Peninsula are of different origin, a

phenomenon also described for the Taymyr Peninsula (Boike, 1997). The similar pattern in the δD - $\delta^{18}O$ diagram of recent precipitation points to the same moisture source for both regions.

4.8.2 Stable isotopes in ice wedges

Melting of snow is generally accepted as the main source for recent ice wedge ice (e. g. MacKay, 1983, Vaikmäe, 1989). Accordingly, the oxygen isotope composition of ice wedges was correlated with mean annual winter temperatures (Vaikmäe, 1991, Vasil'chuk, 1992). For the Bykovsky Peninsula, snow has been identified as the main source for modern ice wedges by Dereviagin *et al.* (2002). For the interpretation of the ice wedge isotope data, the main area of interest is, which effects might influence $\delta^{18}O$ and δD in an ice wedge being is a possible sink for water in the hydrological cycle. Mainly three groups of processes leading to a distinct stable isotope value in an ice vein must be considered: (1) fractionation processes at phase transitions of water in (winter) precipitation and in frost cracks, (2) alteration of the isotopic signal in the ice wedge after its formation, (3) different sources and pathways of water vapour including mixing.

The isotopic composition of discrete snowfall events is influenced by various processes from the formation of an air mass moving from a moisture source to the deposition site and influenced by changes in the atmospheric circulation (Jouzel *et al.*, 1997). Additionally, the seasonality of precipitation events within one year must be taken into account. Two climatically identical years might give different $\delta^{18}O$ in ice veins, e. g. when in one year, the frost crack is mainly fed by colder November snow and in the other by warmer March snow. Changes in seasonality of precipitation therefore have a great impact on stable isotopes and related paleothermometry (Jouzel *et al.*, 1997). Evaporation, sublimation and melting of a snow mass can be assumed to have a small effect on isotopes in the working area because the snow sampled in summer 1998 still shows a slope of 8 in the $\delta^{18}O$ - δD diagram, and consequently has not been modified isotopically.

Tab. 4.2: Stable isotope ($\delta^{18}\text{O}$, δD and d excess) minimum, mean and maximum values, standard deviations (s. d.), as well as slopes and intercepts in the $\delta^{18}\text{O}$ - δD diagram for all ice wedges of three genetic units Ice Complex, alas and log.

Ice wedge	Remarks	N	height a.s.l. (m)	width (m)	$\delta^{18}\text{O}$ (‰) min.	$\delta^{18}\text{O}$ (‰) mean	$\delta^{18}\text{O}$ (‰) max.	$\delta^{18}\text{O}$ (‰) s.d.	δD (‰) min.	δD (‰) mean	δD (‰) max.	δD (‰) s. d.	d (‰) min.	d (‰) mean	d (‰) max.	d (‰) s. d.	slope	Inter- cept	R^2
LOG																			
MKh-1.1	complete ice wedge	5	17.0-16.5	0.5	-28.93	-27.79	-26.39	1.06	-216.8	-208.0	-197.4	8.0	13.7	14.3	15.0	0.5	7.58	2.7	0.99
MKh-1.3	complete ice wedge	10	17.5-16.9	0.8	-29.02	-26.27	-23.32	1.86	-217.3	-197.3	-173.8	14.7	9.9	12.8	14.8	1.3	7.86	9.1	0.99
MKh-1.6	complete ice wedge	5	20.0-19.4	0.5	-25.08	-23.64	-22.52	1.05	-189.2	-177.1	-168.5	8.6	11.3	12.1	13.4	0.9	8.12	14.8	0.99
MKh-4.13	Holocene part	19	23.9-22.5	0.8	-26.96	-25.79	-24.01	0.83	-206.0	-194.0	-179.8	6.7	8.8	12.3	13.9	1.1	7.99	12.0	0.97
ALAS																			
BYK-H	complete ice wedge	15	5.1	1.5	-29.07	-26.14	-24.14	1.50	-219.6	-197.7	-182.8	11.3	8.5	11.4	13.0	1.2	7.51	-1.3	0.99
BYK-A1 (Hol)	Holocene part	6	0.8	3.0	-28.72	-28.26	-27.89	0.38	-213.8	-210.6	-207.7	2.6	14.1	15.5	16.2	0.8	6.55	-25.6	0.94
BYK-A2	complete ice wedge	109	4.5-2.1	3.3	-30.16	-28.18	-23.73	1.07	-224.3	-210.9	-177.1	7.6	10.7	14.5	17.8	1.5	7.08	-11.5	0.98
BYK-A2	upper horizontal	36	4.5	3.6	-30.16	-27.95	-23.73	1.13	-224.3	-209.3	-177.1	8.2	11.3	14.3	17.0	1.6	7.19	-8.5	0.98
BYK-A2	lower horizontal	59	2.5	2.7	-30.09	-28.25	-24.44	1.11	-224.0	-211.4	-184.1	7.9	10.7	14.6	17.8	1.5	7.00	-13.6	0.98
BYK-A2	vertical transect	14	4.5-2.1	-	-29.38	-28.46	-27.23	0.53	-219.7	-212.9	-203.8	3.9	13.0	14.8	16.1	0.7	7.32	-4.5	0.97
ICE COMPLEX																			
MKh-4.6	complete ice wedge	50	37.2-36.2	3.0	-30.03	-25.76	-23.07	1.67	-232.6	-195.7	-174.5	13.9	7.5	10.4	12.6	1.4	8.31	18.3	0.99
MKh-00	complete ice wedge	35	30.0	3.5	-31.08	-29.52	-28.16	0.80	-243.9	-230.2	-217.7	7.8	1.9	6.0	9.1	1.8	9.53	51.3	0.97
MKh-4.13	Pleistocene part	36	22.5-21.5	3.5	-32.12	-31.17	-28.28	0.71	-253.5	-245.0	-221.8	5.8	3.2	4.4	5.7	0.6	8.24	11.9	0.99
MKh-5	horizontal transect	72	19.7-19.0	3.5	-31.89	-30.80	-29.25	0.61	-250.4	-241.3	-228.8	5.0	3.4	5.0	6.5	0.6	8.16	9.9	0.99
MKh-3	complete ice wedge	112	12.75-8.35	5.0	-32.27	-30.09	-24.97	1.86	-253.2	-237.3	-205.4	13.0	-5.6	3.3	6.5	2.2	6.96	-27.9	0.99
MKh-3	upper horizontal	48	11.1	5.0	-32.15	-30.41	-25.91	1.64	-253.1	-239.6	-207.2	11.9	0.0	3.7	5.8	1.5	7.28	-18.2	1.00
MKh-3	lower horizontal	21	9.1	3.1	-31.06	-29.74	-27.56	1.13	-244.4	-235.1	-219.9	8.2	0.0	2.7	4.5	1.3	7.22	-20.1	0.99
MKh-3	vertical transect	23	12.75-8.35	-	-32.27	-31.42	-30.32	0.58	-251.7	-246.2	-238.1	3.8	2.8	5.2	6.5	1.0	6.50	-42.0	0.98
MKh-1.2	complete ice wedge	49	3.0	4.5	-33.92	-31.56	-30.02	0.94	-267.5	-247.9	-232.3	8.1	2.7	4.6	7.9	1.0	8.54	21.7	0.99
MKh-1.2	horizontal transect	45	3.0	4.5	-33.92	-31.63	-30.02	0.95	-267.5	-248.5	-232.3	8.1	2.7	4.5	7.9	1.0	8.54	21.7	0.99
MKh-1.2	vertical transect	5	2.8-3.6	-	-30.81	-30.73	-30.47	0.15	-242.1	-240.9	-238.1	1.6	4.3	4.9	5.7	0.5	10.90	94.2	0.98
BYK-A1	Pleistocene part	6	0.8	2.0	-33.41	-32.71	-31.44	0.71	-262.2	-256.8	-247.2	5.3	4.1	4.9	5.4	0.6	7.50	-11.5	0.99
MKh-00-10	complete ice wedge	18	0.5	3.0	-32.53	-31.55	-30.53	0.52	-259.2	-251.7	-244.5	4.0	-0.4	0.7	2.1	0.8	7.45	-16.7	0.96
SEGREGATED ICE		66			-30.45	-23.42	-17.72	3.25	-231.7	-187.7	-134.8	24.9	-11.7	-0.4	15.6	7.8	7.33	-16.1	0.91
RECENT WATER/ICE																			
Rain water		10			-16.97	-14.80	-11.43	1.95	-132.6	-115.7	-91.4	13.4	-3.4	2.7	6.1	3.2	6.77	-15.5	0.98
Snow patches		9			-27.50	-23.19	-19.74	3.01	-211.2	-176.2	-149.8	24.3	6.2	9.3	13.4	2.2	8.01	9.6	0.99
Recent ice wcdges		22			-29.02	-24.86	-22.38	1.89	-217.3	-186.5	-167.1	14.8	9.9	12.4	14.8	1.0	7.80	7.5	1.00

Melting of the annual snow cover leads to the formation of one single elementary ice veinlet. This means a meteoric water line of snow is transferred into one point in the $\delta^{18}\text{O}$ - δD diagram. If we consider isotope fractionation for snow melting, the first melt water will have a lighter $\delta^{18}\text{O}$ and δD than the last. Additionally, mixing with water of different origin must be considered. At the time the snow starts melting, the active layer is still frozen and can therefore be ruled out as major source, but flooding may have an effect on ice wedges (especially at river and lake terraces).

The frequency of ice wedge cracking is highly variable (MacKay, 1992) and subject to seasonality. Cracking mainly tends to occur in winter between mid-January and mid-March (MacKay, 1974). For the growth of ice wedges, the existence of a thin snow cover is necessary, because of the insulating effect of the snow impeding frost cracking. When (melt) water enters frost cracks in spring, no fractionation takes place when the freezing process is faster than 2 mm/h, which is the critical value (Michel, 1982).

Possible processes for the alteration of the isotope signal in an ice wedge after its formation are diffusion of water vapour and water migration due to gradients in hydrochemical composition. These effects may best be studied at the interface between ice wedge and segregated ice, which are both fed by waters of different origin. Here, a gradient in isotopic composition and in hydrochemistry can be expected. In Figs. 4.6.1-4.6.3, the electrical conductivity, $\delta^{18}\text{O}$ and d are displayed for a 5 m long horizontal sampling transect across Pleistocene ice wedge MKh-3. The middle part of the ice wedge shows only slight variations in conductivity between 150 and 250 $\mu\text{S}/\text{cm}$. At the interface of the ice wedge and sediment, a higher conductivity of up to 530 $\mu\text{S}/\text{cm}$ was measured. The enclosing segregated ice is characterised by a much higher conductivity of up to 5500 $\mu\text{S}/\text{cm}$. For oxygen isotopes and d excess, a similar effect is observed. An isotopic composition of -22.5‰ in $\delta^{18}\text{O}$ and low d of -6‰ are measured close to the edges of the ice wedge, whereas the middle part shows $\delta^{18}\text{O}$ of -30‰ and d of up to 6‰ . Segregated ice has a low mean $\delta^{18}\text{O}$ of -23.4‰ and d of -0.4‰ , respectively (see Tab. 4.2). The observed changes of $\delta^{18}\text{O}$, d and conductivity indicate exchange processes from the enclosing

sediment to the ice wedge. Segregated ice has a low mean $\delta^{18}\text{O}$ of -23.4‰ and d of -0.4‰ , respectively (see Tab. 4.2). The observed changes of $\delta^{18}\text{O}$, d and conductivity indicate exchange processes from the enclosing sediment to the ice wedge. The hydrochemical (and isotopic) gradient between the ice wedge and segregated ice is partly compensated during the existence of the 42 ky old ice wedge. It is important to note that this effect is only found in some Ice Complex ice wedges.

Solomatin (1986) postulated a migration of moisture from the host sediment towards the ice wedge was caused by differences in heat capacities and dilation coefficients of ice and ice-rich sediment. As a consequence, small cracks are formed at the sides of an ice wedge and filled with water. This process indicates the possibility of moisture exchange in the contact zone between an ice wedge and the sediment, which could compensate hydrochemical and isotopic gradients. The transfer of water molecules in permafrost depends on composition and structural characteristics of soil and water. Yershov (1998) emphasises that the migration of bound water in frozen ground is driven by potential differences (such as temperature or ion concentration). Only in the case of soil pores relatively empty of water and ice must vapour transfer be considered. We conclude that in the fine-grained and ice-rich Ice Complex, water migration is the driving force for the isotope and ion exchange between ice wedge and segregated ice, which was identified for the first time by means of stable isotopes and hydrochemistry.

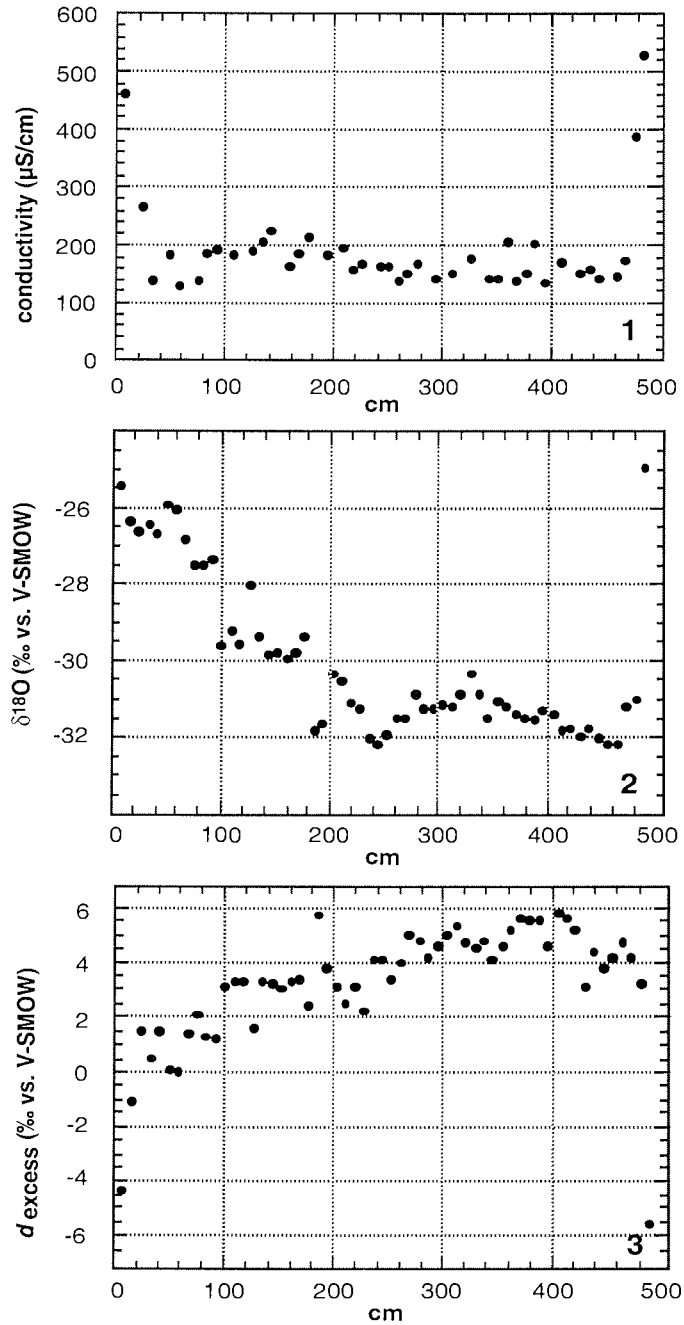


Fig. 4.6.1-4.6.3: Electrical conductivity, $\delta^{18}\text{O}$ and d excess of 5 m long horizontal sampling transect of Pleistocene ice wedge MKh-3 (height a.s.l.: 11.1 m). For the location of the sampling transect in the outcrop see Fig. 4.3, for a general sampling scheme, see Fig. 3.7.

4.8.3 Paleoclimatic evolution as revealed from stable isotope data

A wide range of hydrogen and oxygen isotopic compositions is observed for ice wedges on the Bykovsky Peninsula. Stable isotope minimum, mean and maximum values, standard deviation for 15 ice wedges of the three genetic units on the Bykovsky Peninsula Ice Complex (8 ice wedges), alas (3) and log (4) are presented in Tab. 4.2. Additionally, the slope and the intercept in the $\delta^{18}\text{O}$ - δD diagram as well as the sampling heights (a.s.l.) and the widths of all ice wedges are given. Variations in δD and $\delta^{18}\text{O}$ of 100‰ and 11.5‰, respectively, were measured for all ice wedges, with a mean isotopic composition of $\delta\text{D} = -218.0\text{‰}$ and $\delta^{18}\text{O} = -28.4\text{‰}$. This reflects changing, but always very cold climatic conditions in the working area during winter.

For some ice wedges (e. g. MKh-3 in the Ice Complex) horizontal and vertical transects were sampled. Stable isotopes of vertical transects of ice wedges show up to four times lower standard deviations than horizontal transects, because vertical sampling (Fig. 3.7) is carried out along the cracking direction (following one vein). Therefore, a randomly sampled vertical profile does not necessarily reflect climatic trends. In earlier studies, small and medium-sized ice wedges were considered to be important for paleoclimate, stratigraphic and genetic studies (Vaikmäe, 1991). Because of the possibility of exchange processes between ice wedges and the enclosing sediments, as discussed above, we chose a statistical approach for a paleoclimatic reconstruction, using big ice wedges of the Ice Complex. Eliminating the samples influenced by segregated ice and using mean values and ranges for horizontal sampling transects of ice wedges, we expect to find isotopic trends, which in a second step could be attributed to climatic variability, especially to changes in winter temperatures. The variability within an ice wedge surely also contains climatic information, but it is difficult to attribute an ice vein to a discrete year.

The differences in mean $\delta^{18}\text{O}$ and δD of Ice Complex, alas and log ice wedges represent the development of mean winter temperatures throughout time (Figs. 4.7.1-4.7.4). In general, samples from the Pleistocene Ice Complex shows an isotopic composition of -29‰ to -32‰ for $\delta^{18}\text{O}$ and of -230‰ to -250‰ for δD . The mean $\delta^{18}\text{O}$ values of all Pleistocene Ice Complex ice

wedges are between -33‰ and 29.5‰ . Because of the close relationship between temperatures and isotopic composition, mean winter temperatures can be assumed as constantly relatively cold for the investigated time interval between 58 ka and 20 ka.

The lightest isotopic composition (as low as $\delta^{18}\text{O} = -33.9\text{‰}$ and $\delta\text{D} = -267.5\text{‰}$) is observed in the oldest Ice Complex ice wedges located close to sea level. We assumed that in the period of ice wedge formation (at about 60 to 55 ka), the mean annual winter temperatures must have been the lowest. Relatively heavy $\delta^{18}\text{O}$ and δD values for ice wedges of the Ice Complex of up to -25‰ and -190‰ are observed in the left half of the upper horizontal transect of ice wedge MKh-3 (Fig. 4.6.2). Only in parts, this could be attributed to exchange processes between ice wedge and adjacent sediment. Consequently, during the formation of this part of ice wedge MKh-3, less severe winter temperatures can be assumed.

Relatively constant cold climatic conditions according to the mean values varying between -31.2‰ and -29.5‰ for $\delta^{18}\text{O}$ and -245‰ and -230‰ for δD are characteristic for the next younger ice wedge transects (MKh-5, MKh-4.13, MKh-00) between about 26 to 20 ka. All samples of the Late Pleistocene Ice Complex (Fig. 4.7.1) lie on a straight line parallel to the GMWL and in general show low d excess values of 0‰ - 5‰ . The mean d excess is constantly between 3.7‰ and 5.0‰ . Samples of MKh-00 (30 m a.s.l.) exhibit a different signature. They show an isotopic range, which seems to be typical for the Ice Complex, but a slope in the $\delta^{18}\text{O}$ - δD diagram of 9.5 and a mean d excess of 6.0‰ are higher than for all previously formed Ice Complex samples. The steep slope is apparently caused by a change from low to high d excess, which will be discussed later.

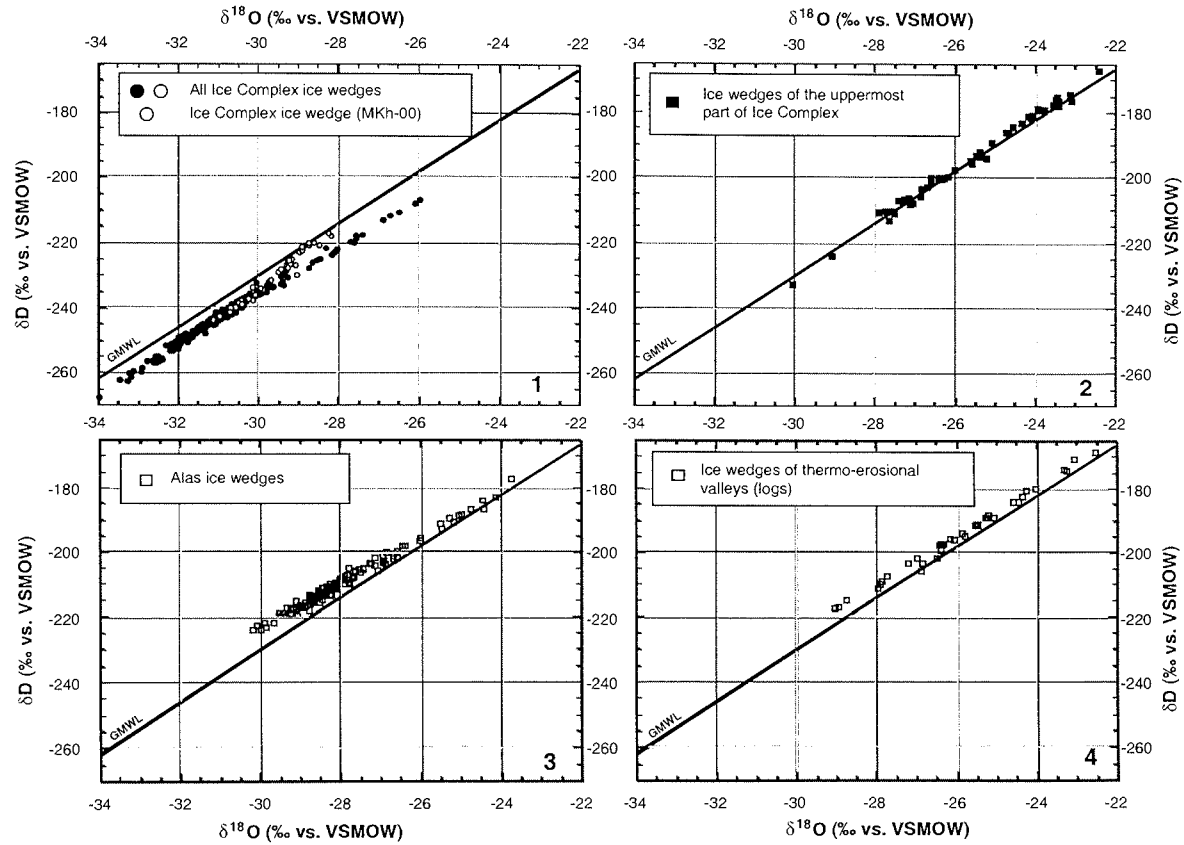


Fig. 4.7.1-4.7.4: $\delta^{18}O$ - δD diagrams for ice wedges in all genetic units: 1. Late Pleistocene part of the Ice Complex. Samples of the ice wedge Mkh-00 are represented by white dots; 2. Uppermost part of the Ice Complex (ice wedge Mkh-4.6); 3. Alas; 4. Thermo-erosional valley (Log). GMWL is the Global Meteoric Water Line.

Ice wedge MKh-4.6 (36 m a.s.l.) in the uppermost part of the Ice Complex represents a special case (Fig. 4.7.2). The $\delta^{18}\text{O}$ and δD values range mostly between -28‰ and -23‰ and -210‰ and -270‰ , respectively, with mean values of -25.8‰ and -196‰ indicating much warmer winters than before. All samples plot on the GMWL, with a high mean d excess of about 10.4‰ . In the $\delta^{18}\text{O}$ - δD diagram, a slope of 8.3 indicates no significant evaporation effects.

In Figs. 4.7.3 and 4.7.4, all samples for the younger genetic units, alas and log are displayed. The $\delta^{18}\text{O}$ values are generally significantly heavier than in the Ice Complex, but similar to those in Fig. 4.7.2 ranging from -30‰ to -24‰ for the alas and -29‰ to -22.5‰ for the log. Thus, a similar range of winter temperatures is reflected. For the formation of log ice wedges, winters might have been slightly warmer, as indicated by mean $\delta^{18}\text{O}$ and δD . d excess values of both Holocene genetic units are in general higher than 10‰ pointing to a similar source for winter precipitation as for the uppermost part of Ice Complex. Log ice wedges are characterised by a mean slope close to 8 in the $\delta^{18}\text{O}$ - δD diagram, whereas alas ice wedges have lower slopes of about 7.0. The latter evidently points to the participation of water, which has been subject to evaporation effects before the formation of ice veins. Both ice wedges located close to the slope near the Ice Complex (BYK-A2 and BYK-A1) show these effects, whereas BYK-H situated at greater distance is different (lower d , $\delta^{18}\text{O}$ and δD and higher slope of 7.5). Thus, mixing of snow meltwater with surface water from slopes has to be taken into account for the formation of BYK-A1 and BYK-A2. Both log ice wedges containing tritium (MKh-1.6, MKh-1.3) show differences in isotopic composition of up to 2.5‰ in $\delta^{18}\text{O}$ and 20‰ in δD , which may be explained by the small number ($N=5$) of samples measured.

In Fig. 4.8, the development of $\delta^{18}\text{O}$, δD and d excess of all Ice Complex ice wedges (without samples evidently influenced by exchange processes) are displayed for the interval between 10 and 60 ka. The differences between mean and median are in general negligible, except for the upper horizontal transect of MKh-3.

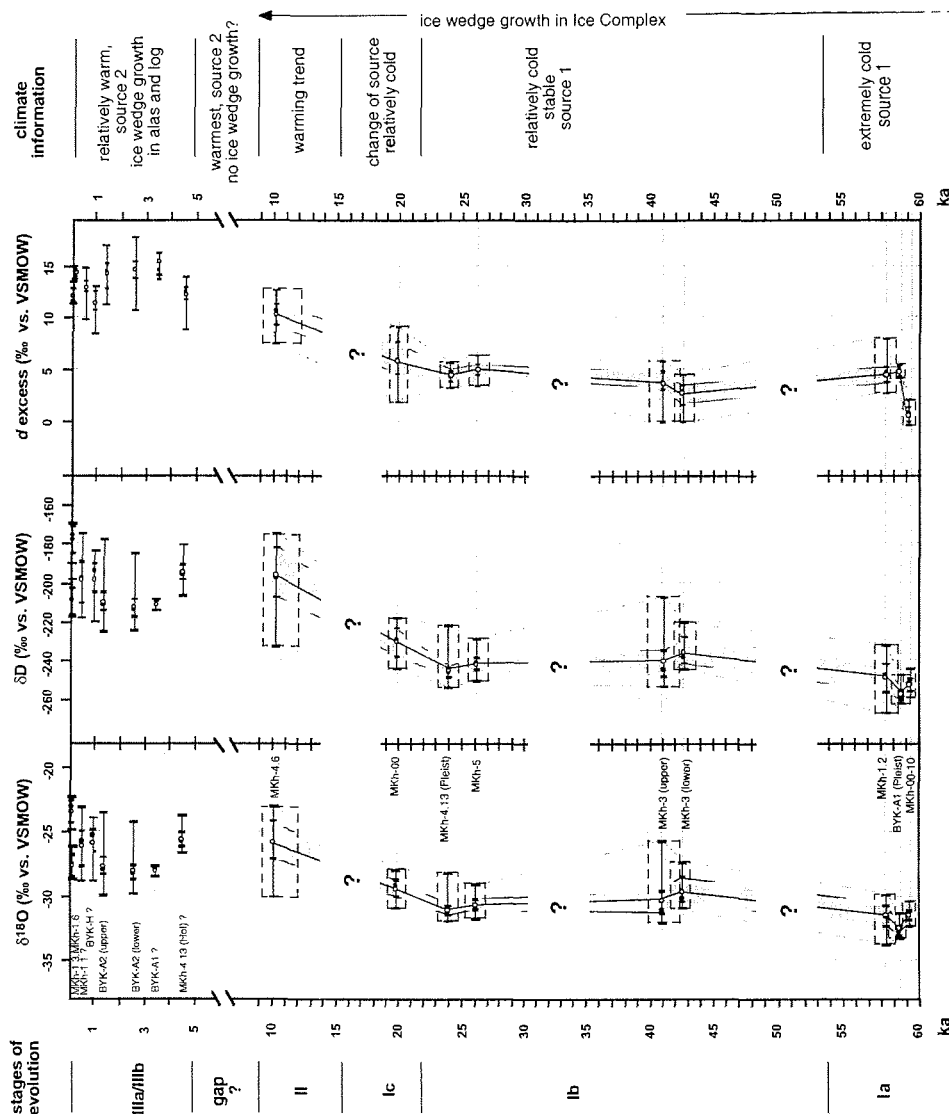


Fig. 4.8: Development of $\delta^{18}O$, δD and d excess of all Ice Complex ice wedges (without samples evidently influenced by exchange processes) and for the younger units alas and log through time. White dots are the mean isotopic composition, black dots the median of horizontal transects. A straight black line follows the development of the mean isotopic composition through time. The respective angle (light grey field) and an intermediate area (dark grey field) between the quartiles Q1 and Q3 (dotted lines) are held out for visualisation. A (white or black) dot does not correctly represent a horizontal ice wedge transect, because for horizontal ice wedge growth a time span is also needed. Therefore, estimated ages as calculated above). White gaps were left where no ice wedges were sampled. Additionally, Holocene ice wedges are displayed. When no age determinations were available, ice wedges were put into a "logical" order (marked with "?").

The development of the Ice Complex can be subdivided into three intervals. The coldest period (Ia) was between 60 and 55 ka as indicated by low stable isotope values in ice wedges, followed by a slight rise of winter temperatures. This trend is supported by pollen data (Andreev *et al.*, 2002) and sediment analysed from the Mamontovy Khayata section on Bykovsky Peninsula (Schirrmeyer *et al.*, 2002a; Siegert *et al.*, 2002). Period (Ib) between about 45 and 22 ka is characterised by very stable, still cold winter conditions as indicated by low $\delta^{18}\text{O}$, δD and d excess. Both, pollen and sediment data as well as numerous soil horizons in the middle level of the Ice Complex show strong variations of the paleoenvironmental conditions at that interval. From 40 to 30 ka, the highest number of insect and mammal remains were found, pointing to favourable conditions for fauna and flora (Siegert, pers. comm.). After 22 ka, a rise in d excess is observed in Ice Complex ice wedges proceeding to the Holocene. This stage Ic was relatively cold in winter and reflects changing climatic conditions in the source of precipitation.

The Late Pleistocene cold period (or Sartanian in Russian stratigraphy), reflected in pollen from 26 to 16 ka, is apparently not reflected in the isotopic composition of ice wedges. This may be due to missing samples for that time slice. A strong rise in the mean $\delta^{18}\text{O}$ of 5‰ and in δD of 25‰ is observed for the Pleistocene-Holocene transition. The rise in δ values is also well known from Greenland (Grootes *et al.*, 1993) and Antarctic ice cores (Petit *et al.*, 1999). Period (II) is interpreted as a transitional stage with climate warming. The trend of a rise in $\delta^{18}\text{O}$ in ice wedges from the Bykovsky Peninsula has already been measured by Fukuda (1994), albeit with a much lower resolution.

A gap in ice wedge growth is indicated by a lack of data from about 8 - 4.5 ka. Limited or missing ice wedge growth during that time was presumably caused by the occurrence of extensive lakes (Schirrmeyer *et al.*, 2002a). According to Andreev *et al.* (2002), the highest amount of tree pollen data was found in the sediment from 8.2 - 4 ka indicating a most favourable climate or the "Holocene climatic optimum" at this time interval. Additionally, numerous tree remains from this time were found in Northern Siberia (Siegert *et al.*, 1999). Despite insecure age estimates for some ice wedges, two overlapping stages

(IIIa and IIIb) of ice wedge growth in log and alas can be distinguished for the second half of the Holocene. Both show similar climatic situations, which is confirmed by pollen data (Andreev *et al.*, 2002). Nevertheless, alas ice wedges reflect slightly colder winters than log ice wedges. After 4.5 ka, climate deterioration and drying up of lakes is known from Taymyr Peninsula, Northern Siberia (Siegert *et al.*, 1999), which is followed by new ice wedge growth (French, 1996).

4.8.4 Sources

The existence of a strong linear correlation ($R^2=0.99$) of all Ice Complex ice wedges (except MKh-00 and MKh-4.6) in the $\delta^{18}\text{O}$ - δD diagram clearly indicates that ice wedge growth is only weakly influenced by fractionation processes. Only in the contact zone between ice wedge MKh-3 (Figs. 4.6.1-4.6.3) and adjacent sediment, water from the segregated ice formerly subjected to evaporation has been transferred to the ice wedge leading to a deviation from the linear correlation towards a lower slope in the $\delta^{18}\text{O}$ - δD diagram. We conclude that fractionation during melting and winter sublimation of snow, which would both lead to a shift in d excess, must have been of small influence during Ice Complex ice wedge growth. This leads to the assumption that first meltwater feeds the frost crack. Additionally, the main source of the precipitation incorporated in ice wedges on the Bykovsky Peninsula must have been constant, or, in the case of two or more different sources, their relative amount. Another explanation for the strong linear correlation of Ice Complex and other ice wedges could be diffusion within the ice wedge. The stable isotope records of $\delta^{18}\text{O}$ and δD in ice cores show that the isotopic gradients are smoothed with time by diffusion (Jean-Baptiste *et al.*, 1998). Transport of hydrogen and oxygen atoms through solid ice is slow, whereas water vapour diffusion through the interconnected porosity is much faster. Diffusion in ice wedges would be supported by (1) small variations and the absence of abrupt shifts in the isotopic composition of two adjacent samples and (2) lower correlation in younger ice wedges because of limited time for "isotopic smoothing". But all analysed ice wedges have very high correlation coefficients (Tab. 4.2) showing no increasing

"smoothing" with time. To prove this, a closer view of the differences in the isotopic composition between single veinlets is necessary.

For the shift in d excess between the Pleistocene and the Holocene, various explanations are possible. First, a change of the main source for the precipitation or a change of the pathways may have led to a higher d excess in the Holocene (and Latest Pleistocene). The source of the winter precipitation today is probably located in the Northern Atlantic. The western air transfer dominates all over Northern Eurasia (Rinke *et al.*, 1999), fed by Atlantic moisture (Kuznetsova, 1998). Especially in January, the Siberian anticyclone remains in a stable position over the Arctic Ocean, north of the Laptev Sea. The Arctic Ocean is frozen in winter, leaving only a thin polynya with open water. In coastal regions this polynya has to be taken into account as a moisture source. Continental areas of Northern Siberia with open water are also frozen in winter, but the low temperatures in the Arctic regions impede the moisture transfer to the atmosphere. Moreover, a large amount of snow originating from a source with reprecipitated water is detectable in the $\delta^{18}\text{O}$ - δD diagram by a low slope. The advection of moisture from the Pacific Ocean is restricted by atmospheric circulation patterns and the mountain relief (Leroux, 1993). Therefore, the boundary between regions influenced by Pacific and Atlantic moisture is situated far to the East between 130°E and 150°E . In winter, the lowest moisture content is observed in this area and eastern moisture transport in the North of the Aleutian depression from the Pacific meets Atlantic air masses (Kuznetsova, 1998). Nevertheless, the Pacific can be ruled out, because the present climatic conditions on the Bykovsky Peninsula are similar to those on the Taymyr Peninsula (Boike, 1997), with snow presumably deriving from the same moisture source (see above). Additionally, according to (Clark & Fritz, 1997), Atlantic marine-influenced stations in Northern Canada today have a much higher d excess (about 10.6‰) than Pacific marine-influenced stations ($d = 3.6\text{‰}$).

Little is known about past Arctic atmospheric circulation. But, Atlantic derived precipitation was presumably influenced by two major changes in the paleoenvironmental history: the existence of ice sheets covering large areas of

Western Siberia during periods in the Weichselian (Svendsen *et al.*, 1999), and the more continental position of the working area with respect to the sea (Alekseev, 1997).

A higher continentality is generally accompanied by a larger amplitude of temperatures. Therefore, marine-influenced precipitation has a narrower range of isotopic composition compared to continental areas (Clark & Fritz, 1997) and consequently higher $\delta^{18}\text{O}$ and δD in the ice wedges. During the late glacial maximum (LGM, 15-18 ka ^{14}C), the sea level was much lower than today and the Arctic shelves were subaerially exposed. A distance from the Bykovsky Peninsula to the sea of about 500 km (Romanovskij *et al.*, 1999) has been estimated. "Colder" winter temperatures are not indicated by the stable isotopic composition of ice wedges during the Sartanian cold period. Thus, continentality does not seem to have a major influence on winter temperatures. Brezgunov *et al.* (1998) correlated $\delta^{18}\text{O}$ of precipitation with mean monthly temperatures at Russian meteorological stations. Their map shows latitudinal gradients and strong continentality effects on variations of $\delta^{18}\text{O}$ in precipitation for Northern Siberia. The Lena Delta area is located in the region with the lowest $\delta^{18}\text{O}$ values (-24‰), indicating a high degree of continentality even though presently it is close to the Laptev Sea coast.

The position and extent of a possible LGM ice sheet in Northern Siberia is still being controversially discussed (e. g. Grosswald, 1998; Grosswald *et al.*, 1999, Astakhov, 1998). The presence of the Ice Complex with syngenetic ice wedges, which were growing between >60 ka and 9 ka on the Bykovsky Peninsula are evidence for the absence of a large ice sheet in this area. But even the existence of a West Siberian LGM ice sheet should have had an influence on atmospheric circulation patterns and thus on the isotopic composition of precipitation. Any ice sheet must have acted as a morphological barrier changing the pathways of moisture transport, and blocking or deviating the Atlantic air masses. During the LGM, moist tropical air masses were forced northward both in the North Pacific and in the Atlantic regions (Leroux, 1993). Higher humidity in the source region leads to lower d excess. Consequently, both are possible source regions for moisture feeding our ice wedges. A change

of the source of the precipitation from the Northern Pacific to the Atlantic after the decay of the LGM ice sheet is a possible explanation for the shift in d excess. A second possibility, is moisture originating from lower latitudes of the Atlantic (Johnsen & White, 1989) which has been slightly colder during the LGM (CLIMAP, 1976), combined with a southward displacement of the sea ice boundary. Despite the larger distance to the study area, colder sea surface temperatures or higher moisture in the source region may explain the low d excess in winter precipitation. On the Taymyr Peninsula, a rise in d excess is observed between Pleistocene and Holocene ice wedges (Siegert *et al.*, 1999). We conclude that winter precipitation originated from the west, presumably at lower latitudes in the Atlantic.

Another possible explanation for the shift in d excess is related to the modification of isotopic composition in the snow cover feeding the frost cracks during spring. In the case of a very thin snow cover, the importance of sublimation, evaporation and diffusion within the snow cover as well as percolation of melt water through it would increase leading to a change in the d excess. After Gasanov (1977), sublimation of ice wedge ice may occur in an open frost crack and desublimation from a moist air mass in the upper part of the crack. This is caused by a gradient between low air temperature and higher permafrost temperature in winter. Cold air enters into the frost crack, where it becomes undersaturated in water vapour when the air temperature rises. Depending on humidity, this process could also change the d excess.

4.9 Conclusions

The following results were obtained during the study of ice wedges carried out on the Bykovsky Peninsula, Northern Siberia:

The presence of ice wedges since more than 60 ka points to permafrost conditions and to the absence of a glacier cover in this area. For these remote non-glaciated areas of Northern Siberia, ice wedges are important climate archives for isotope studies.

Ice wedges of three different genetic units and of different ages could be distinguished by means of oxygen and hydrogen isotopes. The Ice Complex

was subdivided isotopically into a period of very cold winter temperatures between 60-55 ka, followed by a long stable period of cold winters from 50 to 24 ka. A rise of 5‰ in $\delta^{18}\text{O}$ and of 25‰ in δD probably after the Late Glacial Maximum indicates a climate warming trend.

For the Ice Complex, a continuous age-height relationship of 0.7 m/ky was established, pointing to syngenetic freezing and relatively constant vertical ice wedge growth and sediment accumulation rates. Ice wedge growth was limited during the Holocene optimum, because of wide-spread lake formation processes. The following climate deterioration led to initial Holocene ice wedge growth (in alas) after 4.5 ka continuing until today at relatively warm winter temperatures as compared to the Pleistocene.

The isotopic composition of old ice wedges may be altered by migration of water between the ice wedge and the enclosing segregated ice, which must be considered for paleoclimatic interpretation. The d excess of ice wedges contains information about the moisture source region for winter precipitation. A shift in the d excess after about 20 ka is probably related to a change of the main marine source of the precipitation. In the Pleistocene, the moisture source region (presently the North Atlantic) lay further to the south.

5. PALEOCLIMATE RECONSTRUCTION ON BIG LYAKHOVSKY ISLAND, NORTH SIBERIA – HYDROGEN AND OXYGEN ISOTOPES IN ICE WEDGES

Hanno Meyer, Alexander Dereviagin, Christine Siegert, Lutz Schirrmeister, Hans-W. Hubberten

Reprinted from **Permafrost and Periglacial Processes** 13, p. 91-105, 2002 ;
Copyright © John Wiley and Sons, Ltd. Reproduced with permission.

5.1 Abstract

Late Quaternary permafrost deposits on Big Lyakhovsky Island (New Siberian Islands, Russian Arctic) were studied with the aim of reconstructing the paleoclimatic and paleoenvironmental conditions in Northern Siberia. Hydrogen and oxygen stable isotope analyses are presented for six different generations of ice wedges as well as for recent ice wedges and precipitation.

An age of about 200 ka BP was determined for an autochthonous peat layer in ice-rich deposits by U/Th method, containing the oldest ice wedges ever analysed for H and O isotopes. The paleoclimatic reconstruction revealed a period of severe winter temperatures at that time. After a gap in the sedimentation history of several tens of thousands of years, ice wedge growth was reinitiated around 50 ka BP by a short period of extremely cold winters and rapid sedimentation leading to ice wedge burial and characteristic ice-soil wedges ("polosatics"). This corresponds to the initial stage for the Late Weichselian Ice Complex, a peculiar cryolithogenic periglacial formation typical of the lowlands of Northern Siberia. The Ice Complex ice wedges reflect cold winters and similar climatic conditions as around 200 ka BP. With a sharp rise in $\delta^{18}\text{O}$ of 6‰ and δD of 40‰, the warming trend between Pleistocene and Holocene ice wedges is documented. Stable isotope data of recent ice wedges show that Big Lyakhovsky Island has never been as warm in winter as today.

5.2 Introduction

For paleoclimatic studies in the continental areas of northern Siberia, only a few archives are available, which cover periods of more than 10,000 years. These are mainly ice caps occurring in a few limited areas such as on Severnaya Zemlya (Vaikmäe & Punning, 1984) or lake deposits such as in Lake Baikal (Colman *et al.*, 1995).

On Big Lyakhovsky Island as well as in other lowland areas in northeast Siberia, deep lakes with long records are also rare and glacier ice is not available. Therefore, we selected different generations of ice wedges embedded in mostly ice-rich deposits of different ages as archives for paleoclimatic reconstruction. For paleotemperature reconstruction (Petit *et al.*, 1999) and the identification of moisture sources (Merlivat and Jouzel, 1979), stable water isotopes are widely used in paleoclimatology.

The first pioneer work using ice wedges for paleoclimatic studies was performed by Michel (1982), MacKay (1983), Vaikmäe (1989) and Vasil'chuk (1991), who considered oxygen isotope variations in ice wedges as indicators for winter temperature changes. Ice wedges are excellent objects for paleoclimatic research, especially when ice wedges of different generations covering a long time span are available. Ice wedges, as strictly periglacial features, are indicative for permafrost conditions and the absence of glacier ice. The source of wedge ice is mainly snowmelt water, which penetrates into frost cracks. Melt water freezes rapidly enough to prevent fractionation (Michel, 1982), and an ice vein is formed, containing the isotope signal of one discrete winter. Frost cracks are formed preferentially between Mid-January and Mid-March (MacKay, 1974). In general, frost cracking occurs in a zone of weakness preformed by the ice vein of the previous cracking event (MacKay, 1974). Therefore, stable isotope composition of ice wedges can be correlated with mean annual winter and January temperatures (Vasil'chuk, 1992, Nikolayev and Mikhalev, 1995, Vasil'chuk and Vasil'chuk, 1998). Wedge ice may also serve for stratigraphical distinctions (Vasil'chuk and Trofimov, 1988, Vaikmäe, 1989). A detailed work of paleoclimatic studies by means of oxygen and hydrogen isotopes on ice wedges based on precise age determinations has recently been

presented for the Bykovsky Peninsula, near the Lena Delta, by Meyer *et al.* (2002). In order to understand which factors may influence the isotopic composition of an ice wedge, we used recent snow and ice veins as a base for the paleoclimatic interpretation (Lauriol *et al.*, 1995; Meyer *et al.*, 2002). The influence of moisture exchange between ice wedges and adjacent segregated ice in the sediment is demonstrated by Meyer *et al.* (2002). Segregated ice is mainly formed by the freezing of suprapermafrost pore water at the bottom of the active layer (International Permafrost Association, 1998) and is thus fed by water sources other than ice wedges. Therefore, samples taken near the boundary between ice wedge and ice-rich sediment were discarded from our paleoclimatic interpretation.

Our stable isotope studies are embedded in the German-Russian research project "System Laptev Sea 2000" being part of a multidisciplinary approach dedicated to a better understanding of paleoclimatic and paleoenvironmental change during the Late Quaternary.

5.3 Working area and climatic background

The working area is situated on the south coast of Big Lyakhovsky Island in the Eastern Laptev Sea region. Big Lyakhovsky Island is the most southern of the New Siberian Islands, separated from the continent by the Dimitri Laptev Strait. A NE-SW striking coastal outcrop with a length of about 6 km was studied at both sides of the Zimov'e River mouth (Fig. 5.1). The study area belongs to the Arctic Tundra (Atlas Arktiki, 1988). A first description of the Quaternary sequences of Big Lyakhovsky Island was performed by Romanovsky (1958).

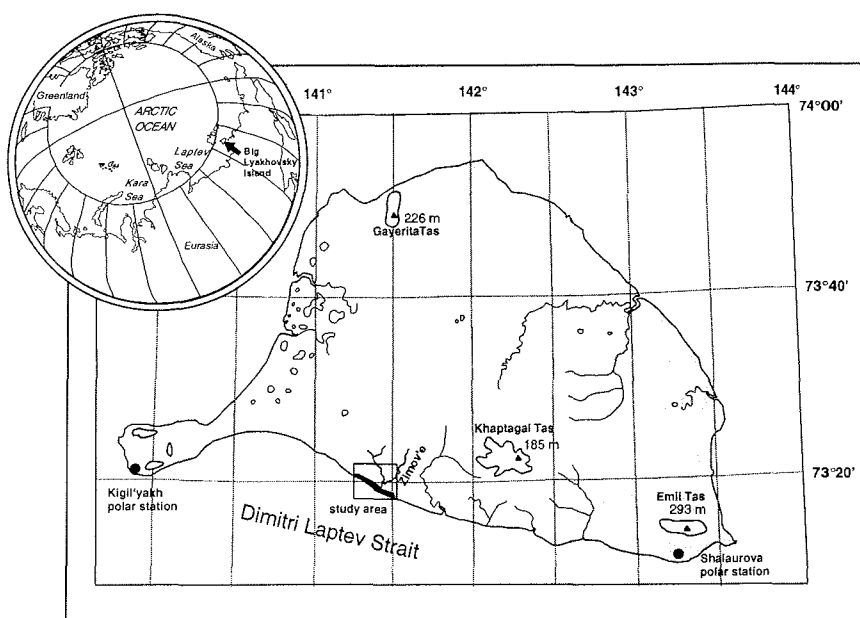


Fig. 5.1: Location of the working area on Big Lyakhovsky Island

The closest meteorological station is located at Cape Shalaurova, SE coast of Big Lyakhovsky Island ($73^{\circ}11'N$ $143^{\circ}56'E$). The present climatic situation is characterized by a low mean precipitation and temperature of 184 mm/year and $-13.6^{\circ}C$, respectively, calculated for a seven year period between April 1994 and September 2000 (National Oceanic and Atmospheric Administration (NOAA) data archive). The main period of precipitation is between June and September, when about two thirds of the annual volume occurs. The coldest month is January (mean temperature $-31.0^{\circ}C$), the warmest month August (mean temperature $2.4^{\circ}C$). Mean daily temperatures as low as $-40.5^{\circ}C$ and as high as $9.4^{\circ}C$ were measured pointing to a highly continental climate despite the proximity of the Laptev Sea.

5.4 Methods

Several generations of ice wedges were studied on Big Lyakhovsky Island. According to new datings, these span over the last 200 ka (Schirmermeister *et al.*, 2002b). Sampling of ice wedges was performed at 10 cm intervals in the

horizontal direction. Sampling was carried out for horizontal transects of all ice wedges, at different height levels of the outcrop corresponding to discrete time intervals. The mean stable isotopic composition of one horizontal sampling transect is supposed to be characteristic for the winter temperature of the time this transect was formed. Samples were taken by means of a chain saw (in vertical slices 1.5 cm thick) and an ice screw (\varnothing 14 mm), then thawed and poured into plastic bottles, which were sealed tightly. The widths of single veinlets vary between 1 and 6 mm. Thus, one sample represents an integral signal of several (up to 15) ice veins. "Heads" of ice wedges were sampled separately from the lower ice wedge and are not included into the statistics (Table 5.1). Hydrogen and oxygen isotope ratios were measured with a Finnigan MAT Delta-S mass spectrometer, at the Alfred Wegener Institute Potsdam, using equilibration techniques. They are given as permil difference to V-SMOW, with internal 1σ errors of better than 0.8‰ and 0.1‰ for δD and $\delta^{18}O$, respectively (Meyer *et al.*, 2000). The results are presented in $\delta^{18}O$ - δD diagrams with respect to the Global Meteoric Water Line (GMWL), in which fresh surface waters are correlated on a global scale (Craig, 1961). In general, the most negative $\delta^{18}O$ and δD values reflect the coldest temperatures. Slope and intercept in the $\delta^{18}O$ - δD diagram are valuable indicators for the identification of (1) precipitation deriving from the evaporation of ocean water in different regions and (2) participation of secondary evaporation processes (Dansgaard, 1964). The deuterium excess ($d = \delta D - 8\delta^{18}O$) introduced by Dansgaard (1964) is an indicator for non-equilibrium fractionation processes.

The ages of the sediments in the outcrop were estimated by accelerator mass spectrometry (AMS) ^{14}C dating of plant remains (mainly small roots, leaves or twigs). The measurements were carried out in the Leibniz Laboratory in Kiel, Germany. Details of the AMS facility in Kiel are given in Nadeau *et al.* (1997) and Nadeau *et al.* (1998). In order to eliminate contamination by younger organic acids, only the leached tissue was used for dating. For a better comparability of Pleistocene and Holocene samples, uncalibrated AMS ^{14}C ages were used.

5.5 Results of the field studies

At least 11 different geocryological units can be distinguished in the section (Kunitzky & Schirrmeister, 2000). Seven of these units contain different generations of ice wedges, six of which were sampled for stable isotope analyses (Fig. 5.2). In all sampled units, ice wedges of different size, colour and genesis enclose mostly ice-rich sediment with finely-dispersed segregated ice.

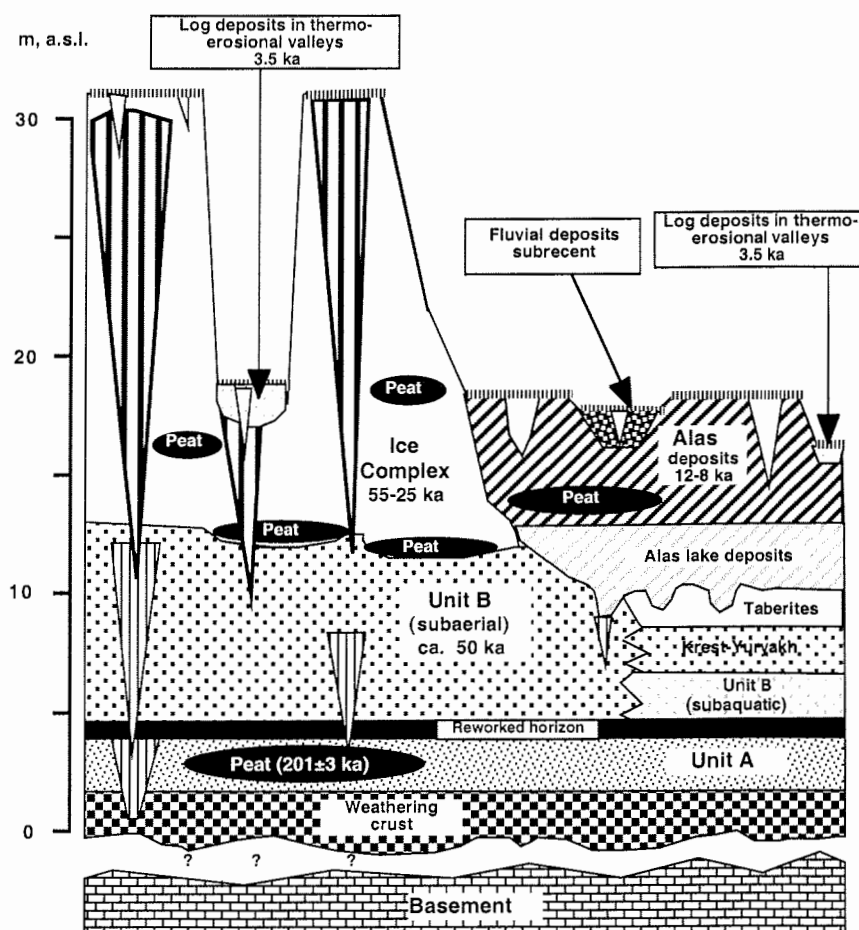


Fig. 5.2: Schematic profile of the study site at the South coast of Big Lyakhovsky Island with cryolithogenetic units (modified after Grosse, 2000)

The oldest stratigraphic unit is a horizon composed of weathered Permian sandstone, which outcrops in parts of the working area near sea level. This weathering crust consists of eluvial clay and silt with poorly-rounded rock fragments and is characterized by basal and cellular cryostructures. The oldest generation of ice wedges, being in general narrower than 0.5 m, penetrates from the next younger Unit A into the weathering crust.

Unit A is composed of greyish-brown silt to fine-grained sand with some peat inclusions and cryoturbated paleosols. A peculiarity of Unit A is the inclusion of the underlying weathering crust of yellowish rock debris in the sediment and in ice wedges. Ice wedges in Unit A sediments reach widths of 3.5 m. Two types of ice wedges occurring side-by-side can be distinguished: (1) with light grey transparent ice, gas bubbles ≥ 1 mm and low sediment content and (2) ice-soil-wedges called "polosatic" in Russian literature (Kunitsky, 1998). "Polosatics" are related presumably to the next youngest Unit B and are explained later. Horizontal ice belts of up to 15 mm thickness characterise the cryolithogenic structure of Unit A. Ice wedge growth was probably both syngenetic as shown by ice belts bound upward near ice wedges, and epigenetic (the "polosatic" part) to the sedimentation.

Unit B consists of yellowish to greyish-brown "loess-like" fine-grained sands with many subvertically oriented *in situ* grass roots. Unit B has a relatively low ice content of 30-40 wt% (relative to the dry-weight) in sediment of mostly massive cryostructure. Ice wedges are rather rare compared to other units, and some soil wedges occur. The ice wedges in Unit B are between 1 m and 2.5 m wide and contain in most cases ice-soil-wedges or "polosatics". "Polosatics" (Fig. 5.3) are phenomena where very sediment-rich vertical bands are interrupted by single ice veins. The ice veins are in general turbid and yellowish, about 1 to 3 mm thick, but may attain up to 1 cm. The thickness of mineral strips is normally about of 1 to 2 mm, but it may be significantly higher. Vertical zebra-striped "polosatic" structures can be found at different height levels from 1-17 m a.s.l., both in contact to the Ice Complex and the Unit A ice wedges. Similar structures were described as ice-sand wedges by Romanovsky (1976).

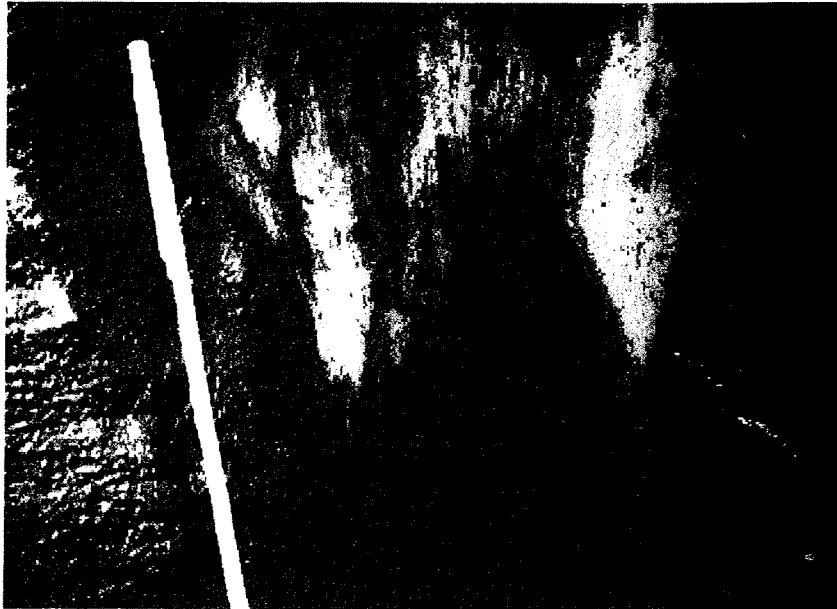


Fig. 5.3: Subvertical oriented ice-soil wedges ("polosatic") of Unit B. Interfingering of single ice veinlets with the sediment is observed.

In general, we observed an uneven upper part of Unit B ice wedges with several vertical extensions. The width of these "heads" may reach up to 20 cm and in some cases, they are buried under Unit B sediments, and are therefore considered to be of Unit B age. The phenomenon of buried ice wedge heads may be explained by a reduced thaw depth in the active layer or, most likely, by a sudden rise in the sedimentation rate. Melting processes may have caused a degradation of the ice wedge from above prior to the growth of ice wedge heads. The contact between Unit B and the Late Pleistocene Ice Complex is not clearly defined and not uniformly at the same height above sea level. Some parts of the permafrost profile of Unit B sediments have visible marks of thawed ice wedges. These ice-wedge pseudomorphs belong to a subaquatic facies of Unit B and are usually associated with lake depressions.

The next younger unit is the Ice Complex with typical geomorphological forms such as steep ice cliffs reaching 35 m a.s.l. and thermo-erosional cirques extending some 100 m in length. They are characterized by a 50-100 m wide "thermo-terrace" with numerous thermokarst mounds (baydzherakhii). The

sediments are composed of silty to fine-grained sand of greyish-brown colour, some cryoturbated peaty paleosols and peat inclusions especially in the lower part of the unit. Yellowish-grey coloured ice wedges are up to 6 m wide and more than 20 m high. Well-defined subvertical structures such as elementary ice veins of about 1-4 mm thickness, oval gas bubbles and thin mineral layers are common. Massive subhorizontal, 2-4 cm thick ice belts in the sediment, always bound upward in contact with the ice wedges point to the syngenetic formation of the ice wedges.

Three younger facies overlie the Ice Complex and older deposits. The formation of these younger facies such as deposits in thermokarst depressions (alases) and in thermo-erosional valleys (logs) as well as fluvial deposits is linked with the destruction of the older units. Ice wedges of two alas depressions of different depth were sampled. Alas deposits are determined by polygonal ice wedge systems attaining 10-15 m in diameter and by alternating horizontal layers of thin ice belts and reticulate cryostructures. The layers are observed to be inclined upwards near their contacts with the ice wedges. Typically, the alas sediments are composed of grey fine-grained sands with layered bedding, high organic contents and some peaty paleosol horizons. Alas ice wedges may reach widths of about 3.5 m and contain subvertical structures such as up to 3 mm thick elementary ice veins and orientated small gas bubbles. The ice wedges are white and milky and contain datable organic material. In alas deposits, recent ice-wedge growth with single 1-4 cm wide ice veins in the lowermost part of the active layer are very common.

Logs and their respective thermo-erosional channels are typical features in the whole working area. They are mainly associated with the Ice Complex, and their sediments consist of grey and silty fine-grained sands partly organic-rich and dissected by roots. Ice wedges in logs are up to 1.5 m wide and characterized by white to grey, milky ice with subvertically elongated gas bubbles resembling a string of beads. Single ice veins are between 1 and 4 mm thick. Low-centred ice wedge polygons with diameters of 8 to 12 m are found in the Holocene fluvial terrace at the mouth of the Zimov'e River. The maximum thickness of these deposits is about 5 m, being composed of light brown fine- to medium-

grained sand with ripple and cross-bedding structures. The width of ice wedges may reach 1.5 m. The ice wedges are still active and show subvertically orientated, 2 to 6 mm thick, ice veins, very thin sediment layers and elongated gas bubbles. The ice is relatively clear and colourless. Enclosing sediments are characterized by a layered cryostructure that bounds upward near ice wedges.

One to 4 cm wide recent ice veins have been observed in various parts of the outcrop, especially in alas depressions, thermo-erosional valleys, and fluvial deposits. Recent ice wedges were identified by tritium analyses and sampled as a base for the climatic interpretation of the older ice wedges.

In some units, no ice wedges were available. Unit B and alas deposits are both characterized by a subaquatic facies, which consist of sediments with relatively low ice content and the presence of lacustrine shells (bivalves and gastropods). These deposits were formed when the heat capacity of overlying water bodies was high enough to cause thaw of the underlying deposits. Subsequently, they refroze after the lake dried out. In all these units, ice wedge pseudomorphs document the melting of ice wedges caused by temporary open water bodies (Fig. 5.2). The upper part of subaquatic Unit B is considered separately by some authors (Gavrilov *et al.*, 2000) and interpreted as the Krest-Yuryakh suite, which corresponds to the Eemian. Further information about the units where no ice wedges are available for stable isotope analyses are found in Kunitsky & Schirrmeyer (2000) and Grosse (2000).

5.6 Geochronology

Thermoluminescence (TL) dating carried out on silty sands close to the Zimov'e River point to ages around 1 Mio a for Unit A (Arkhangelov *et al.*, 1996). Paleomagnetic investigations in the upper part of Unit A sediments show the Jaramillo magnetic reversal (Arkhangelov *et al.*, 1996). Schirrmeyer *et al.* (2002b) showed that a pre-Eemian $^{230}\text{Th}/\text{U}$ age of a sample taken near the top of Unit A deposits from a frozen peat layer several tens of meters long revealed a younger age of 201 ± 3 ka. This requires attribution to another magnetic inverse period such as Biwa I or II. We have assumed that this U/Th age is highly reliable because (1) frozen peat in permafrost behaves like a closed

system for uranium and thorium (Schirmer *et al.*, 2002b), and (2) it is within the dating range of the method (which is questionable for TL ages of 1 Mio a). Unit B sediments were also TL dated by Arkhangelov *et al.* (1996) to 360 ± 90 ka and by Kunitsky *et al.* (1996, 1998) to ages between 94 ± 26 and 35 ± 10 ka. Our AMS ^{14}C ages derived from the Unit B sediments are 50.1 ± 3.0 ka BP and 49.8 ± 3.2 ka BP, thus close to the limit of AMS dating range. Nevertheless, these two ages are reliable, because we dated *in situ* grass roots. Consequently, we assume a hiatus of 150 ka or more (possibly including the Eemian) between the deposition of Unit A and Unit B. The deposition of the Krest-Yuryakh suite was attributed to the Eemian (Gavrilov *et al.*, 2000) based on the TL dating by Arkhangelov *et al.* (1996). In earlier studies, Units A and B were classified as Olyor and Kuchchuguy sediments (Arkhangelov *et al.*, 1996). Since the new geochronology for these two units differs considerably from ancient TL dates on which the stratigraphical classification was based, we decided to use the terms Unit A (for the Olyor) and Unit B (for the Kuchchuguy). But, the controversial state of the age of these two units is still insufficiently understood and requires further research and dating.

Conventional ^{14}C dates published by Japanese scientists (Nagaoka *et al.*, 1995) show that the Ice Complex on Big Lyakhovsky Island was deposited between >42.2 ka and 28.7 ± 0.4 ka BP and covered by Holocene deposits of 7.4 ± 0.8 ka BP. According to our age determinations the Ice Complex on Big Lyakhovsky Island started forming around 50 ka BP as indicated by AMS ^{14}C ages (54.1 ± 3.1 ka BP, 52.9 ± 4.6 ka BP, 51.2 ± 4.7 ka BP, 50.3 ± 2.6 ka BP). These ages are in the same range or slightly older than those of the underlying Unit B. In the Ice Complex, a small salix leaf found in an ice wedge at 15.8 m a.s.l. was dated by AMS to 35.0 ± 2.1 ka BP. A lemming coprolith in an Ice Complex ice wedge at 8.2 m a.s.l. revealed an AMS age of 49.2 ± 2.1 ka BP, and at 9 m a.s.l. an AMS ^{14}C age of 39.7 ± 1.3 ka BP was derived. According to available data, the age of the Ice Complex formation is now proved for the time interval between around 55 ka and 28.7 ka BP. It must be mentioned that we were unable to sample the uppermost part of the Ice Complex. Consequently, younger ages are to be expected for the Ice Complex.

According to AMS ^{14}C dated organic material, formation of the two thermokarst depressions started at 12.4 ka BP and 11.3 ka BP, respectively, proceeding at least until 8 ka BP. Alas ice wedges were formed in the last 1 ka epigenetically, as shown by two AMS ^{14}C datings of organic matter in ice wedges (135 ± 30 a BP and 835 ± 50 a BP). Tritium analyses prove the occurrence of recent ice-wedge growth in alas and fluvial deposits (Dereviagin *et al.*, 2002). The Holocene development of thermo-erosional valley deposits was confirmed by an AMS ^{14}C age of 3.43 ± 0.03 ka BP. However, whether thermo-erosional valley or alas ice wedges are younger cannot be solved yet. Uncertain age estimates and large differences obtained from different methods, particularly from the Pleistocene deposits, reveal the necessity of more detailed age determinations on Big Lyakhovsky Island. Nevertheless, it is concluded that: (1) there is a gap in the sedimentation history between Unit A and Unit B, (2) Unit B was deposited rapidly before the formation of the Late Pleistocene Ice Complex started, (3) mostly Holocene deposits are linked with the destruction of the older units.

5.7 Recent precipitation

The range of stable isotopes in precipitation reflects seasonal variations of condensation temperatures. Recent precipitation is displayed in the $\delta^{18}\text{O}$ - δD diagram for rain water, snow patches and for recent ice wedges of Big Lyakhovsky Island (Fig. 5.4). The isotopic composition for rain, snow and recent ice wedges can be drawn from Table 5.1.

Rain water ($N = 13$) was collected for all precipitation events in July and August 1999. The mean isotopic composition is $\delta^{18}\text{O} = -12.1\text{‰}$ and $\delta\text{D} = -101\text{‰}$. The samples are characterized by a low mean d excess of -4.4‰ and a slope of 6.8 in the $\delta^{18}\text{O}$ - δD diagram. The deviation from the GMWL points to the participation of kinetic fractionation processes. We assume that this enrichment in heavy isotopes is due to evaporation processes, probably originating either from surface waters or from the open Laptev Sea.

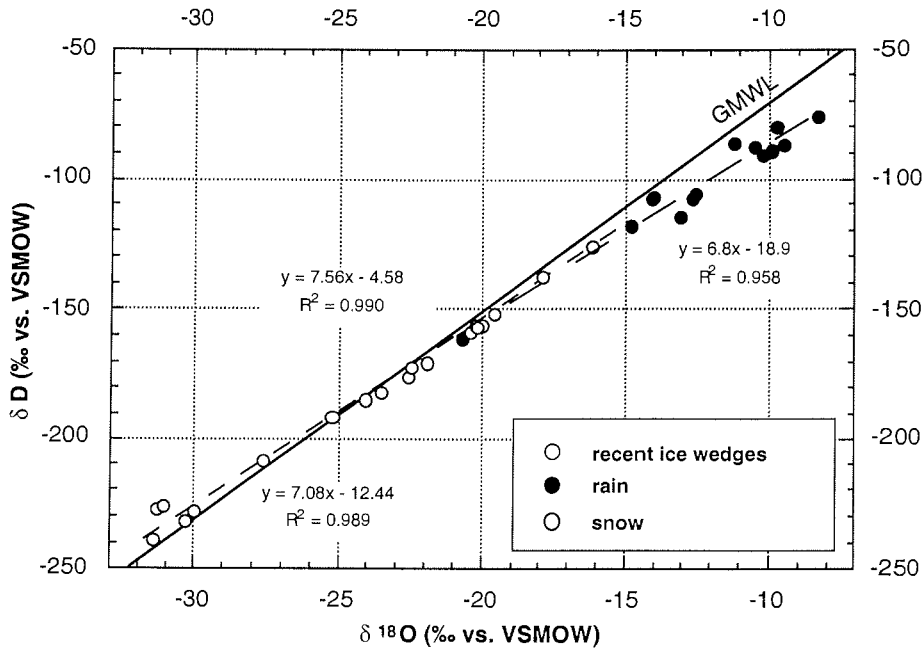


Fig. 5.4: $\delta^{18}\text{O}$ - δD diagram for snow patch, rain water and recent ice wedge samples collected in summer 1999 on Big Lyakhovsky Island. GMWL is the Global Meteoric Water Line.

During the field season in summer 1999, remains of snow patches ($N = 10$) were sampled on Big Lyakhovsky Island. The mean isotopic composition of snow patches is -26.3‰ for $\delta^{18}\text{O}$ and -199‰ for δD . The d excess of snow is highly variable between 23‰ and 3.5‰ , with a mean d of 11.6‰ . In the $\delta^{18}\text{O}$ - δD diagram (Fig. 5.4), snow samples have a slope of 7.1 and an intercept of -12 . The isotopically heavier snow samples are located below the GMWL, whereas "colder" snow is located above the GMWL. This shift in d excess may be explained by percolation of rain water or melt water through the snow cover or by evaporation or sublimation processes of snow. The notable influence on d excess is possibly also due to the low amount of winter precipitation on Big Lyakhovsky Island. Another possibility for the shift of d excess in snow is the participation of a local isotopically depleted moisture source. Since the Laptev Sea and lakes are frozen in winter, the polynya, a belt of open water conditions in the sea, would be the only possible local source.

On Big Lyakhovsky Island, the isotopic composition of snow differs significantly from that of recent ice wedges (Fig. 5.4, Table 5.1, Dereviagin *et al.*, 2002), with mean $\delta^{18}\text{O} = -20.5\text{‰}$, $\delta\text{D} = -152\text{‰}$ and $d = 4.5\text{‰}$. In the $\delta^{18}\text{O}$ - δD diagram, recent ice wedges have a slope of 7.6 and an intercept of -4.6 , and correspond isotopically to relatively heavy snow samples, but also to light rain (Fig. 5.4). This leads to two possible scenarios: (1) the recent ice wedges on Big Lyakhovsky Island are fed by a mixture of snow-melt water and rain, e.g. by percolation of rain through the snow cover; (2) ice wedges are fed by snow-melt water, which was changed isotopically before entering the frost crack. This contrasts with results from Taymyr (Dereviagin *et al.*, 2002) and the Bykovsky Peninsula (Meyer *et al.*, 2002), where fractionation and mixing did not change the d excess in snow melt before trickling into the frost crack.

Melting of the annual snow cover leads to the formation of one single elementary ice vein. Consequently, a meteoric water line of snow is transferred into one point in the $\delta^{18}\text{O}$ - δD diagram. If we consider isotope fractionation for snow melting, the first melt water will be characterized by lighter $\delta^{18}\text{O}$ and δD and higher d excess than the last (Lauriol *et al.*, 1995). This means, the recent ice wedges on Big Lyakhovsky Island with their heavier mean isotopic composition compared to the remains of snow patches, are most likely fed during the later stages of snow melt. According to Lauriol *et al.* (1995), the same process is observed for Holocene ice wedges along the Yukon River in Canada.

Another possible process for the isotope fractionation between snow and recent ice wedges is evaporation or sublimation of the snow cover, which would also result in lower d excess. This could be due to the relatively low amount of winter precipitation on Big Lyakhovsky Island (and thus a thin snow cover, the isotopic composition of which could be changed isotopically relatively easy). Flooding of frost cracks can be ruled out, because of the position of recent ice veins, which were sampled 10-15 m above sea (and river) level.

Additionally, the seasonality of precipitation events and frost cracking within one year has to be taken into account. Two climatically identical years might give different $\delta^{18}\text{O}$ in ice veins, e. g. when in one year, the frost crack is mainly

fed by colder January snow and in the next year by warmer March snow. Since we do not know the precise time of frost cracking events and the formation of ice veins, we refer to winter temperatures when considering the isotope composition of ice wedges.

5.8 Stable isotopes in ice wedges and their paleoclimatic interpretation

For Big Lyakhovsky Island, stable isotope compositions for different generations of ice wedges were analysed for a reconstruction of the paleoclimatic evolution. In Tab. 5.1, hydrogen and oxygen isotope minimum, mean, and maximum values, standard deviations, slopes and intercepts in the $\delta^{18}\text{O}$ - δD diagram are given for 17 ice wedges of six geocryological units. For comparison, stable isotopic composition of recent ice wedges and precipitation as well as for segregated ice are presented. The isotopic composition of ice wedges on Big Lyakhovsky Island is highly variable throughout time, ranging between -37.3‰ and -19.2‰ for $\delta^{18}\text{O}$ and from -290‰ to -150‰ for δD . Within one ice wedge, we observed relatively constant stable isotopic composition with variations, in general, less than 4‰ and 30‰ for $\delta^{18}\text{O}$ and δD . For all ice wedges on Big Lyakhovsky Island including recent ice wedges, the mean d excess varies between 4.5‰ and 12‰ .

The isotopic composition of ice wedges is valuable for stratigraphic subdivision of the outcrop (Meyer *et al.*, 2002). The three Pleistocene units can be differentiated by means of stable isotopes, despite light isotopic composition in all of them. The ice wedges of the oldest Unit A show a mean isotopic composition around -32‰ for $\delta^{18}\text{O}$ and -250‰ for δD (Fig. 5.5.1). For ice wedges of Unit B, much lighter $\delta^{18}\text{O}$ as low as -37.3‰ and $\delta\text{D} = -290\text{‰}$ are observed, with a respective mean isotopic composition of -35.5‰ and -280‰ (Fig. 5.5.2). Unit A and B ice wedges are characterized by relatively low mean d excess of 5 to 7‰ . The mean $\delta^{18}\text{O}$ and δD values of the Ice Complex ice wedges range from -32.5‰ to -28.5‰ and from -250‰ to -220‰ (Fig. 5.5.3), and are thus similar to those of Unit A. In the lower part of the Ice Complex, the mean d excess is between 8 and 10.3‰ . In the upper part a d excess around 5‰ is observed (an exception is R10-2).

Tab. 5.1: Stable isotope ($\delta^{18}\text{O}$, δD and d excess) minimum, mean and maximum values, standard deviations as well as slopes and intercepts in the $\delta^{18}\text{O}$ - δD diagram for all sampled ice wedges and for recent precipitation samples of Big Lyakhovsky Island.

ICE WEDGE TYPE	N	height a.s.l. (m)	width (m)	$\delta^{18}\text{O}$ (‰) min.	$\delta^{18}\text{O}$ (‰) mean	$\delta^{18}\text{O}$ (‰) max.	$\delta^{18}\text{O}$ (‰) std. dev.	δD (‰) min.	δD (‰) mean	δD (‰) max.	δD (‰) std. dev.	d (‰) min.	d (‰) mean	d (‰) max.	d (‰) std. dev.	slope	intercept	R^2
Recent ice wedges	8	varying	< 0.05	-22.48	-20.42	-19.21	1.27	-175.5	-158.9	-149.2	9.6	3.3	4.5	6.6	1.1	7.56	-4.58	0.99
FLUVIAL DEPOSITS																		
L2-1	14	3.0	1.5	-23.74	-23.12	-21.55	0.53	-183.1	-178.3	-166.7	4.1	5.7	6.6	7.2	0.4	7.71	-0.01	0.99
LOG																		
R19-1	5	16.0	1.5	-27.83	-27.04	-26.38	0.58	-211.0	-205.9	-201.2	3.9	9.4	10.3	11.6	0.9	6.64	-26.52	0.99
TZ2-3	4	19.0	0.5	-28.61	-27.89	-26.76	0.81	-216.6	-211.1	-202.4	6.3	11.6	12.0	12.4	0.4	7.75	5.12	1.00
ALAS																		
L21-1	32	9.0	2.4	-26.52	-24.42	-23.03	0.76	-203.5	-187.7	-177.9	5.5	5.3	7.7	8.8	0.9	7.23	-11.21	0.99
R32-2	33	14.0	2.9	-26.27	-24.56	-21.05	1.27	-200.0	-189.0	-164.1	9.1	2.9	7.4	10.2	1.7	7.06	-15.61	0.98
ICE COMPLEX																		
TZ3-1	28	27.5	2.5	-32.62	-31.35	-26.10	1.15	-257.5	-246.2	-204.1	9.4	3.2	4.7	5.7	0.7	8.12	8.38	1.00
R10-2	6	23.0	0.5	-32.57	-32.40	-32.10	0.18	-251.9	-247.9	-241.5	4.4	8.4	11.3	15.4	3.1	23.27	505.76	0.87
R10-1	57	22.0	4.7	-32.87	-31.56	-24.47	1.54	-258.1	-247.4	-192.4	12.2	2.7	5.1	8.5	1.1	7.90	2.00	0.99
TZ2-2	24	19.0	2.1	-31.07	-30.39	-28.32	0.77	-244.0	-235.0	-219.7	7.2	4.6	8.1	12.2	1.7	9.23	45.44	0.96
TZ2-4	19	19.0	1.2	-30.91	-28.68	-27.18	0.94	-239.1	-220.1	-207.6	7.9	8.0	9.3	11.3	0.9	8.33	18.77	0.99
TZ2-5	4	16.8	0.9	-30.91	-30.48	-29.95	0.48	-239.7	-235.4	-231.3	4.3	7.5	8.5	10.3	1.3	8.60	26.67	0.91
R8-1	10	15.4	0.8	-32.74	-32.05	-30.32	0.70	-251.6	-246.1	-232.8	5.2	8.6	10.3	15.1	1.9	7.04	-20.46	0.89
R9-1	26	9.0	2.2	-30.64	-30.09	-28.71	0.44	-237.1	-232.3	-221.0	3.5	7.7	8.4	10.2	0.5	7.85	3.86	0.98
UNIT B																		
R6-1	14	6.5	0.7	-37.34	-35.96	-34.82	0.88	-289.3	-281.0	-274.6	5.0	3.0	6.7	9.4	2.1	5.63	-78.40	0.99
R7-1	24	6.5	2.2	-36.23	-35.55	-34.61	0.46	-284.1	-278.2	-261.2	4.9	4.7	6.2	15.7	2.1	9.87	72.85	0.85
UNIT A																		
R17-1	30	7.0	3.2	-34.77	-31.98	-29.90	1.65	-273.2	-250.0	-232.2	14.2	2.7	5.9	8.3	1.6	8.60	25.21	0.99
R17-2	23	3.0	2.6	-32.31	-31.56	-30.81	0.40	-255.5	-247.4	-240.4	3.9	2.4	5.1	7.1	1.3	9.55	53.98	0.92
SEGREGATED ICE																		
segregated ice	100	varying		-32.30	-24.50	-14.07	4.66	-235.2	-188.0	-118.4	30.2	-12.0	7.9	33.5	9.8	6.35	-32.48	0.96
RECENT PRECIPITATION																		
rain water	13			-20.69	-12.09	-8.27	3.24	-161.3	-101.1	-76.6	22.5	-10.9	-4.4	5.1	6.0	6.80	-18.92	0.96
snow patches	17			-31.43	-19.95	-9.44	8.99	-239.0	-151.6	-73.3	66.1	1.2	8.0	23.4	6.8	7.35	-4.99	1.00

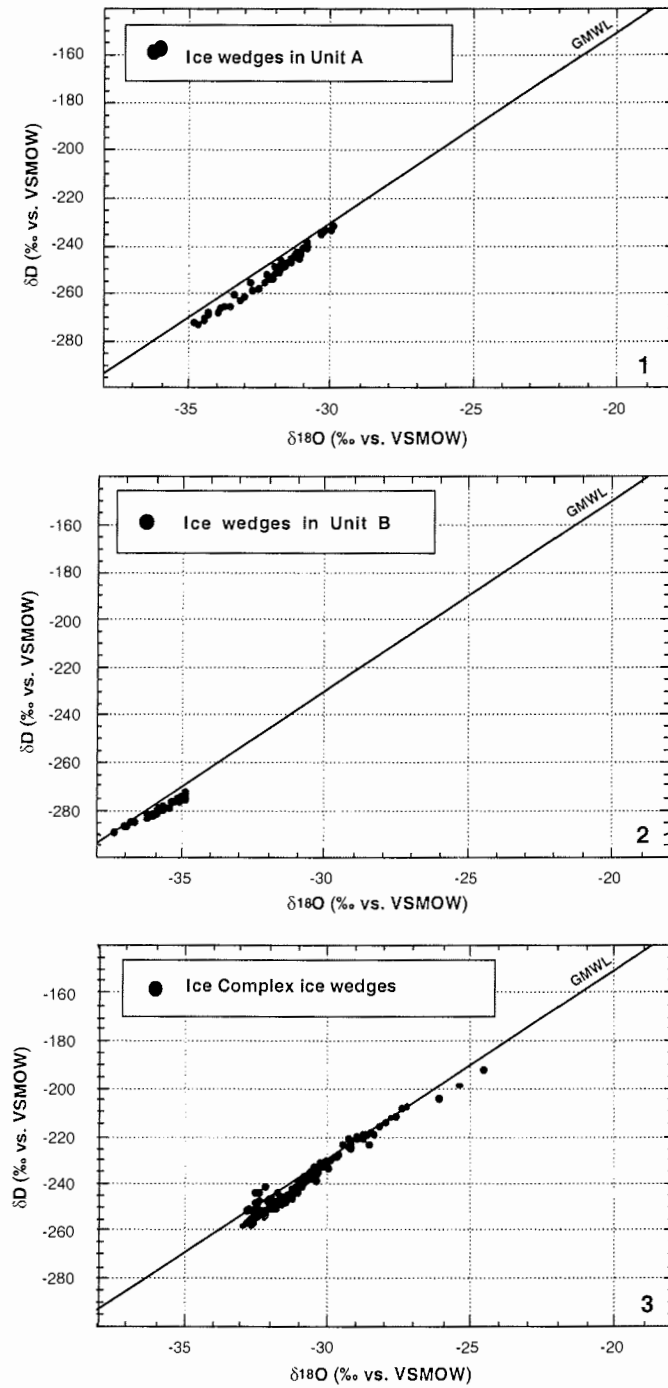


Fig. 5.5.1-5.5.3: $\delta^{18}\text{O}$ - δD diagrams for ice wedges in the older geocryological units:
 1. Unit A; 2. Unit B; 3. Ice Complex. GMWL is the Global Meteoric Water Line.

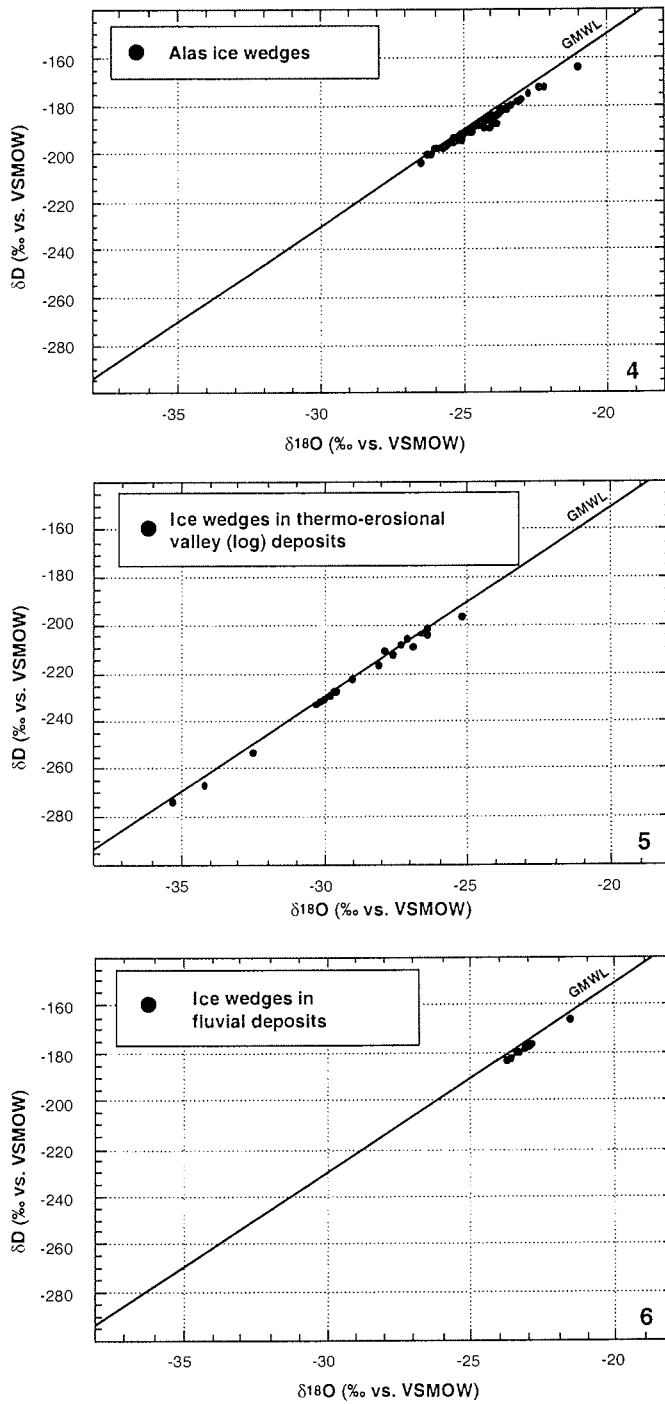


Fig. 5.5.4-5.5.6: $\delta^{18}\text{O}$ - δD diagrams for ice wedges in the younger geocryological units: 4. Alas; 5. Thermo-erosional valley (Log); 6. Fluvial deposits of Zimov'e River. GMWL is the Global Meteoric Water Line.

For ice wedges in two alases, $\delta^{18}\text{O}$ and δD values range from -26.5‰ to -21‰ and -200‰ to -160‰ (Fig. 5.5.4), reflecting much heavier isotopic composition than in all older units. The mean $\delta^{18}\text{O}$ and δD in alas ice wedges are -24.5‰ and -190‰ , with a mean d excess around 7.5. The sampled ice wedges in thermo-erosional valley deposits (Fig. 5.5.5) are of Holocene age with mean $\delta^{18}\text{O}$ and δD values of -27.5‰ and -200‰ , respectively. The ice wedge sampled in fluvial deposits of Zimov'e River exhibits subrecent to modern ice wedge growth and the heaviest mean isotopic composition with mean $\delta^{18}\text{O}$ of -23‰ and δD of -178‰ compared to all other units (Fig. 5.5.6). Only recent ice wedges, sampled in the active layer above thermo-erosional valley, alas and fluvial deposits, have heavier isotopic compositions.

The temporal development of stable isotopic composition in ice wedges is depicted in Fig. 5.6 for the different units in chronological order. Severe winter conditions are reflected in stable isotopes of the oldest Unit A. The ice wedges sampled here may be as old as 200 ka, and thus, are the oldest ice wedges ever analysed for hydrogen and oxygen isotopes. The pollen spectra of enclosing deposits (Andreev *et al.*, 2001) are dominated by taxa of grass-sedge tundra, which indicate a relatively warm and wet (summer) climate for this unit. The combination of stable isotope and pollen data leads to the assumption that the annual temperature amplitude of Big Lyakhovsky Island must have been high at that time.

In the period of ice wedge growth in Unit B, about 50 ka ago, the winter temperatures are assumed to have been extremely cold as indicated by Unit B stable isotope data. The presence of cryoxerophytic taxa in the pollen spectrum also indicate cold and dry climatic conditions (Andreev *et al.*, 2001) for the time when Unit B was formed. This is in good agreement with ice wedge morphology and stable isotope data. Interfingering of various ice veinlets and subvertical structures in the sediment ("polosatics") are related only to Unit B ice wedge growth, which is also observed in contact with the upper part of Unit A and the lower part of the Ice Complex.

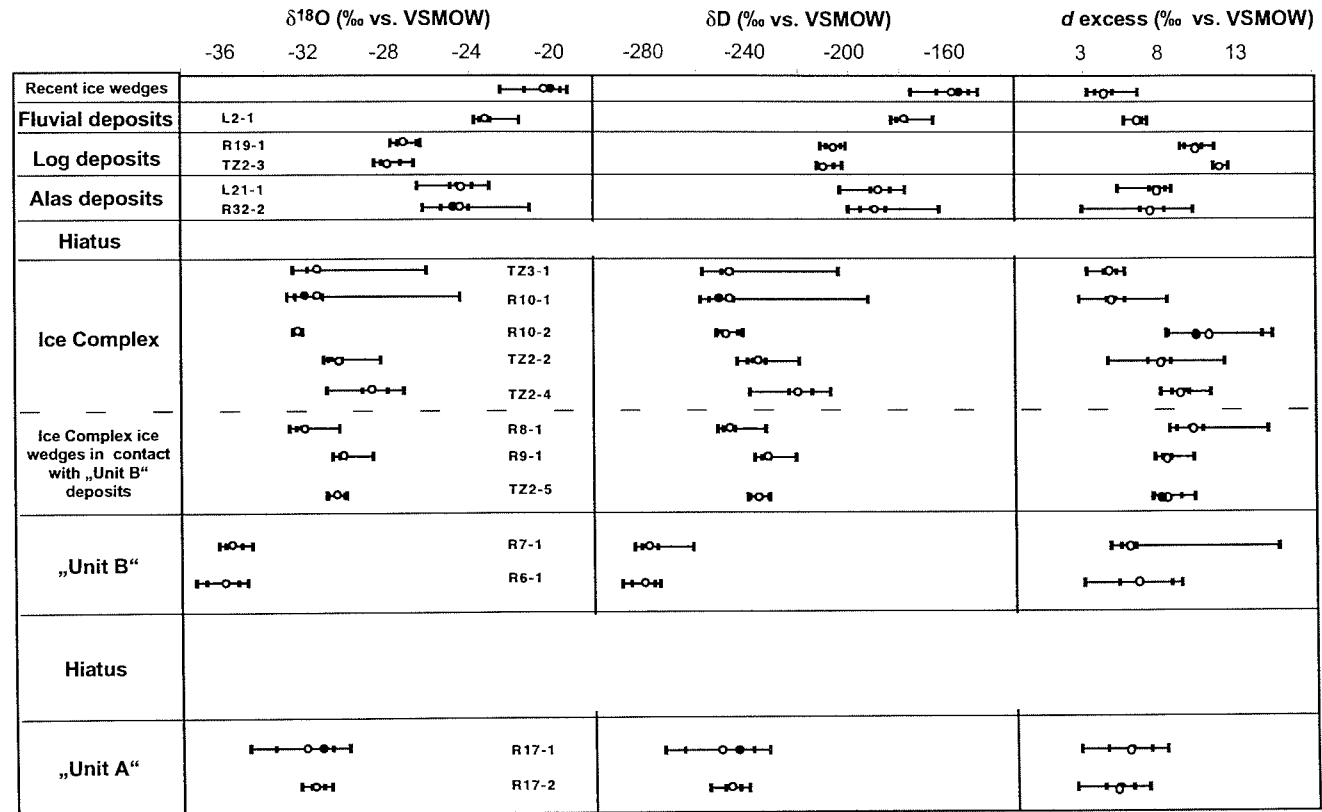


Fig. 5.6: Development of $\delta^{18}\text{O}$, δD and d excess of all ice wedges (without samples influenced by exchange processes) in "logical" stratigraphic order. White dots represent the mean isotopic composition of every ice wedge, the median (black dots) is given when different to the mean value. The respective ranges (outer bars) and the quartiles Q1 and Q3 (inner bars) are held out.

A high number of buried and multiple ice wedges in Unit B suggests a rapid deposition of the sediments. Other explanations for the burial of ice wedge „heads“ may be linked with changes in the thermal or hydrological regime, i. e. a reduced thaw depth of the active layer. There is no evidence in the sediment structures near the buried ice wedge "heads" pointing to one of these hypotheses. But the hypothesis of a high sedimentation rate is also supported by similar AMS ¹⁴C dates of *in situ* grass roots around 50 ka in the 5 to 8 m thick Unit B sediments. With high sedimentation rates, not only ice wedges, but also the vertical structures of frost cracks (these being zones of weakness) can be buried. This would lead to interfingering of ice veins (MacKay, 1974), because frost cracking could not originate in the same place. This is a possible explanation for the "polosatic" phenomenon, which consists of numerous single ice veinlets interrupted by vertical sediment-rich bands.

Another possibility to explain "polosatics", as well as the relatively low water content and the small number of ice wedges in Unit B sediments may be linked to a low amount of winter precipitation or a well-drained accumulation surface. A relatively dry climate with a thin snow cover would result in low heat insulation and less melt water entering frost cracks, possibly without forming an ice vein at every frost cracking event. A consequence would be frequent and deep frost cracking, which could also explain the interfingering ice-soil-wedges entering sediments of Unit A.

In summary, the numerous phenomena found in Unit B are certainly linked with the competition of sedimentation and winter precipitation. Nevertheless, the existing data do not allow deciding whether the higher sedimentation rate or relatively lower precipitation is the responsible process. Since "polosatics" are also found near the lower boundary to the Ice Complex with heavier isotopic composition, we interpret "polosatics" as being indicative of the initial stage of ice wedge growth and perhaps represent the beginning of the Late Pleistocene Ice Complex formation on Big Lyakhovsky Island. This is supported by the occurrence of relatively small ice wedges in the lower part of the Ice Complex.

For the Ice Complex, winter temperatures were assumed as relatively cold for the investigated time interval between about 50 ka BP and 28.7 ka BP. Low

total pollen concentration dominated by typical tundra species also reflects cold climatic conditions, more humid than before (A. Andreev, pers. comm.). However, compared to Unit B a climate warming of both winter and summer temperatures has to be assumed. Winter temperatures were slightly warmer but comparable to ice wedges from Unit A. Due to the similar stable isotopic composition, we consider Unit A as an older equivalent of the Ice Complex. This is supported by a similar sediment matrix, a high gravimetric ice content (60 to 170wt%), a similar type of ice wedges and the presence of paleosols and ice belts interrupted by lens-like reticulate cryostructures in both units.

The Holocene ice wedges reflect much warmer winter temperatures compared to the Pleistocene ice wedges. The rise in $\delta^{18}\text{O}$ of about 6‰ and in δD of 40‰ reflects the amelioration of the global climate at the Pleistocene-Holocene boundary, which is known from several climate archives worldwide such as glacier and ground ice (e. g. Cuffey *et al.*, 1995; Meyer *et al.*, 2002). An increase of the total pollen content and the occurrence of shrub pollen confirms this climate warming trend, with most favourable climatic conditions between 9 ka BP and 4.5 ka BP and subsequent cooling of the climate after 4.2 ka BP (Andreev *et al.*, 2001) Ice wedge growth in alas and thermo-erosional valleys probably started after this climate deterioration. In alas ice wedges, slightly warmer winter conditions are seen, as compared to ice wedges in thermo-erosional valleys. A subrecent ice wedge in fluvial deposits of the Zimov'e River indicates even warmer winter temperatures in the Holocene. Only recent ice wedges identified by high tritium concentrations (Dereviagin *et al.*, 2002) show heavier isotopic composition. Hence, Big Lyakhovsky Island has never been as warm in winter than at the present time. For ice wedges of the Holocene fluvial and thermo-erosional valley deposits and recent ice wedges, slopes in the $\delta^{18}\text{O}$ - δD diagram vary around 7.5. Alas ice wedges with relatively low slopes of 7.1 may be influenced by further evaporation, possibly due to the participation of melt water running down slopes (Meyer *et al.*, 2002).

Evidently, the recent synoptic situation for the winter precipitation on Big Lyakhovsky Island is different compared to Bykovsky Peninsula (Meyer *et al.*,

2002), which is fed by Atlantic moisture. This can be seen in the slope of 7.1 in the $\delta^{18}\text{O}$ - δD diagram for snow samples of Big Lyakhovsky Island, pointing to either moisture from a source region enriched in heavy isotopes, or to a change of the low amount of snow by mixing, melting or evaporation/sublimation. Kuznetsova (1998) reports that in winter, the influence of moisture originating from the Pacific easterlies and Atlantic Ocean westerlies meet between 130° and 150° E. Precipitation in Canada originating in the Pacific Ocean is characterized by a low d excess (Clark and Fritz, 1997). Consequently, the Pacific Ocean is a possible winter precipitation source for Big Lyakhovsky Island. Recent ice wedges on Big Lyakhovsky Island show an isotopic composition different to that of snow. Therefore, variations in the isotopic composition (especially in the d excess) of ice wedges through time cannot simply be related to the moisture source of the precipitation. Other local processes such as fractionation in the snow cover, i. e. by melting or sublimation/evaporation have to be taken into account for the temporal variations in the d excess of ice wedges.

On the Bykovsky Peninsula, 50 km SE of the Lena Delta, a shift towards high d excess was found around 20 ka BP. This was interpreted as a change of the moisture source (Meyer *et al.*, 2002). If a similar change of the main winter precipitation source took place, we should expect a sharp increase in d excess between the youngest Ice Complex and Holocene ice wedges. On Big Lyakhovsky Island, a slight increase from 5‰ (in the Ice Complex) to 7‰ (in alas and in fluvial deposits) is observed. Despite the lack of ^{14}C dated samples for the time interval between 28 ka BP and 12 ka BP, the slight increase in d excess indicates no significant change of the main precipitation source at that time.

5.9 Conclusions

The study of ice wedges on Big Lyakhovsky Island in the eastern Laptev Sea, northern Siberia, reveals permafrost conditions for periods of the last 200 ka. By means of stable isotope analyses, six generations of ice wedges are distinguished and used for the reconstruction of paleoclimatic variations. This

paleoreconstruction is based on the comparison between the stable isotope composition of recent precipitation (both snow and rain) with recent ice wedges, which were identified by means of tritium analyses. On Big Lyakhovsky Island, recent ice wedges are most likely fed by melt water of the later stages of snow melt, and consequently winter temperatures are derived from ice wedges.

The variations of the oxygen and hydrogen isotopic composition reveal distinct changes in the winter climate history on Big Lyakhovsky Island. A period of cold winter temperatures was determined for an old equivalent of the Late Pleistocene "Ice Complex" at about 200 ka. According to radiocarbon data, a hiatus of more than 100 ka in the sedimentation history including the Eemian was followed by a short period of extremely cold winters around 50 ka BP characterized by high sediment accumulation rates sometimes exceeding vertical ice-wedge growth rates. Peculiar ice-soil wedges ("polosatics") initiate the ice wedge growth for the classical Late Weichselian Ice Complex. During Ice Complex formation, winters must have been cold. A warming trend between Pleistocene and Holocene ice wedges is found in sharply increasing $\delta^{18}\text{O}$ and δD values. The warmest winter temperatures were derived from recent ice wedges on Big Lyakhovsky Island.

6. SYNTHESIS

6.1 Paleoclimatic history of Northern Siberia

Hydrogen and oxygen isotopes and hydrochemistry of ice wedges from Bykovsky Peninsula and Big Lyakhovsky Island have been used to reconstruct the Late Quaternary climate history of the Laptev Sea area, Northern Siberia. The stable isotopic composition of ice wedges is fed by winter precipitation (MacKay, 1983, Vaikmäe, 1991) and, thus, may be correlated with mean winter or January temperatures (Vasil'chuk, 1992). Being part of the ongoing research, stable isotope data from two sites in the western part of the Lena delta add supplementary information for the paleoclimatic interpretation. Combined with literature data from the Taymyr Peninsula (Siegert *et al.*, 1999; Boike, 1997), we were able to gain an understanding of the (1) temperature development through time, (2) moisture sources for the winter precipitation, (3) processes and site-specific properties influencing the stable isotopic composition in ground ice. This enables us to draw and to interpret the picture of the regional climatic history.

Age determinations are crucial for every paleoclimatic reconstruction. The studied sequences on Bykovsky Peninsula reveal a clear age model. The continuous record of Ice Complex deposits and ground ice as well as the Holocene ground ice of alás and log cover about 60 ka of paleoclimatic evolution. The situation on Big Lyakhovsky Island is a bit more complicated, because (1) the record covers more than 200 ka, and (2) it is interrupted by gaps in the sedimentation history and in ground ice formation due to thermokarst.

On Big Lyakhovsky Island, the Late Pleistocene Ice Complex is underlain by two older Units A and B (Fig. 5.2). In the upper part of Unit A, a frozen peat sample was dated to 200 ka BP by $^{230}\text{Th}/\text{U}$ method (Schirrmeister *et al.*, 2002b). The ice-rich permafrost in Unit A represents the oldest ground ice ever analysed by means of hydrogen and oxygen isotopes. Unit A, which we interpret as an old equivalent of the Late Pleistocene Ice Complex, is characterised by low winter temperatures reflected in a mean isotopic composition of -31.5‰ in $\delta^{18}\text{O}$

and -250‰ in δD . According to $^{230}\text{Th}/\text{U}$ and radiocarbon age determinations, a hiatus of about 150 ka between Unit A and B can be assumed.

According to our AMS ^{14}C dating, Unit B was rapidly deposited around 50 ka BP on Big Lyakhovsky Island. In this unit, the stable isotope analyses of ice wedges revealed the lightest mean $\delta^{18}\text{O}$ and δD values (-35.5‰ and -280‰) of all sampled ice wedges, respectively. Consequently, the coldest winters for Big Lyakhovsky Island are assumed during the deposition of Unit B. At that time, the Bykovsky Peninsula was already subject to Ice Complex formation.

On Bykovsky Peninsula, the coldest winter temperatures were reflected around 55 to 60 ka BP in the stable isotopic composition of ice wedges ($\delta^{18}\text{O} = -32\text{‰}$; $\delta\text{D} = -250\text{‰}$) sampled near the sea level. On Bykovsky Peninsula, the Ice Complex is extended beneath the sea level and therefore the underlying unit could not be studied. However, Grigoryev *et al.* (1996) reported the occurrence of the Ice Complex 15 m below the sea level in the coastal area near the Mamontovy Khayata outcrop, Bykovsky Peninsula. Since the age model for the Bykovsky Peninsula reveals a relatively continuous vertical accumulation rate for the Ice Complex of about 0.7 m/ky, a maximum age of about 80 ka BP can be derived for the Ice Complex. Sites such as the Bykovsky Peninsula, where the base of the Ice Complex is situated below sea level, are often connected with neotectonic subsidence (Romanovskii *et al.*, 2000).

In contrast, on Big Lyakhovsky Island and in the western Lena delta, the base of the Ice Complex is located above sea level. In the Lena delta, fluvial sediments of the Lena River underlay the Ice Complex deposits, dated to 40-80 ka BP by infrared optical stimulated luminescence (IR-OSL) (Schwamborn *et al.*, 2002). The sparseness of ice wedges in these sandy deposits resembles Unit B on Big Lyakhovsky Island. However, the mean isotopic composition of ice wedges in the Lena sediments is different in $\delta^{18}\text{O} = -20\text{‰}$, $\delta\text{D} = -165\text{‰}$ and d excess of -2‰ (Meyer, unpubl. data). Relatively heavy δ values and low d excess are probably related to ice wedge growth fed by river water. This hypothesis is supported by a similar $\delta^{18}\text{O}$ value for recent water of the Lena River ($\delta^{18}\text{O} = -20.6\text{‰}$; Bauch, 1995). River waters reflect (1) the isotopic composition of the precipitation in the hinterland integrating the whole year and

(2) evaporation effects, and thus are assumed as poor indicators for climatic variations.

According to AMS ^{14}C ages, the formation of the Late Pleistocene Ice Complex started around 50 ka BP on Big Lyakhovsky Island and at about 43 ka BP in the western Lena delta (Schwamborn *et al.*, 2002). The winter temperatures during the Ice Complex formation are reflected in the stable isotopic composition of huge syngenetic ice wedges of the locations Big Lyakhovsky Island, Bykovsky Peninsula and the western Lena delta. These three regions show constant mean $\delta^{18}\text{O}$ values between -28‰ and -32‰ and mean δD values from -210‰ to -245‰ reflecting cold and stable winter temperatures without large regional differences for the whole period of the Ice Complex formation. In the Labaz Lake region, Taymyr Peninsula, Late Pleistocene ice wedges attributed to the Karginian time (Middle Weichselian interstadial, 50-25 ka BP) revealed heavier isotopic composition of -24‰ in $\delta^{18}\text{O}$ and -180‰ in δD (Siegert *et al.*, 1999) and possibly warmer winter temperatures.

For the same time interval, large variations in the isotope record and several interstadial periods with heavy $\delta^{18}\text{O}$ values are described in Greenland glacier ice cores (Dansgaard *et al.*, 1993). Schirrneister *et al.* (2002a) distinguish a middle horizon in the Bykovsky outcrop (between 10 m and 25 m a.s.l., corresponding to the time interval between 50 and 28 ka BP) by the presence of numerous peaty soil horizons and changing geochemical parameters. The alternations of peaty horizons and mineral layers are interpreted as possible equivalent of Dansgaard-Oeschger cycles and as a period of changing surface conditions (Schirrneister *et al.*, 2002a). Nevertheless, large variations as revealed in the stable isotope record of Greenland ice cores are definitively not found in the stable isotopic composition of ice wedges in Northern Siberia. This fact is interpreted as relatively stable climatic situation of cold winter temperatures between 50 and 20 ka BP, which is accompanied by an increased influence of the Siberian anticyclone during the cold periods (Rozenbaum & Shpolyanskaya, 1998).

The well-dated record of Bykovsky Peninsula reveals only one stage of slightly warmer winter temperature around 42 ka. This is indicated by relatively heavy $\delta^{18}\text{O}$ values of parts of a horizontal sampling transect (11.1 m a.s.l.) in an Ice Complex ice wedge (Fig. 4.6.2). On Big Lyakhovsky Island, a similar heavy isotopic composition of a (yet undated) ice wedge is found at 22 m a.s.l.. The problems related to the interpretation of variations in the stable isotope data within horizontal sampling transects are discussed in detail in Chapter 4. Especially old ice wedges may be changed isotopically due to lateral moisture exchange with the adjacent sediments. For the interval between 40 to 30 ka BP, more favourable and relatively moist climatic conditions with slightly higher summer temperatures are revealed by pollen analyses and other bioindicators for the Bykovsky Peninsula and Big Lyakhovsky Island (Andreev *et al.*, 2001, Kienast *et al.*, 2001). Between 25 and 12 ka BP, relatively stable sedimentary conditions are indicated by low variations in the geochemical parameters and a low intensity of soil formation (Schirmer *et al.*, 2002a). The Late Pleistocene cold period is reflected in the pollen spectra between 26 and 16 ka (Andreev *et al.*, 2002), but evidently not found in the isotopic composition of Ice Complex ice wedges. Apparently, the formation of Ice Complex is linked to relatively constant cold winter temperatures. Variations in the summer temperatures are not necessarily reflected in the ice wedges.

For the Ice Complex of Bykovsky Peninsula, ice wedge growth in the uppermost layer (36-37 m) can be differentiated by means of stable hydrogen and oxygen isotopes. Here, the heaviest mean isotopic composition for Ice Complex ice wedges is observed ($\delta^{18}\text{O} = -25.8\text{‰}$ and $\delta\text{D} = -195.7$), corresponding to a warming of the mean winter temperatures. The ice wedge was dated to AMS ^{14}C ages of 11.2 and 9.3 ka BP. This signifies that ice wedge growth in the Ice Complex proceeded to the Early Holocene, when the sedimentation had already stopped. However, at other locations thermokarst already started to destroy the Ice Complex around 13 ka, when the shoreline was located 45 to 60 m below the present sea level (Romanovskii *et al.*, 2000).

Significant climate and environmental changes marked the Pleistocene-Holocene transition. A characteristic of all isotope records is a sharp rise in $\delta^{18}\text{O}$

and δD values between Pleistocene and Holocene ice wedges. For the Bykovsky Peninsula, Big Lyakhovsky Island and the western Lena delta, this rise comprises about 5‰ in $\delta^{18}O$. A similar difference of 6 ‰ in $\delta^{18}O$ between Pleistocene and Holocene ice wedges is described for the Lower Kolyma region (Vaikmäe, 1989). The abrupt shift in the isotopic composition of ice wedges is also found in the stable isotopic composition of Greenland glacier ice cores, and according to that, interpreted as significant warming trend. This climate change is confirmed by increasing tree and shrub pollen in the pollen spectra of the Bykovsky Peninsula (Andreev *et al.*, 2001, 2002) pointing to most favourable climatic conditions around 8.2 ka. For the Taymyr Peninsula, a large number of ^{14}C ages on trees around 8-7 ka BP (Siegert *et al.*, 1999) indicate that the tree line lay further to the north at that time. At 7.5 ka BP, the Laptev shelf was flooded to an isobath of 20 m below the present sea level (Romanovskii *et al.*, 2000).

On Bykovsky Peninsula, between the end of the Ice Complex accumulation and the beginning of ice wedge growth in alas around 4.5 ka, ice wedge growth was limited due to the existence of numerous thermokarst lakes. Despite a dense vegetation cover in the Holocene warm period, no organic material could be dated in ice wedges at that time. To compare between the Pleistocene and the Holocene, this "gap" in ice wedge formation must be considered. On Big Lyakhovsky Island, the alas ice wedges are younger than the enclosing sediment and formed in the last 1 ka, after the thermokarst lakes fell dry. The oldest AMS ^{14}C dating of organic matter gives an age of around 3 ka in alas ice wedges of the Bykovsky Peninsula.

Because of the different time of ice wedge growth at both localities, alas ice wedges are more difficult to interpret. Additionally, alas ice wedges of Bykovsky Peninsula and Big Lyakhovsky Island in general show slopes of 7 in the $\delta^{18}O$ - δD diagram (Fig. 4.7.3). This deviation from the GMWL points to kinetic fractionation processes (Dansgaard, 1964) taking part in ice wedge formation. A possible explanation for this effect is the participation of evaporated water in ice wedge formation. This could happen due to the influence of water running down the slopes of the Ice Complex as assumed for the Bykovsky Peninsula or due to

flooding events. Therefore, the paleoclimatic information of alas ice wedges is reduced, because either the isotopic composition of the snow has been changed or snow was not the only source for alas ice wedges. These site-specific characteristics must be considered.

Ice wedges in thermo-erosional valleys (logs), which have been formed in the last 1000 years at both sampling sites, in general do not show kinetic fractionation effects. The mean $\delta^{18}\text{O}$ values of log ice wedges range around -27‰ on Big Lyakhovsky Island and between -23.5‰ and -28‰ on Bykovsky Peninsula. Accordingly, Big Lyakhovsky Island was colder in winter during the time of log ice wedge growth. On Big Lyakhovsky Island, a subrecent ice wedge in fluvial deposits of the Zimov'e River is characterised by a mean $\delta^{18}\text{O}$ of -23‰ , thus by relatively warm winter temperatures.

The Holocene ice wedge history shows a period of restricted ice wedge growth until 4.5 ka BP. After a climate deterioration, indicated by pollen data from Bykovsky Peninsula at that time (Andreev *et al.*, 2002), ice wedge growth was reinitiated, when the thermokarst lakes fell dry. Log and alas ice wedges of Big Lyakhovsky Island and Bykovsky Peninsula show variable mean $\delta^{18}\text{O}$ between -23‰ and -28‰ . In the western Lena delta, slightly warmer winter temperatures are indicated by the mean oxygen isotope data ($\delta^{18}\text{O} = -22\text{‰}$ to -26‰) of Holocene ice wedges. According to the mean isotopic composition of ice wedges, the Holocene is relatively variable in winter temperatures. This is in contrast to results from the Greenland ice cores, which contain only slight variations in stable isotopes in the Holocene ice (Dansgaard *et al.*, 1993).

The comparison of the stable isotopic composition of snow and recent ice wedges provides the base for the interpretation of ice wedges as paleoclimatic indicators and for absolute winter temperature reconstruction (Vasil'chuk, 1992). For all study areas, it was demonstrated that mean $\delta^{18}\text{O}$ and δD values of snow and recent ice veins correspond very well to each other (Tab. 6.1) proving that ice wedges are fed by snow meltwater. The isotopic composition of rain with slopes of 6.8 in the $\delta^{18}\text{O}$ - δD diagram and low d excess differs considerably from that of snow and recent ice veins (Fig. 4.5 and 5.4). Consequently, summer precipitation originates, at least in parts, from a different moisture source

enriched in heavy isotopes, such as terrestrial surface waters. Tritium analyses from Big Lyakhovsky Island revealed high ^3H values in modern snow and ice veins (Dereviagin *et al.*, 2002) proofing (1) modern ice wedge growth and (2) the close relationship between snow and ice wedges in all sampling sites. Comparing different locations, Big Lyakhovsky Island shows the heaviest isotopic composition for both, recent ice wedges and snow differing in mean $\delta^{18}\text{O}$ by about 5‰ from samples of the Bykovsky Peninsula and the western Lena delta. This is surprising, because the mean annual air temperature on Big Lyakhovsky Island is even lower than on Bykovsky Peninsula. For Big Lyakhovsky Island, a mean $\delta^{18}\text{O}$ of -20‰ in recent ice wedges and snow demonstrates that the winter temperatures have never been as warm as today. The spatial difference in d excess may be explained by different moisture sources for the western regions compared to the Big Lyakhovsky Island, and will be discussed in the next chapter.

Tab. 6.1: Mean isotopic composition of snow, recent, Holocene and Pleistocene ice wedges for different locations of the Laptev Sea region

Region (sampling year)	Bykovsky Peninsula (1998)			Big Lyakhovsky Island (1999)			Western Lena Delta (2000)			Taymyr (Labaz Lake) (1994/1995)			
type	δD (‰)	$\delta^{18}\text{O}$ (‰)	d (‰)	δD (‰)	$\delta^{18}\text{O}$ (‰)	d (‰)	δD (‰)	$\delta^{18}\text{O}$ (‰)	d (‰)	δD (‰) ⁽¹⁾	$\delta^{18}\text{O}$ (‰) ⁽¹⁾	d (‰) ⁽²⁾	
Rain	-116	-14.8	2.7	-101	-12.1	-4.4							
Snow	-176	-23.2	9.3	-152	-20.0	8.0	-190	-24	12.5	-180	-24	11	
Recent ice wedges	-186	-24.8	12.4	-159	-20.4	4.5	-190	-26	13				
Holocene ice wedges (<4.5 ka) (fluvial) (alas) (log)	-190 -190	-28 -25.5	14 12.5	-180 -190 -205	-23 -24.5 -27.5	6.6 7.5 11	-160 to -190	-22 to -26	12	-117 to -165 (range)	-16 to -23 (range)	6 to 14 (range)	
Ice Complex	Early Holocene (11-9 ka)	-195	-25.8	10.5									
	Sartanian (25-12 ka)	-230	-29.5	6	-220 to -250	-28.5 to -31.5	5 to 11	-230	-29	5 to 7	-210 -180 to -230	-26 to -28.5 -24 to -30	6.5 to 11 8 to 13
	Karginian (55-25 ka)	-230 to -245	-29 to -31.5	2 to 5									
	60-55 ka	-250	-32	4.5									
Fluvial deposits (40-80 ka)							-165	-20	-2				
Unit B (~ 50 ka)				-280	-35.5	5.5 to 10							
Unit A (~200ka)				-250	-31.5	6							

(1) Siegert *et al.* (1999); (2) Dereviagin (pers. comm)

6.2 Moisture sources for ice wedges

On Bykovsky Peninsula, in the western Lena delta and on Taymyr Peninsula (Boike, 1997), snow samples are located on the global meteoric water line (GMWL), with a slope of 8 in the $\delta^{18}\text{O}$ - δD diagram (Fig. 4.5). This points to (1) no significant fractionation of the snow and (2) a common oceanic moisture source. This is confirmed by a very uniform mean isotopic composition around $\delta^{18}\text{O} = -23.5\text{‰}$ in snow of the three western sites (Tab. 6.1). The present moisture source of the winter precipitation of this "western province" is located in the Northern Atlantic (Spielhagen, 2001, Boike, 1997). This is in good agreement with the cyclone trajectories during the winter months (Murray & Simmonds, 1995), when westerlies dominate all over Northern Eurasia (Kuznetsova, 1998). The influence of moisture originating from the Pacific Ocean (Leroux, 1993) and the Indian Ocean (Aizen *et al.*, 1996) is limited by high mountains acting as orographic barriers and by the atmospheric circulation. In winter, Pacific air masses meet Atlantic moisture in a region between 130°E and 150°E in Northern Siberia (Kuznetsova, 1998). The Arctic Ocean and lakes are frozen in winter, except the polynya, an ice-free belt in the Laptev Sea, which is a possible local moisture source.

For Big Lyakhovsky Island, the situation is different. The snow shows a relatively heavy isotopic composition and the influence of kinetic fractionation processes, such as a slope of 7.4 in the $\delta^{18}\text{O}$ - δD diagram and relatively low d excess (Fig. 5.4). These spatial differences in the isotopic composition of snow are confirmed by relatively heavy $\delta^{18}\text{O}$ and δD values and low d excess in recent ice wedges of Big Lyakhovsky Island as compared to the western region (Tab. 6.1). Consequently, an isotopically different moisture source is assumed for the winter precipitation of Big Lyakhovsky Island. A possible source is Pacific-derived moisture (Kuznetsova, 1998), which is characterised by higher humidity and low d excess (Clark & Fritz, 1997) or a local source such as the polynya, but also a mixture of two or more sources.

For the Holocene, the ice wedges of the "western province" in general show high d excess around 10‰ , including the youngest Ice Complex ice wedge on Bykovsky Peninsula. In contrast, the Holocene ice wedges on Big Lyakhovsky

Island are characterised by lower mean d excess. Consequently, the differences in the moisture source regions for both provinces must have been existed through the Holocene, even though the differences in d excess are smaller than for snow and recent ice wedges between these regions.

A sharp increase in mean d excess of 5-6‰ between Pleistocene and Holocene ice wedges is found on Bykovsky Peninsula (Fig. 4.8) and confirmed for the western Lena delta (Tab. 6.1). This is interpreted as a change of the winter precipitation source, leading to higher d excess in the Holocene compared to the Pleistocene. The change of the moisture source must have been happened between 18.5 ka and 11.2 ka BP, according to a new AMS ^{14}C dating in the sediment near ice wedge MKh-00 (Figs. 4.3 and 4.7.1). On Big Lyakhovsky Island, the situation is different, because the mean d excess of recent, Holocene and Pleistocene ice wedges is in general lower than 10‰ (Tab. 5.1). Accordingly, a distinct increase in d excess between the youngest Ice Complex ice wedge and the Holocene ice wedges is not found. The moisture source region in winter was constant for Big Lyakhovsky Island through the whole period of ice wedge formation. Consequently, we assume the Pacific Ocean to be the moisture source for Big Lyakhovsky ice wedge growth. The reason, why some of the ice wedges of Big Lyakhovsky Island show higher d excess is not solved yet.

The shift in d excess between Pleistocene and Holocene ice wedges of the western province, where the moisture presently derives from the Atlantic Ocean, indicates a change of the main source for the winter precipitation. Two scenarios are possible explaining the change of the moisture source for Pleistocene winter precipitation reaching Northern Siberia: (1) the moisture source was located in the Pacific Ocean or (2) the winter precipitation originated at lower latitudes in the Atlantic.

During the LGM, a glacier occupied large areas of Western Siberia (Svendsen *et al.*, 1999) and acted as a morphological barrier (Leroux, 1993). Atlantic air masses were deviated or even blocked. This would favourise a change of the winter precipitation source from the Atlantic to the Pacific. The Northern Atlantic was covered by sea ice during LGM (Koç *et al.*, 1993). As a

consequence, moisture reaching the western province from the West must have originated further to the south. Variations in $\delta^{18}\text{O}$ and δD profiles of Greenland ice cores were interpreted as a southward displacement of the polar front during periods of cold climatic conditions (Johnsen & White, 1989). Moreover, for an Antarctic glacier ice core, Jouzel *et al.* (1982) interpreted an increase in the d excess from 4‰ to 8‰ across the Pleistocene-Holocene transition as a result of higher humidity in the moisture source region under glacial conditions. Accordingly, both proposed changes in the atmospheric circulation pattern are possible reasons for low d excess in the western regions before LGM and through the whole period of Ice Complex formation. However, moisture supply is the main factor to determine at what time and what place ice sheets grow. The ice sheets of Western Eurasia were formed in periods when the snow fall rate exceeded the summer melting (Spielhagen, 2001), evidently deriving from the West. Therefore, we favourise an Atlantic moisture source region for the Pleistocene winter precipitation in the “western province”, located further to the south as compared to the present situation.

6.3 Absolute temperatures

A linear relationship between annual (or monthly) values of $\delta^{18}\text{O}$ and δD with mean annual (or monthly) temperatures at a precipitation site is the base of all climatological reconstruction with stable isotopes. The spatial and temporal relationship between surface temperatures and $\delta^{18}\text{O}$ or δD is assumed to be relatively constant (Jouzel *et al.*, 1997). The accuracy of the $\delta^{18}\text{O}$ paleothermometer is reduced by the seasonality of precipitation and evaporation effects.

Ice wedges have been shown to be useful archives for a relative winter temperature reconstruction. For a reconstruction of absolute winter temperatures with ice wedges, the calibration of the paleothermometer is necessary. Most approaches dedicated to derive temperatures from ice wedge isotope data are based on the hypothesis, that single ice veins in the still frozen part of the active layer reflect winter (or January) temperatures. Ice veins from

different locations sampled in different years should form a linear relationship in the $\delta^{18}\text{O}$ /temperature (δ/T) diagram. For Northern Russia, Vasil'chuk (1992) calculated a relationship between $\delta^{18}\text{O}$ of elementary ice veins and mean annual winter temperature of 1‰ per °C as well as mean January temperature of 1.5‰ per °C. Neither the quality of the correlation nor the exact ages of the ice veins are provable. Nikolayev & Mikhalev (1995) calculated a δ/T correlation of 0.83-0.86‰ per 1°C for $\delta^{18}\text{O}$ of single ice veins from 15 regions in Russia for the "cold" season, when precipitation falls as snow, and 0.48‰ per 1°C for January temperatures.

Therefore, we plotted all available data (Vasil'chuk, 1992; Nikolayev & Mikhalev, 1995; Fukuda, 1994; Dereviagin *et al.*, 2002) in a δ/T diagram deriving new δ/T equations for winter and January temperatures (Figs. 6.1 and 6.2):

$$\text{mean winter temperature } (T_w) \quad \delta^{18}\text{O} = 1.02 T_w - 0.72 \quad (R^2=0.81) \quad (1)$$

$$\text{mean January temperature } (T_{\text{Jan.}}) \quad \delta^{18}\text{O} = 0.59 T_{\text{Jan.}} - 3.46 \quad (R^2=0.72) \quad (2)$$

The mean winter temperature is related to the period, when the precipitation falls as snow. Since most of the samples were published by Vasil'chuk (1992), it is evident that the new equations are similar to his calculations. The results for recent ice veins of Big Lyakhovsky Island (N=8) and Bykovsky Peninsula (N=22) fit these correlations.

For the identification of the most recent ice veins in our working areas, we performed tritium analyses. The ^3H concentrations in recent ice wedges are too high to be explained by an old thermonuclear reaction (Dereviagin *et al.*, 2002). Even though the beginning and cause for this new regional tritium mark are unknown, it enables us to recognise the most recent ice veins, which we correlated with mean winter and January temperatures from the NOAA data archive. This improvement of the method still lacks the attribution of one discrete single ice vein to a distinct year.

Synthesis

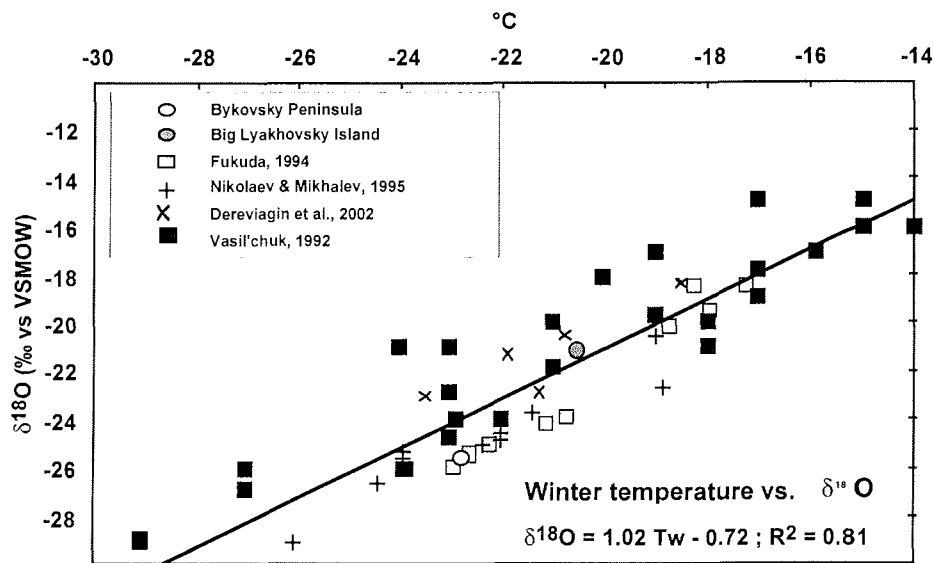


Fig. 6.1: Absolute temperature reconstruction of the mean annual winter temperature by means of a correlation with recent ice veins

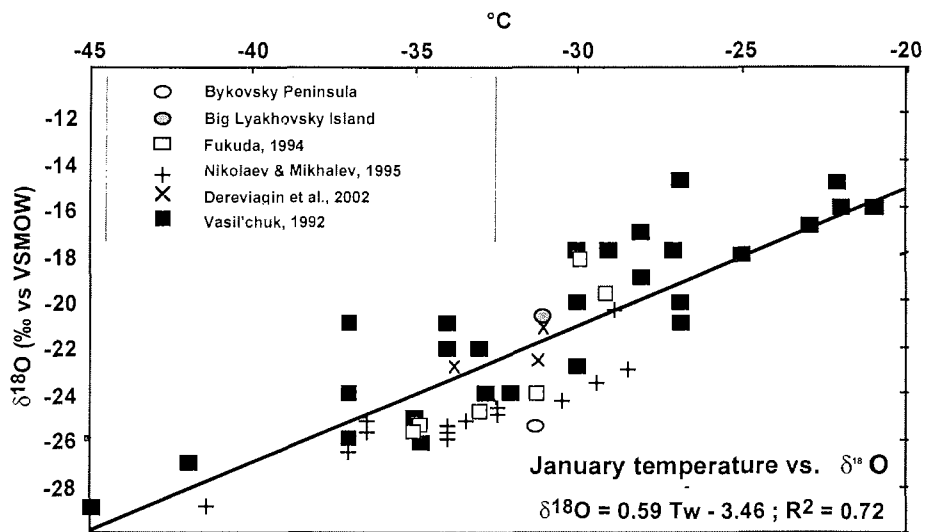


Fig. 6.2: Absolute temperature reconstruction of the mean January temperature by means of a correlation with recent ice veins

The next step is the application of the δ/T relationship to Holocene and Pleistocene ice wedges. We applied the equations one by one to the older ice

wedges of Unit A and Unit B from Big Lyakhovsky Island, and to ice wedges of the Ice Complex and of the Holocene units from all sampled regions. The results were compared with the present temperatures for the Bykovsky Peninsula and Big Lyakhovsky Island being $T_{Jan.} = -31.3^{\circ}\text{C}$ and -31.0°C and $T_w = -22.9^{\circ}\text{C}$ and -20.6°C , respectively. The resulting winter temperatures are of about 9°C colder for Unit A, 13°C colder for Unit B, 5 to 9°C colder for the Ice Complex and around the same temperature for Holocene ice wedges. For January temperatures the same calculation was performed leading to about 16°C colder temperatures for Unit A, 23°C colder for Unit B, 11 to 17°C colder for the Ice Complex and 2 to 10°C colder for Holocene ice wedges. The error of this reconstruction is estimated to $\pm 2^{\circ}\text{C}$ and $\pm 3^{\circ}\text{C}$ for the winter and January temperatures, respectively. According to Nikolayev & Mikhalev (1995), temporal variations of $\delta^{18}\text{O}$ in the ocean water from which the moisture originates, of the relative air humidity and of the sea surface temperature have to be taken into account for the calculation of absolute temperatures. They estimated the respective January and winter temperatures to be 3°C and 2°C higher during the cold marine oxygen isotope stages 2, 4 and 6, than calculated by the equations (1) and (2). This reconstruction of absolute temperatures is a first approach and the present state of an ongoing research.

7. CONCLUSIONS

The aim of this research was to reconstruct the Late Quaternary paleoclimatic and paleoenvironmental changes in Northern Siberia. We used the following strategy to accomplish this goal:

The first step was to establish a method suitable for a large amount of samples for oxygen and hydrogen isotope analyses on ground ice. For this purpose, the mass spectrometer was calibrated and a laboratory standard NGT1 was introduced, apt for isotopically light samples such as ground ice. If water samples smaller than 1 ml are measured in the Delta-S mass spectrometer, a balance correction has to be applied. This is important for future studies with higher-resolution sampling on ice wedges.

Hydrogen and oxygen isotopes of ground ice, especially of ice wedges, proved to be important proxies for the reconstruction of the Late Quaternary climate history in the non-glaciated areas of Northern Siberia. The stable isotopic composition of ice wedges is fed by winter precipitation and, thus can be correlated with mean winter or January temperatures. Lateral migration of bound water to ice wedges may alter the isotopic composition at the interface ice wedge-segregated ice, especially for old ice wedges. This fact has to be considered to interpret stable isotope data for paleoclimate studies.

The permafrost sequences of Big Lyakhovsky Island and Bykovsky Peninsula reflect the climate history of the last 200 ka. The stable isotopic composition of ice wedges allows to distinguish a period of very cold winters (60-55 ka), from a following long stable period of cold winter temperatures (50-20 ka). In stable isotope data of ice wedges, an abrupt climatic warming trend is indicated for the Pleistocene-Holocene boundary, also known from Greenland ice cores. In the Holocene warm period between 8 to 4.5 ka BP, ice wedge growth was limited due to thermokarst processes. From 4.5 ka until present, ice wedge growth occurred in thermokarst depressions and thermo-erosional valleys. In general, Holocene ice wedges point to more variable winter temperatures as compared to the Pleistocene ones. This is in contrast to results from the Greenland ice cores, which contain larger variations in stable isotopes

in the Pleistocene ice compared to the Holocene ice. Northern Siberia, especially in winter, is dominated by the influence of the Siberian anticyclone, whereas Greenland is subject to variations in the North Atlantic current.

The deuterium excess of ice wedges is a useful tool to identify moisture source regions for the winter precipitation. A northward displacement of the marine source of the winter precipitation to the present North Atlantic source region is possibly linked with to decay of the LGM ice sheet and occurred between 18.5 ka and 11.2 ka BP.

The presence of syngenetic ice wedges as typical permafrost feature since about 60 ka, implies that no large glacier extended over the Laptev Sea shelf during that time. This result contradicts the theory of Grosswald *et al.* (1999).

Ideas for future research

- 1 The main problem in using the stable isotope method on ice wedges for paleotemperature studies are the difficulties in attributing an ice veinlet or a sequence of ice veins to a discrete year or a discrete time interval, respectively. The use of tracers such as coloured *Lycopodia* spores could help to identify frost cracking processes and enable the attribution of an ice vein to a discrete year. Therefore, a selected field site easy to reach (because it should be visited more than once) with recent frost cracking activity is necessary.
- 2 A method for stable isotope analyses of small sample volumes has been developed (see Chapter 3). For the use of this method on ground ice samples, a complete horizontal sampling transect of ice wedges ice has been recovered on Big Lyakhovsky Island. This ground ice, presently stored in the freezing cellar at the AWI Bremerhaven, will enable us to perform a higher (maybe annual) sampling resolution for stable isotope and hydrochemical analyses and of ground ice, which is important to understand i. e. "isotopic smoothing" by diffusion.
- 3 The influence of surface water on ground ice formation (both ice wedges and segregated ice) should be examined in shallow water environment (i. e.

Conclusions

near the shore of a thermokarst lake), where frost cracking penetrates the permafrost table.

- 4 We suggest a monitoring programme, which combines recent climate data acquisition, sampling of recent precipitation on an annual scale and the study of recent ground ice formation processes with stable isotope and hydrochemical analyses.
- 5 The stable isotope studies on ground ice should be extended to other regions of Northern Siberia in order to distinguish local, regional and global variations in temperatures and moisture sources through time.
- 6 A high amount of stable isotope data has been obtained from ground ice. This information could be archived and used on a broader scale in a ground ice data base.

8. REFERENCES

- Aagaard, K., Swift, J. H. & Carmack, E. C. (1985): Thermohaline circulation in the Arctic Mediterranean Seas.- *J. Geophys. Res.* 90 (C5): 4833-4846.
- Aizen, V., Aizen, E., Melack, J. & Martma, T. (1996): Isotopic measurements of precipitation on central Asian glaciers (southeastern Tibet, northern Himalayas, central Tien Shan).- *J. Geophys. Res.* 101: 9185-9196.
- Alekseev, M. N. (1997): Paleogeography and geochronology in the Russian Eastern Arctic during the second half of the Quaternary.- *Quatern. Int.* 41/42: 11-15.
- Andreev, A., Novenko, E. Yu., Schirrmeister, L., Siegert, C. & Hubberten, H. W. (2001): Vegetation and climate changes in the Laptev Sea region during the Late Quaternary by pollen data. In: EUG XI Strasbourg, Conference Proceedings. Strasbourg, France, 211.
- Andreev, A. A., Schirrmeister, L., Siegert, C., Bobrov, A. A., Demske, D., Seiffert, M. & Hubberten, H.-W. (2002): Paleoenvironmental changes in Northeastern Siberia during the Late Pleistocene - evidences from pollen records of the Bykovsky Peninsula.- *Polarforschung* 70: 13-25.
- Arkhangelov, A. A., Vaikmyae, R. E., Mikhalev, D. V., Punning, Ya. M. & Solomatin, V. I. (1986): Stratigraphic subdivision of syngenetic permafrost by means of oxygen-isotope analysis.- *Transactions (Doklady) of the U.S.S.R* 290 (2): 94-96.
- Arkhangelov, A. A., Mikhalev, D. V. & Nikolaev, V. I. (1996): Reconstruction of formation conditions of permafrost and climates in Northern Eurasia.- In: Velichko, A. A., Arkhangelov, A. A., Borisova, O. K. (eds.). History of permafrost regions and periglacial zones of northern Eurasia and conditions of old human settlement. Institute of Geography, Russian Academy of Science, Moscow: 85-109 (in Russian).
- Astakhov, V. (1998): The last ice sheet of the Kara Sea: Terrestrial constraints on its age.- *Quatern. Int.* 45/46: 19-28.
- Atlas Arktiki (Atlas of the Arctic) (1985): Treshnikov, A. F. (ed.). G.U.G.K., Moscow (in Russian).
- Bauch, D. (1995): The distribution of $\delta^{18}\text{O}$ in the Arctic Ocean: Implications for the freshwater balance of the halocline and the sources of deep and bottom waters.- *Rep. Polar Res.* 159: 144 pp.
- Bauch, H. A., Kassens, H., Erlenkeuser, J., Grootes, P. M. & Thiede, J. (1999): Depositional environment of the Laptev Sea (Arctic Siberia) during the Holocene.- *Boreas* 28: 194-204.
- Boike, J. (1997): Thermal, hydrological and geochemical dynamics of the active layer at continuous permafrost site Taymyr Peninsula, Siberia.- *Rep. Polar Res.* 242: 104 pp.
- Bond, G., Heinrich, H., Broecker, W., Labeyrie, L., McManus, J., Andrews, J., Huon, S., Jantschik, R., Clausen, S., Simet, C., Tedesco, K., Klas, M., Bonani, G. & Ivy, S. (1992): Evidence for massive discharges of icebergs into the North Atlantic ocean during the last glacial period.- *Nature* 360: 245-249.
- Brezgunov, B. S., Yesikov, A. D., Ferronsky, V. I. & Sal'nova, L. V. (1998): Spatial-temporal variations of oxygen isotope composition in precipitation and

References

- river water of Northern Eurasia and their relation to temperature changes.- *Vodnye Resursy* 25, No. 1: 99-104 (in Russian).
- Burn, C. R., Michel, F. A. & Smith M. W. (1986): Stratigraphic, isotopic, and mineralogical evidence for an early Holocene thaw unconformity at Mayo, Yukon Territory.- *Can. J. Earth Sci.* 23: 794-803.
- Buzek, F. (1983): A rapid procedure for preparing oxygen-18 determination in water samples.- *Isotopenpraxis* 19: 70-72.
- Chappellaz, J., Davis, M., Delaygue, G., Delmotte, M., Kotiyakov, V. M., Legrand, M. & Stievenard, M. (1999): Climate and atmospheric history of the past 420,000 years from the Vostok ice core, Antarctica.- *Nature* 399: 429-436.
- Chizhov, A. B. & Dereviagin, A. Yu. (1998): Tritium in Siberian permafrost.- *Permafrost; Seventh international Conference, Proceedings, Yellowknife, Canada, Collection Nordiana, Quebec*: 151-156.
- Clark, I. D. & Fritz, P. (1997): *Environmental Isotopes in Hydrology*.- Lewis Publishers, Boca Raton: 328 pp.
- CLIMAP Project Members (1976): The surface of the Ice-Age Earth.- *Science* 191: 1131-1137.
- Colman, S. M., Peck, J. A., Karabanov, E. B., Carter, S. J., Bradbury, J. P., King, J. W. & Williams, D. F. (1995): Continental climate response to orbital forcing from biogenic silica records in Lake Baikal. *Nature* 378: 769-771.
- Craig, H. (1961): Isotopic variations in meteoric waters.- *Science* 133: 1702-1703.
- Cuffey, K. M., Clow, G. D., Alley, R. B., Stuiver, M., Waddington, E. D. & Saltus, R. W. (1995): Large Arctic temperature change at the Wisconsin-Holocene glacial transition.- *Science* 270: 455-458.
- Dansgaard, W. (1964): Stable isotopes in precipitation.- *Tellus* 16: 436-468.
- Dansgaard, W., Johnsen, S. J., Clausen, H. B., Dahl-Jensen, D., Gundestrup, N., Hammer, C. U. & Oeschger, H. (1984): North Atlantic climatic oscillations revealed by deep Greenland ice cores.- In: Hansen, J. E. & Takahashi, T. (eds.). *Climate Processes and Climate Sensitivity*. Washington, DC: American Geophysical Union: 288-298.
- Dansgaard, W., Johnsen, S. J., Clausen, H. B., Dahl-Jensen, D., Gundestrup, N. S., Hammer, C. U., Hvidberg, C. S., Steffensen, J. P., Sveinbjornsdottir, A. E., Jouzel, J. & Bond, G. (1993): Evidence for general instability of past climate from a 250-kyr ice-core record.- *Nature* 364: 218-220.
- Dereviagin, A. Yu., Meyer, H., Chizhov, A. B., Hubberten, H.-W. & Simonov, E. F. (2002): New data on the isotopic composition and evolution of modern ice wedges in the Laptev Sea Region.- *Polarforschung* 70: 27-35.
- Drachev, S. S., Johnson, G. L., Laxon, S. W., McAdoo, D. C. & Kassens, H. (1999): Main Structural Elements of Eastern Russian Arctic Continental Margin Derived from Satellite Gravity and Multichannel Seismic Reflection Data.- In: Kassens, H., Bauch, H. A., Dmitrenko, I. A., Eicken, H., Hubberten, H.-W., Melles, M., Thiede, J. & Timokhov, L. A. (eds.). *Land-Ocean Systems in the Siberian Arctic: Dynamics and History*. Lecture Notes in Earth Sciences, Springer, Berlin: 667-682.
- Epstein, S. & Mayeda, T. (1953): Variations of O¹⁸ content of waters from natural sources.- *Geochim. Cosmochim. Acta* 4: 213-224.

References

- Fairbanks, R. G. (1989): A 17,000-year glacial-eustatic sea level: influences of glacial melting rates on Younger Dryas event and deep ocean circulation.- *Nature* 342: 637-642.
- French, H. M. (1996): *The Periglacial Environment*.- 2nd Edition. London, Longman Publ.: 341 pp.
- Friedman, I. & O'Neil, J. R. (1977): Compilation of stable isotope fractionation factors of geochemical interest.- U.S. Geol. Surv. Prof. Pap. 440-KK: 49 pp.
- Fukuda, M. (1994): Occurrence of Ice-complex (Edoma) in Lena River Delta region and Big Lhyavosky Island, High Arctic Eastern Siberia.- In: Inoue, G. (ed.). *Proceedings of the Second Symposium on the joint Siberian Permafrost Studies between Japan and Russia in 1993*, Tsukuba, Japan: 1-9.
- Gasarov, Sh. Sh. (1977): Sublimation redistribution of material in ice wedges.- *Problems of Cryolithology* 6: 224-229 (in Russian).
- Gavrilov, A. V., Tumskey, V. E. & Romanovskij, N. N. (2000): Reconstruction of the mean annual ground temperature dynamic on the Yakutian coastal lowlands and adjoining shelf during the last 420 kyr.- *Kryosfera Zemlya* 4 (4): 3-14. (in Russian).
- Gonfiantini, R., Stichler, W. & Rozanski, K. (1995): Standards and intercomparison materials distributed by the International Atomic Energy Agency for stable isotope measurements.- In: *Reference and Intercomparison Materials for Stable Isotopes of Light Elements*, Proceedings of a consultants meeting held in Vienna, 1-3 December 1993, IAEA, Vienna: 13-29 (IAEA-TECDOC-825).
- Gordeev, V. V. & Sidorov, I. S. (1993): Concentrations of major elements and their outflow into the Laptev Sea by the Lena River.- *Mar. Chem.* 43: 33-45.
- Grigoryev, M. N., Imayev, V. S., Imayeva, L. P. *et al.* (1996): *Geology, seismicity and cryogenic processes in the arctic areas of western Yakutia*.- Yakut. Scientific Centre SD RAS: 80 pp. (in Russian).
- Groote, P. M., Stuiver, M., White, J. W., Johnsen, S. & Jouzel, J. (1993): Comparison of oxygen isotope records from the GISP2 and GRIP Greenland ice cores.- *Nature* 366: 552-554.
- Grosse, G. (2000): *Survey of quaternary sediments in permafrost deposits on Bol'shoy Lyakhovsky Island, New Siberian Islands*.- Unpubl. MSc thesis, Bergakademie Freiberg, Germany: 40 pp. (in German).
- Grosswald, M. G. (1998): Late Weichselian ice sheets in Arctic and Pacific Siberia.- *Quatern. Int.* 45/46: 3-18.
- Grosswald, M. G., Hughes, T. J. & Lasca, N. P. (1999): Oriented lake- and ridge assemblages of the Arctic coastal plains: glacial landforms modified by thermokarst and solifluction.- *Polar Record* 194: 215-230.
- Horita, J., Ueda, A., Mizukami, K. & Takatori, I. (1989): Automatic δD and $\delta^{18}O$ analyses of multi-water samples using H_2 - and CO_2 -water equilibration methods with a common equilibration set-up.- *Appl. Radiat. Isot.* 40: 801-805.
- International Permafrost Association (1998): *Multi-Language Glossary of Permafrost and Related Ground-Ice Terms*.- Van Everdingen, R. O. (ed.). The Arctic Institute of North America, Calgary, Canada: 78 pp.
- Jean-Baptiste, P., Jouzel, J., Stievenard, M. & Ciais, P. (1998): Experimental determination of the diffusion rate of deuterated water vapor in ice and

References

- application to the stable isotopes smoothing of ice cores.- *Earth Planet. Sc. Lett.* 158: 81-90.
- Johnsen, S. J., Dansgaard, W., Clausen, H. B. & Langway, C. C. (1972): Oxygen isotope profiles through the Antarctic and Greenland ice sheets.- *Nature* 235: 429-434.
- Johnsen, S. J. & White, J. (1989): The origin of Arctic precipitation under present and glacial conditions.- *Tellus* 41B: 452-468.
- Jouzel, J., Merlivat, L. & Lorius, C. (1982): Deuterium excess in an East Antarctic ice core suggests higher relative humidity at the oceanic surface during the last glacial maximum.- *Nature* 299: 688-691.
- Jouzel, J., Alley, R. B., Cuffey, K. M., Dansgaard, W., Grootes, P., Hoffmann, G., Johnsen, S. J., Koster, R. D., Peel, D., Shuman, C. A., Stievenard, M., Stuiver, M. & White, J. (1997): Validity of the temperature reconstruction from water isotopes in ice cores.- *J. Geophys. Res.* 102 (C12): 26,471-26,487.
- Kaplina, T. N. (1981): History of permafrost of north Yakutia in the late Cenozoic.- In: *History of the Development of Perennial Frozen Deposits in Eurasia.* Nauka: Moscow: 153-181 (in Russian).
- Karte, J. (1979): Räumliche Abgrenzung und regionale Differenzierung des Periglaziärs.- *Bochumer Geographische Arbeiten* 35: 211 pp. (in German).
- Kienast, F., Siegert, C., Schirrmeister, L. & Hubberten, H.-W. (2001): Plants as Climate Indicators- Results of Plant Macrofossil Studies on Late Quaternary Permafrost Sequences of the Laptev Sea Region, Northern Siberia.- *EUG XI, Conference Proceedings, Strasbourg*: 213.
- Klementyev, O. L., Nikolaev, V. I., Potapenko, V. Yu. & Savatyugin, L. M. (1991): Structures and thermodynamic conditions of the glaciers on the Severnaya Zemlya Archipelago.- *Data Glaciol. Stud.* 73: 103-109 (in Russian).
- Koç, N., Jansen, E. & Hafliðason, H. (1993): Paleoceanographic reconstructions of surface ocean conditions in the Greenland, Iceland and Norwegian Seas through the last 14 ka based on diatoms.- *Quaternary Sci. Rev.* 12: 115-140.
- Kunitsky, V. V. (1989): Cryolithogenesis of the lower Lena.- *Permafrost Institute, Academy of Science USSR, Siberian Department, Yakutsk*: 162 pp. (in Russian).
- Kunitsky, V. V. (1996): Chemical composition of continuous grown ice wedges of the Ice Complex.- In: *Cryolithozone and groundwater of Siberia, part I.: Morphology of the cryolithozone.* Melnikov Permafrost Institute, Yakutsk, Russian Academy of Science, Siberian Branch, Yakutsk: 93-117 (in Russian).
- Kunitsky, V. V. (1998): The Ice Complex and cryoplanation terraces on Big Lyakhovsky Island.- In: Kamensky, R. M., Kunitsky, V. V., Olovin, B. A., Shepelev, V. V. (eds.). *Problems of Geocryology (collected paper).* Melnikov Permafrost Institute, Russian Academy of Science, Siberian Branch, Yakutsk: 60-72 (in Russian).
- Kunitsky, V. V. & Schirrmeister, L. (2000): Paleoclimate Signals of Ice-Rich Permafrost Deposits.- In: Rachold V. (ed.). *Expeditions in Siberia in 1999.* *Rep. Polar Res.* 354: 113-270.
- Kuznetsova, L. P. (1998): Atmospheric moisture content and transfer over the territory of the former USSR.- Ohata, T., Hiyama, T. (eds.): *Second*

References

- International Workshop on Energy and Water Cycle in GAME-Siberia, 1997. Research Report of IHAS, Institute for Hydrospheric-Atmospheric Sciences, Nagoya, Japan: 145-151.
- Lachenbruch, A. H. (1962): Mechanics of thermal contraction cracks and ice-wedge polygons in permafrost.- *Geol. Soc. Am. Spec. Pap.* 70: 69 pp.
- Lauriol, B., Duchesne, C. & Clark, I. D. (1995): Systématique du remplissage en eau de fentes de gel: les résultats d'une étude oxygène-18 et deutérium.- *Permafrost Periglacial Process.* 6: 47-55.
- Leroux, M. (1993): The Mobile Polar High: a new concept explaining present mechanisms of meridional air-mass and energy exchanges and global propagation of palaeoclimate changes.- *Global Planet. Change* 7: 69-93.
- Lungersgauzen, G. F. (1967): On the geological age of the Verkhoyansk mountains (method of investigations and conclusions).- In: *Tektonicheskie dvizheniya i noveishie struktury zemnoi kory.* Moscow, Nedra.
- MacKay, J. R. (1972): Offshore permafrost and ground ice, southern Beaufort Sea, Canada.- *Can. J. Earth Sci.* 9: 1550-1561.
- MacKay, J. R. (1974): Ice-wedge cracks, Garry Island, Northwest Territories.- *Can. J. Earth Sci.* 11: 1366-1383.
- MacKay, J. R. (1983): Oxygen isotope variations in Permafrost, Tuktoyaktuk peninsula area, Northwest Territories.- *Pap. 83-1B, Geol. Surv. Canada:* 67-74.
- MacKay, J. R. (1992): The frequency of ice-wedge cracking (1967-1987) at Garry Island, western Arctic coast, Canada.- *Can. J. Earth Sci.* 29: 236-248.
- Merlivat, L. & Jouzel, J. (1979): Global climatic interpretation of the deuterium-oxygen 18 relationship for precipitation.- *J. Geophys. Res.* 84 (C8): 5029-5033.
- Meyer, H., Dereviagin, A. & Syromyatnikov, I. (1999): Ground ice studies.- In: *Expeditions in Siberia in 1998.* Rachold, V. (ed.)- *Rep. Polar Res.* 315: 155-163.
- Meyer, H., Schönicke, L., Wand, U., Hubberten, H.-W. & Friedrichsen, H. (2000): Isotope studies of hydrogen and oxygen in ground ice - Experiences with the equilibration technique.- *Isot. Environ. Health S.* 36: 133-149.
- Meyer, H., Dereviagin, A., Siegert, C. & Hubberten, H. W. (2002a): Paleoclimate studies on Bykovsky Peninsula, North Siberia - Hydrogen and oxygen isotopes in ground ice.- *Polarforschung* 70: 37-51.
- Meyer, H., Dereviagin, A., Siegert, C., Schirrmeister, L. & Hubberten, H. W. (2002b): Paleoclimate reconstruction on Big Lyakhovsky Island, North Siberia - Hydrogen and oxygen isotopes in ice wedges.- *Permafrost Periglacial Process.* 13: 91-105.
- Michel, F. A. (1982): Isotope investigations of permafrost waters in Northern Canada.- Ph. D. thesis, Dept. of Earth Sciences, Univ. of Waterloo, Canada: 227 pp.
- Murray, R. J. & Simmonds, I. (1995): Responses of climate and cyclones to reductions in Arctic winter sea ice.- *J. Geophys. Res.* 100: 4791- 4806.
- Nadeau, M. J., Schleicher, M., Grootes, P. M., Erlenkeuser, H., Gottdang, A., Mous, D. J. W., Sarnthein, J. M. & Willkomm, H. (1997): The Leibniz Labor facility at the Christian-Albrechts-University, Kiel, Germany. *Nucl. Instr. Methods Phys. Res.* **B123**: 22-30.

References

- Nadeau, M. J., Grootes, P. M., Schleicher, M., Hasselberg, P., Rieck, A. & Bitterling, M. (1998): Sample throughput and data quality at the Leibniz Labor AMS facility. *Radiocarbon* **40**: 239-245.
- Nagaoka, D. (1994): Properties of Ice Complex deposits in Eastern Siberia. – In: Inoue, G. (ed.). *Proceedings of the Second Symposium on the Joint Siberian Permafrost Studies between Japan and Russia in 1993*, Tsukuba, Japan: 14-18.
- Nagaoka, D., Saijo, K. & Fukuda, M. (1995): Sedimental environment of the Edoma in high Arctic eastern Siberia.- In: Takahashi, K., Osawa, A., Kanazawa, Y. (eds.). *Proceedings of the Third Symposium on the Joint Siberian Permafrost Studies between Japan and Russia in 1994*: 8-13.
- Nikolayev, V. I. & Mikhalev, D. V. (1995): An oxygen-isotope paleothermometer from ice in Siberian permafrost.- *Quat. Res.* **43** (1): 14-21.
- Oeschger, H. (1985): The contribution of ice core studies to the understanding of environmental processes.- In: Langway Jr., C. C., Oeschger, H. & Dansgaard, W. (eds.). *Greenland Ice Core: Geophysics, Geochemistry, and the Environment*. Am. Geophys. Union, Washington/DC, USA. *Geophys. Monograph* **33**: 9-17.
- Petit, J. R., Jouzel, J., Raynaud, D., Barkov, N. I., Barnola, J. M., Basile, I., Bender, M., Chappellaz, J., Davis, M., Delaygue, G., Delmotte, M., Kotlyakov, V. M., Legrand, M. & Stievenard, M. (1999): Climate and atmospheric history of the past 420,000 years from the Vostok ice core, Antarctica.- *Nature* **399**: 429-436.
- Rachold V. (ed.) (1999): *Expeditions in Siberia in 1998*.- *Rep. Polar Res.* **315**: 268 pp.
- Rachold V. (ed.) (2000): *Expeditions in Siberia in 1999*.- *Rep. Polar Res.* **354**: 303 pp.
- Rachold V. & Grigoriev M. (eds.) (2001): *Russian-German Cooperation SYSTEM LAPTEV SEA 2000: The Expedition LENA 2000*.- *Rep. Polar Res.* **388**: 135 pp.
- Rinke, A., Dethloff, K., Spekat, A., Enke, W. & Hesselbjerg Christensen, J. (1999): High resolution climate simulations over the Arctic.- *Polar Res.* **18** (2): 143-150.
- Romanovsky, N. N. (1958): Paleogeographic conditions of formation of the Quaternary deposits on Bol'shoy Lyakhovsky Island (Novosibirsky Islands).- In: *Questions of Physical Geography of Polar region*, Publications of Moscow State University, Moscow: 80-88 (in Russian).
- Romanovsky, N. N. (1976): The scheme of correlation of polygonal wedge structures.- *Biuletyn Peryglacjalny* **26**: 287-294.
- Romanovskii, N. N. (1978): Effect of neotectonic movements on formation of permafrost regions.- In: Sanger, F. J. & Hyde, P. J. (eds.). *Second International Conference on permafrost; USSR contribution*. Washington, D. C., United States, National. Acad. Sci.: 184-188.
- Romanovskii, N. N. (1985): Distribution of recently active ice and soil wedges in the USSR. Field and theory; lectures in geocryology.- Church, M. & Slaymaker, O. (eds.). Vancouver, BC, Canada. Univ. B. C. Press: 154-165.
- Romanovskii, N. N. (1993): *Principles of cryogenesis of the lithozone*. Moscow, Moscow University Press: 344 pp. (in Russian).

References

- Romanovskii, N. N., Kholodov, A. L., Gavrilov, A. V., Tumskoy, V. E., Hubberten, H.-W. & Kassens, H. (1999): Ice-bonded permafrost thickness in the Eastern part of the Laptev Sea shelf (results of computer modelling).- *Kryosfera Zemlya* 3 (2): 22-32 (in Russian).
- Romanovskii, N. N., Hubberten, H. W., Gavrilov, A. V., Tumskoy, V. E., Tipenko, G. S., Grigoryev, M. N. & Siegert, C. (2000): Thermokarst and Land-Ocean Interactions, Laptev Sea Region, Russia.- *Permafrost Periglac. Process.* 11: 137-152.
- Rozenbaum, G. E. & Shpolyanskaya, N. A. (1998): Late Cenozoic history of the Russian Arctic.- *Permafrost Periglac. Process.* 9: 247-273.
- Schirrmeister, L., Siegert, C., Kunitsky V. V., Grootes, P. M. & Erlenkeuser, H. (2002a): Late Quaternary ice-rich permafrost sequences as a paleo-environmental archive for the Laptev Sea Region in Northern Siberia.- *Int. J. Earth Sci. (Geolog. Rundsch.)* 91: 154-167.
- Schirrmeister, L., Oezen, D., & Geyh, M. A. (2002b): $^{230}\text{Th}/\text{U}$ age determination of frozen peat in permafrost deposits of Bol'shoy Lyakhovsky Island (North Siberia).- *Quaternary Res.* 57: 253-258.
- Schwamborn, G., Rachold, V. & Grigoryev, M. (2002): Late Quaternary sedimentation history of the Lena Delta.- *Quatern. Int.* 89: 119-134.
- Scrimgeour, C. M., Rollo, M. M., Mudambo, S. M., Handley, L. L. & Prosser, S. J. (1993): A simplified method for deuterium/hydrogen isotope ratio measurements on water samples of biological origin.- *Biol. Mass Spectrom.* 22: 383-387.
- Sher, A. V., Kaplina, T. N. & Ovander, M. G. (1987): Unified regional stratigraphic chart for the Quaternary deposits in the Yana-Kolyma lowland and its mountainous surroundings.- Explanatory Note. In: Decisions of Interdepartmental Stratigraphic conference on the Quaternary of the East USSR. Magadan: 29-69 (in Russian).
- Siegert, C., Derevyagin, A. Y., Shilova, G. N., Hermichen, W. D. & Hiller, A. (1999): Paleoclimatic indicators from permafrost sequences in the Eastern Taymyr Lowland.- In: Kassens, H., Bauch, H. A., Dmitrenko, I., Eicken, H., Hubberten, H.-W., Melles, M., Thiede, J. & Timokhov, L. (eds.). *Land-Ocean Systems in the Siberian Arctic: Dynamics and History.* Berlin, Springer: 477-499.
- Siegert, C., Schirrmeister, L. & Babiy, O. A. (2002): The composition of Late Pleistocene permafrost deposits - new sedimentological, mineralogical and geochemical data from the Ice Complex of the Bykovsky Peninsula, Northern Siberia.- *Polarforschung* 70: 3-11.
- Slagoda, E. A. (1993): Genesis and microstructure of cryolithogenic deposits at the Bykovsky Peninsula and the Muostakh Island.- unpubl. Diss., RAS Siberian Section, Permafrost Institute, Yakutsk: 218 pp. (in Russian).
- Solomatn, V. I. (1986): Petrogenesis of ground ice.- Novosibirsk, Nauka: 215 pp. (in Russian).
- Spielhagen, R. (2001): Enigmatic Arctic ice sheets.- *Nature* 410: 427-428.
- Stuiver, M., Reimer, P. J., Bard, E., Beck, J. W., Burr, G. S., Hughen, K. A., Kromer, B., McCormac, F. G., van der Plicht, J. & Spurk, M. (1998): INTCAL98 radiocarbon age calibration, 24,000 - 0 cal BP.- *Radiocarbon* 40:1041-1083.

References

- Svendsen, J. I., Astakhov, V. I., Bolshiyarov, D. Yu., Demidov, I., Dowdeswell, J. A., Gataullin, V., Hjort, C., Hubberten, H.-W., Larsen, E., Mangerud, J., Melles, M., Moeller, P., Saarnisto, M. & Siegert, M. J. (1999): Maximum extent of the Eurasian ice sheets in the Barents and Kara Sea region during the Weichselian.- *Boreas* 28: 234-242.
- Thielecke, F., Brand, W. & Noack, R. (1998): Hydrogen isotope determination for small-size water samples using an equilibration technique.- *J. Mass Spec.* 33: 342-345.
- Tomirdiaro, S. V., Arslanov, Kh. A., Chernen'kiy, B. I., Tertychnaya, T. V. & Prokhorova, T. N. (1984): New data on formation of loess-ice sequences in Northern Yakutia and ecological conditions of mammoth fauna in the Arctic during the late Pleistocene.- *Doklady AN SSSR*, 278, 6: 1446-1449. (in Russian).
- Vaikmäe, R. & Punning, J. M. (1984): Isotope-geochemical investigations on glaciers in the Eurasian Arctic.- In: Mahaney, W. C. (ed.). *Correlation of Quaternary chronologies*, Geobooks, Norwich: 385-393.
- Vaikmäe, R. (1989): Oxygen isotopes in permafrost and ground ice - a new tool for paleoclimatic investigations.- In: 5th Working Meeting "Isotopes in Nature", Proceedings, Leipzig, Germany: 543-553.
- Vaikmäe, R. (1991): Oxygen-18 in permafrost ice.- *International Symposium of the Use of Isotope Techniques in Water Resources Development*. Vienna, Austria, March 1991: 1-26.
- Vasil'chuk, Yu. K., Trofimov, V. T. (1988): Oxygen isotope variations in ice-wedges and massive ice. In *Permafrost: Fifth International Conference, Proceedings*. Trondheim, Tapir Publishers, Vol.1: 489-492.
- Vasil'chuk, Yu. K. (1991): Reconstruction of the paleoclimate of the late Pleistocene and Holocene on the basis of isotope studies of subsurface ice and waters of the permafrost zone.- *Water Res.* 17, Issue 6: 640-674.
- Vasil'chuk, Yu. K. (1992): Oxygen isotope composition of ground ice.- Application to paleogeocryological reconstructions.- Vol. 1, Geological Faculty of Moscow State University, Russian Academy of Sciences, Moscow, Russia: 420 pp.
- Vasil'chuk, Yu. K., Vasil'chuk, A. C. (1998): Oxygen isotope and C¹⁴ data associated with Late Pleistocene syngenetic ice-wedges in mountains of Magadan region, Siberia. *Permafrost Periglac. Process.* 9: 177-183.
- Vasil'chuk, Yu. K., van der Plicht, J., Jungner, H., Soininen, E. & Vasil'chuk, A. C. (2000): First direct dating of Late Pleistocene ice wedges by AMS. *Earth Planet. Sci. Lett.* 179: 237-242.
- Washburn, A. L. (1979): *Geocryology - A survey of periglacial processes and environments*.- Edward Arnold Publ.: 406 pp.
- Yefimov, A. I. & Dukhin, I. E. (1966): *Kratkiye i predvaritel'nyye soobshcheniya*.- *Akad. Nauk. SSSR. Sibirskoye Otdelnyye. Geologiya i Geofizika* 7: 92-97.
- Yershov, E. D. (ed.) (1989): *Geocryology of the USSR*.- Moscow, Nedra, vol. Middle Siberia: 415 pp. (in Russian).
- Yershov, E. D. (1998): *General Geocryology*.- *Studies in Polar Research*. English Edition: Cambridge University Press: 580 pp.

List of figures

Fig. 1.1: Permafrost regions in the Northern hemisphere (Karte, 1979)	2
Fig. 2.1: Distribution of the Ice Complex in Northern Siberia (after Romanovskii, 1993) and the position of the study areas	7
Fig. 2.2: Schematics of Ice Complex formation (after Romanovskii, unpublished)	8
Fig. 3.1: 10 hour temperature plot of a water bath (type GFL 1086, modified)	11
Fig. 3.2: Determination of the equilibration time for $\delta^{18}\text{O}$	12
Fig. 3.3.1: δD -calibration of Delta-S mass spectrometer	15
Fig. 3.3.2: $\delta^{18}\text{O}$ -calibration of Delta-S mass spectrometer	15
Fig. 3.4.1: Temporal variation of δD for the laboratory standard NGT1	16
Fig. 3.4.2: Temporal variation of $\delta^{18}\text{O}$ for the laboratory standard NGT1	16
Fig. 3.5: Memory effects (in %) for different idle times between change-over of standard and sample inlet	17
Fig. 3.6: Equilibration technique applied to small sample sizes	20
Fig. 3.7: Sampling strategy for ground ice (ice wedges and segregated ice)	23
Fig. 3.8: First isotopic data of two Siberian ice wedges from the Bykovsky Peninsula. One ice wedge of Holocene age penetrates into a Late Pleistocene ice wedge.	24
Fig. 4.1: Schematic map and geomorphological situation of the Bykovsky Peninsula	29
Fig. 4.2: Air photograph of the working area at the east coast of the Bykovsky Peninsula	31
Fig. 4.3: Schematic profile of the outcrop "Mamontovy Khayata" (Mammoth mountain), east coast of Bykovsky Peninsula: Cryolithogenetic units and the respective sampling locations for ice wedges	33
Fig. 4.4: New AMS ^{14}C ages of organic remains in ice wedges and in the sediments in direct contact to the sampled ice wedges of the Ice Complex "Mamontovy Khayata", with their respective error bars versus the height in the outcrop.	38
Fig. 4.5: $\delta^{18}\text{O}$ - δD diagram for samples from snow patches, rain and recent ice wedges collected in summer 1998 on Bykovsky Peninsula.	42
Fig. 4.6.1-4.6.3: Electrical conductivity, $\delta^{18}\text{O}$ and d excess of 5 m long horizontal sampling transect of Pleistocene ice wedge MKh-3 (height a.s.l.: 11.1m).	47

List of figures

Fig. 4.7.1-4.7.4: $\delta^{18}\text{O}$ - δD diagrams for ice wedges in all genetic units: 1. Late Pleistocene part of the Ice Complex. Samples of the ice wedge Mkh-00 are represented by white dots; 2. Uppermost part of the Ice Complex (ice wedge MKh-4.6); 3. Alas; 4. Thermo-erosional valley (Log).	50
Fig. 4.8: Development of $\delta^{18}\text{O}$, δD and d excess of all Ice Complex ice wedges (without samples evidently influenced by exchange processes) and for the younger units alas and log through time.	52
Fig. 5.1: Location of the working area on Big Lyakhovsky Island	62
Fig. 5.2: Schematic profile of the study site at the South coast of Big Lyakhovsky Island with cryolithogenetic units (modified after Grosse, 2000)	64
Fig. 5.3: Subvertical oriented ice-soil wedges ("polosatic") of Unit B. Interfingering of single ice veinlets with the sediment is observed.	66
Fig. 5.4: $\delta^{18}\text{O}$ - δD diagram for snow patch and rain water samples collected in summer 1999 on Big Lyakhovsky Island.	71
Fig. 5.5.1-5.5.3: $\delta^{18}\text{O}$ - δD diagrams for ice wedges in the older geocryological units: 1. Unit A; 2. Unit B; 3. Ice Complex	75
Fig. 5.5.4-5.5.6: $\delta^{18}\text{O}$ - δD diagrams for ice wedges in the younger geocryological units: 4. Alas; 5. Thermo-erosional valley (Log); 6. Fluvial deposits of Zimov'e River	76
Fig. 5.6: Development of $\delta^{18}\text{O}$, δD and d excess of all ice wedges (without samples influenced by exchange processes) in "logical" stratigraphic order	78
Fig. 6.1: Absolute temperature reconstruction of the mean annual winter temperature by means of a correlation with recent ice veins	93
Fig. 6.2: Absolute temperature reconstruction of the mean January temperature by means of a correlation with recent ice veins	94

List of tables

Tab. 3.1: δD and $\delta^{18}\text{O}$ of IAEA and laboratory standards (vs. V-SMOW)	14
Tab. 3.2: δD values for small sample sizes of between 0.05 and 5 ml for an Antarctic water	19
Tab. 3.3: Small sample sizes and large differences in δD and $\delta^{18}\text{O}$ values	21
Tab. 4.1: New AMS ^{14}C ages of organic material in ice wedges and in sediments enclosing ice wedges of the three genetic units Ice Complex, alas and log	36

List of figures

Tab. 4.2: Stable isotope ($\delta^{18}\text{O}$, δD and d excess) minimum, mean and maximum values, standard deviations (s. d.), as well as slopes and intercepts in the $\delta^{18}\text{O}$ - δD diagram for all ice wedges of three genetic units Ice Complex, alas and log	44
Tab. 5.1: Stable isotope ($\delta^{18}\text{O}$, δD and d excess) minimum, mean and maximum values, standard deviations as well as slopes and intercepts in the $\delta^{18}\text{O}$ - δD diagram for all sampled ice wedges and for recent precipitation samples of Big Lyakhovsky Island	78
Tab. 6.1: Mean isotopic composition of snow, recent, Holocene and Pleistocene ice wedges for different locations of the Laptev Sea region.....	89

ACKNOWLEDGEMENTS

I would like to thank my professors Dr. Hans-W. Hubberten, Dr. Manfred Strecker and Dr. Hans Friedrichsen for the reviews of this PhD thesis, helpful discussions. Research fund was provided by the BMBF for the project "System Laptev Sea 2000" (project number 03G0534).

Many thanks go to all the staff of AWI Potsdam, who created a nice and friendly atmosphere at the institute. Christine Siegert, who initiated the project "Paleoclimate signals in ice-rich permafrost", is highly acknowledged for that. Without the discussions with Christine and Lutz Schirrmeister, this thesis would not exist in its present form. Thank you both very much for your scientific guidance and engagement! Special thanks to Alexander Dereviagin from Moscow State University for fruitful discussions during the last three years and excellent co-operation in the field and in discussions. Thanks to all the members of the expeditions "Lena-Delta 1998 and 1999". I thank the administrations staff for their fast and unbureaucratic way in solving problems. Helga Henschel is highly acknowledged, not only for proofreading of the three papers. Ingeborg Sass got me any literature I needed, and is simply doing a great job in the AWI library. The friendships amongst PhD students and Postdocs helped to manage good and bad times. Therefore, big and special thanks to Johannes Müller, Holger Rieke (GFZ), Georg Schwamborn and Guido Grosse (Freiberg). Bernd Wagner, Holger Cremer, Frank Kienast, Karsten Friedrich, Andrey Andreev, Thomas Kumke, Wolf-Dieter Hermichen, Uli Wand and Volker Rachold gave a helping hand and had open ears, whenever needed.

For laboratory assistance I would like to thank Ute Bastian, Maren Stapke, Lutz Schönicke, who shared my office for the last two years, and Antje Eulenburg for hydrochemical discussions and good concert tips. Frau Birkenstaedt and Holger Müller gave me the possibility to use the ion chromatograph at the Geologisches Landesamt in Kleinmachnow. Thank you for that. In this thesis, data of the National Oceanic and Atmospheric Administration (NOAA) data archive is used. The reviews of R. Spielhagen and R. Vaikmäe substantially improved the "Polarforschung" paper. Additionally, four unknown reviewers

Acknowledgements

gave helpful comments for the improvement of the two other papers. Valuable discussions with people such as Prof. Hugh French from the University of Ottawa encouraged me a lot to proceed.

My family and my friends I would like to thank for their encouragement and support during my time as PhD student.

Last and most special thanks go to my wife Claudia, who accompanied me during the last years and who showed me that there are many more important and interesting things in life than paleoclimate and ice wedges.

All stable isotope and hydrochemical data of ground ice and water are available in the scientific data base PANGAEA (<http://www.pangaea.de>).

„Berichte zur Polarforschung“

Eine Titelübersicht der Hefte 1 bis 376 (1981 - 2000) erschien zuletzt im Heft 413 der nachfolgenden Reihe „Berichte zur Polar- und Meeresforschung“. Ein Verzeichnis aller Hefte beider Reihen sowie eine Zusammenstellung der Abstracts in englischer Sprache finden Sie im Internet unter der Adresse:
<http://www.awi-bremerhaven.de/Resources/publications.html>

Ab dem Heft-Nr. 377 erscheint die Reihe unter dem Namen: „Berichte zur Polar- und Meeresforschung“

- Heft-Nr. 377/2000 – „Rekrutierungsmuster ausgewählter Wattfauna nach unterschiedlich strengen Wintern“ von Matthias Strasser
- Heft-Nr. 378/2001 – „Der Transport von Wärme, Wasser und Salz in den Arktischen Ozean“, von Boris Cisewski
- Heft-Nr. 379/2001 – „Analyse hydrographischer Schnitte mit Satellitenaltimetrie“, von Martin Losch
- Heft-Nr. 380/2001 – „Die Expeditionen ANTARKTIS XI/1-2 des Forschungsschiffes POLARSTERN 1998/1999“, herausgegeben von Eberhard Fahrbach und Saad El Naggar.
- Heft-Nr. 381/2001 – „UV-Schutz- und Reparaturmechanismen bei antarktischen Diatomeen und *Phaeocystis antarctica*“, von Lieselotte Riegger.
- Heft-Nr. 382/2001 – „Age determination in polar Crustacea using the autofluorescent pigment lipofuscin“, by Bodil Bluhm.
- Heft-Nr. 383/2001 – „Zeitliche und räumliche Verteilung, Habitatspräferenzen und Populationsdynamik benthischer Copepoda Harpacticoida in der Potter Cove (King George Island, Antarktis)“, von Gritta Veit-Köhler.
- Heft-Nr. 384/2001 – „Beiträge aus geophysikalischen Messungen in Dronning Maud Land, Antarktis, zur Auffindung eines optimalen Bohrpunktes für eine Eiskerntiefbohrung“, von Daniel Steinhage.
- Heft-Nr. 385/2001 – „Actinium-227 als Tracer für Advektion und Mischung in der Tiefsee“, von Walter Geibert.
- Heft-Nr. 386/2001 – „Messung von optischen Eigenschaften troposphärischer Aerosole in der Arktis“ von Rolf Schumacher.
- Heft-Nr. 387/2001 – „Bestimmung des Ozonabbaus in der arktischen und subarktischen Stratosphäre“, von Astrid Schulz.
- Heft-Nr. 388/2001 – „Russian-German Cooperation SYSTEM LAPTEV SEA 2000: The Expedition LENA 2000“, edited by Volker Rachold and Mikhail N. Grigoriev.
- Heft-Nr. 389/2001 – „The Expeditions ARKTIS XVI/1 and ARKTIS XVI/2 of the Research Vessel 'Polarstern' in 2000“, edited by Gunther Krause and Ursula Schauer.
- Heft-Nr. 390/2001 – „Late Quaternary climate variations recorded in North Atlantic deep-sea ostracodes“, by Claudia Didié.
- Heft-Nr. 391/2001 – „The polar and subpolar North Atlantic during the last five glacial-interglacial cycles“, by Jan. P. Helmke.
- Heft-Nr. 392/2000 – „Geochemische Untersuchungen an hydrothermal beeinflussten Sedimenten der Bransfield Straße (Antarktis)“, von Anke Dählmann.
- Heft-Nr. 393/2001 – „The German-Russian Project on Siberian River Run-off (SIRRO): Scientific Cruise Report of the Kara-Sea Expedition 'SIRRO 2000' of RV 'Boris Petrov' and first results“, edited by Ruediger Stein and Oleg Stepanets.
- Heft-Nr. 394/2001 – „Untersuchung der Photooxidantien Wasserstoffperoxid, Methylhydroperoxid und Formaldehyd in der Troposphäre der Antarktis“, von Katja Riedel.
- Heft-Nr. 395/2001 – „Role of benthic cnidarians in the energy transfer processes in the Southern Ocean marine ecosystem (Antarctica)“, by Covadonga Orejas Saco del Valle.
- Heft-Nr. 396/2001 – „Biogeochemistry of Dissolved Carbohydrates in the Arctic“, by Ralph Engbrodt.
- Heft-Nr. 397/2001 – „Seasonality of marine algae and grazers of an Antarctic rocky intertidal, with emphasis on the role of the limpet *Nacilla concinna* Strebel (Gastropoda: Patellidae)“, by Dohong Kim.
- Heft-Nr. 398/2001 – „Polare Stratosphärenwolken und mesoskalige Dynamik am Polarwirbelrand“, von Marion Müller.
- Heft-Nr. 399/2001 – „North Atlantic Deep Water and Antarctic Bottom Water: Their Interaction and Influence on Modes of the Global Ocean Circulation“, by Holger Brix.
- Heft-Nr. 400/2001 – „The Expeditions ANTARKTIS XVIII/1-2 of the Research Vessel 'Polarstern' in 2000“ edited by Victor Smetacek, Ulrich Bathmann, Saad El Naggar.
- Heft-Nr. 401/2001 – „Variabilität von CH₂O (Formaldehyd) - untersucht mit Hilfe der solaren Absorptionsspektroskopie und Modellen“ von Torsten Albrecht.
- Heft-Nr. 402/2001 – „The Expedition ANTARKTIS XVII/3 (EASIZ III) of RV 'Polarstern' in 2000“, edited by Wolf E. Arntz and Thomas Brey.
- Heft-Nr. 403/2001 – „Mikrohabitatansprüche benthischer Foraminiferen in Sedimenten des Südatlantiks“, von Stefanie Schumacher.
- Heft-Nr. 404/2002 – „Die Expedition ANTARKTIS XVII/2 des Forschungsschiffes 'Polarstern' 2000“, herausgegeben von Jörn Thiede und Hans Oerter.
- Heft-Nr. 405/2002 – „Feeding Ecology of the Arctic Ice-Amphipod *Gammarus wilkitzkii*. Physiological, Morphological and Ecological Studies“, by Carolin E. Arndt.
- Heft-Nr. 406/2002 – „Radiolarienfauna im Ochotskischen Meer - eine aktuopaläontologische Charakterisierung der Biozönose und Taphozönose“, von Anja Nimmergut.
- Heft-Nr. 407/2002 – „The Expedition ANTARKTIS XVIII/5b of the Research Vessel 'Polarstern' in 2001“, edited by Ulrich Bathmann.
- Heft-Nr. 408/2002 – „Siedlungsmuster und Wechselbeziehungen von Seepocken (Cirripedia) auf Muschelbänken (*Mytilus edulis* L.) im Wattenmeer“, von Christian Buschbaum.